Helsinki University of Technology Publications in Machine Design 2/2004
Teknillisen korkeakoulun Koneensuunnittelun julkaisuja 2/2004
Espoo 2004

PREDICTIVE 3D ROLL GRINDING METHOD FOR REDUCING PAPER QUALITY VARIATIONS IN COATING MACHINES

Petri Kuosmanen

Dissertation for the degree of Doctor of Science (Technology) to be presented with due permission for public examination and debate in Auditorium K216 at Helsinki University of Technology (Espoo, Finland) on the 7th of May, 2004, at 12 o'clock noon.

Helsinki University of Technology
Department of Mechanical Engineering
Machine design

Teknillinen korkeakoulu
Konetekniikan osasto
Koneensuunnittelu

Distribution:
Helsinki University of Technology
Machine Design
P.O. Box 4100
FIN-02015 HUT
Tel. +358 9 451 3555
Fax +359 9 451 3549
E-mail: tiina.nikander@hut.fi

ISBN 951-22-7014-5
ISSN 1456-4955

Otamedia Oy
Espoo 2004

ABSTRACT

The predominant trend in paper machines is towards an increased running speed. At the same time, the paper produced must have a higher and more even quality. In printing papers the main end-use properties and quality components are runnability, printability, and print quality. These coexistent requirements create new demands for the behaviour of rolls under production conditions. High quality printing paper grades are coated. In blade coating the thickness of the coating film on the paper surface is found to be heavily dependent on the run-out of the backing roll which supports the paper web against the metering blade. The run-out tolerance of backing rolls at running speed has lately been 50 µm and should be substantially reduced in the future. The new tolerances can no longer be met by tightening the traditional roll manufacturing tolerances.

A new predictive 3D grinding method has been developed to improve roll behaviour in the paper production environment. It consists of a measuring system, which can verify the rotational and geometry errors of the roll at running speed, and a 3D grinding system, which controls the grinding process according to the information gained by these measurements. In this study, the new method was applied to the backing rolls of a coating station. The experiments were carried out in a paper mill, on a medium-weight coated (MWC) paper production line. The paper was analysed before and after the predictive 3D grinding.

The predictive 3D grinding reduced the machine direction (MD) ash variation caused by the backing rolls by an average of 76%. Ash variation correlates well with coating variation. As a result of a more even coating film, MD gloss variation was reduced by 82%. Reduced gloss variation improves the print quality of LWC paper. The variation in thickness caused by the backing rolls was reduced by 74%. More even paper thickness reduces excitations and therefore improves runnability in calendering, winding, and printing.

A new paradigm for roll grinding was set. The applications of the technology are not limited to high-speed paper machine rolls; the method can also be applied to different kinds of nips of rolls. The method can compensate for a systematic error causing nip force variation, such as uneven thermal expansion or the uneven flexural stiffness of a roll. The technology can be applied in different industries, such as the steel, plastics, or aluminium industries. With this method, it is also possible to use rolls in applications which have requirements too high to be met by traditional technology.

Keywords: roll, roundness, measuring, non-circular machining, dynamic roundness, backing roll, coating, paper machine, coating machine.

PREFACE

I wish to extend my thanks to everyone who has helped me to finish this thesis.

Mauri Airila deserves thanks for his commitment to the supervision of this work. His experience, together with his stable and kind attitude, was indispensable during the final stages. Kalevi Ekman deserves thanks for his support and understanding during this work.

Thanks to Jukka Pullinen, who performed the calibrations of the dynamic measuring device and took the measurements in the paper mill. Thanks to Jari Juhanko for his valuable help with paper analysis data handling and comments on the manuscript. Thanks to Esa Porkka for his great help with data analysis and calculations. Thanks to the research group of Paper Machinery for their support. Thanks to Reijo Hellsten for the paper analysis and Miikka Hernesaho, Timo Häkkinen, and Jari Neejärvi at Myllykoski Paper Oy. Thanks to Repa and others at the roll grinding shop at Myllykoski Paper for always being ready for tests with professional skill. Thanks to Kalervo Salomäki, Ilkka Mustonen, Jyrki Laari, and others at Tapio Technologies for the free software licence and advice on how to use it.

Thanks to Pekka Väänänen, who was my inspiring research colleague for many years.

Thanks to my mother and brothers for support. My warmest thanks go to Sari, Markus, Katariina, and Susanna, who made many sacrifices to give me the time to finalise this work.

Espoo, December 2003 Petri Kuosmanen

TABLE OF CONTENTS

ABSTRACT

1 INTRODUCTION

1.1 Background

The Finnish economy has always been heavily dependent on forests. The forest industry represented one quarter of Finland's total export value of 47.1 billion euros in 2002 (Figure 1). The electronic and electric industry overtook the forest industry as the leading exporter in 1999. In addition, a remarkable portion of the Finnish metal industry produces machines, such as paper machines, for the forest industry.

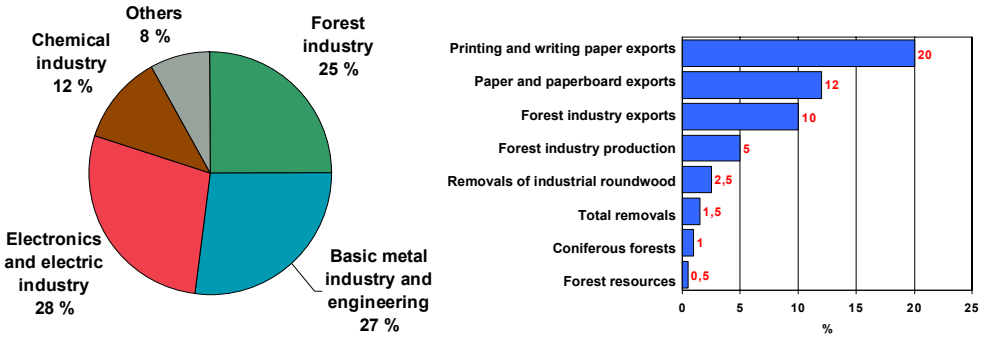

Figure 1 *Total exports from Finland in 2002 and the share in global exports of printing and writing paper and forest resources (Finnish Forest Industries Federation 2002).*

In the Finnish paper industry, the trend is towards high-quality printing papers. Almost all that is produced is exported and globally Finland accounts for 20% of all printing paper exports (Finnish Forest Industries Federation 2002).

Printing paper is calendered to achieve good gloss and smoothness properties. A considerable amount of printing paper is coated. In consequence, Finnish paper mills have a large number of coating machines and calenders. Paper machines, like coating machines and calenders, consist of rolls and the frame for supporting them. Up to 60% of the cost of a paper machine line comes from the rolls.

In increasing the production capacity of paper machines, the predominant trend is towards higher running speeds rather than wider machines. It is forecast that this trend will also continue in the future. As a result of higher running speeds, the rotational speeds of rolls, and thus vibration problems, have increased. The latest paper machines being sold are designed for a running speed of 2000 m/min. The paper-making process itself does not seem to be a limiting factor in increasing running speeds. For example, a pilot coating machine has a speed record of over 3100 m/min (Oinonen 1998) and pilot paper machines have been running at over 2500 m/min. The difference in speed between pilot and production machines is the result of difficulties in making a wide machine rather than a narrow one. A wide machine has longer rolls,

which means reduced natural frequency. In rolls with a steel body, the only effective way to increase the natural frequency is to increase the bending stiffness by increasing the diameter of the roll. Consequently, with a cylindrical shell of constant thickness, the mass of the roll is increased and shell stiffness is reduced.

There are only a few studies dealing with the correlation between roll geometry and variations in paper quality. Normally, the roll is considered as an ideally round component in all circumstances. One exception was a study by Parker (1965) that mentioned roll roundness error as one source of excitation for calender barring problems. A study was made of the barring of newsprint by four-roll calender stacks. He also developed a theory that corrugation of certain wavelengths would grow spontaneously from certain irregularities left after grinding. In addition, a curvature gauge was constructed, which proved that bar-marked rolls were corrugated. Later, roll corrugation was mentioned as a source of excitation in studies by Tervonen (1984) and Nevaranta (1984).

The first study of non-circular machining technology applied to compensate for the effects of structural errors in a roll was published by Kuosmanen (1992). The aim of the study was to optimise the contact pressure in the nip of two cylinders, one of which has varying flexural stiffness. Non-circular turning of the roll reduced nip-pressure changes to one third in comparison with a conventional machined roll. Another important step was the development of the four-point roundness measurement method and apparatus by Kuosmanen and Väänänen (1996). By means of this technology, it became possible for the first time to take effective roundness measurements of paper machine rolls. Later, Pullinen et al. (1997) and Juhanko (1999) applied this technology to a roll dynamic measuring device, which measures the dynamic behaviour of rolls rotating at high speeds. In this study, 3D geometry means the roll geometry at different speeds including roundness, diameter variation, and the movement of the centre axis.

The main objective in coating is to increase the smoothness of paper considerably. Besides this, coating increases gloss, surface strength, and opacity. Coating also decreases ink absorption (Lehtinen 2000). In printing, the smoothness of the gloss is important. This research is focused on improving coating film evenness in the coating process by reducing the errors derived from backing rolls. Thus, paper quality in this research refers to the quality of coated paper. The main quality properties to be measured in coated paper are ash, basis weight (also known as grammage), thickness, and gloss. Ash variation has a good correlation to coating variation because the base paper has a low ash content compared with the coating material.

Rather than SI units, this study uses m/min units to describe running speeds, because this is the normal practice in the pulp and paper industry.

1.2 Research problem

The increased running speeds of coating machines have exacerbated the problems of roll behaviour. At the same time, the paper produced must have a higher and more even quality and the paper machine line better runnability. One of the most sensitive unit processes in paper production is paper coating. In blade coating, the thickness of the coating film on the paper surface is heavily dependent on the run-out of the backing rolls which support the paper web during the process. The run-out tolerance of the backing rolls at running speed has recently been around 50 µm and it should be reduced to 30 µm. The new demands can no longer be met by tightening the roll manufacturing tolerances, which has traditionally been the solution to the problem. The accuracy of traditional manufacturing technology can no longer be increased at reasonable cost. The run-out at running speed is not only created by manufacturing tolerances but there are also problems with bearing accuracy and material homogeneity, especially with cast roll bodies. Variations in material stiffness and heat expansion cause geometrical and rotational errors in the roll.

Machine-direction (MD) variations also cause cross-direction (CD) variation. Fu and Nuyan (2002) proved that the aliasing effect of MD variability is present in CD profiles measured by scanning sensors. Originally, the aliasing problem is not truly a CD problem but the CD controller acting on these false wavelengths introduces actual CD problems.

The problems with new high-speed machines are similar to the old machines whose speed needs to be increased over the original design speed. Roll behaviour under production conditions is no longer satisfactory and major investment is needed to replace the old rolls with new and more accurate ones.

Could it be possible to increase the running speed of a paper machine and at the same time reduce variations in paper quality by using a non-conventional grinding method? This new predictive 3D grinding method should measure roll behaviour in a production environment and consider it in roll grinding. The geometry after non-circular grinding would be far from cylindrical but, in the production environment, the roll would work better than conventionally-machined rolls.

1.3 Aim of the research

The aim of this study is to confirm experimentally that the predictive 3D grinding method improves the roll function under running conditions in the production environment.

In the coating process, better working rolls improve coating film evenness, which affects such paper properties as ash, basis weight, thickness, and gloss. The method will be tested in a real production environment in a paper mill. The specimens are two backing rolls which

are situated in the coating stations of a coating machine on a medium-weight coated (MWC) paper production line.

The improvements in roll behaviour resulting from the use of the new method will be verified by rotational and geometric accuracy measurements at running speed. Finally, the results of the method are verified by paper quality analyses, which are taken before and after this new method is applied.

1.4 Research methods

This work focuses on experimental research and the analysis of calculated and measured quantities. The results of roll measurements are compared with paper analyses in both the time and frequency domains. The calculation of the transfer function between the roll grinding shop and the production environment is based on static and dynamic measurements of the roll. The roll measurement system developed utilises the Fourier transform. The paper analysis is carried out by means of time domain and frequency analyses.

This research applies an experimental approach in order to measure roundness and run-out directly. Another possibility is to model a roll and calculate the dynamic behaviour according to the available information, such as roll thickness and material stiffness. The main problem in modelling is the inaccuracy of the source data, and thus the calculated results cannot reach a useful level of accuracy. The experimental research supplements model development with verification measurements.

1.5 Scope of the research

The effects of thermal expansion are not included in this study because it is not seen as an essential problem in the case of backing rolls. The effects of external loads are not included in the study, either. Resonance vibrations have been studied in other papers and they are not included in this study. The focus in paper analysis is on harmonic MD variations caused by the rolls under study and thus cross-direction CD profiles are not presented in the results of the experimental part. Small-scale variations (formation) in paper are excluded from this study.

1.6 Original features

A new paradigm for roll grinding has been created. This breakthrough study indicates for the first time that the predictive roll grinding method can improve roll behaviour under production conditions. The evenness of the coating film improved remarkably as the method was applied to the backing rolls of the coating stations in the coating machine of a full-scale paper production line. The MD ash variation caused by the backing rolls was reduced by an average of 76%. The gloss variation, which is a very important optical property affecting printing

quality, was reduced in MD by 82% respectively. Thickness variation was also reduced. A more even paper thickness also reduces excitations and therefore improves runnability in calendering, winding, and printing.

The technology developed is cost-effective and can easily be applied to old machines on paper production lines where there is pressure to increase running speeds and paper quality. It has been proved that by means of this technology old rolls will run even better than the new rolls that are available. In new high-speed paper machines this technology provides a new tool to meet the tightening tolerances of rotational and geometric accuracy.

One major advantage of this technology is that in roll manufacturing emphasis can be placed on long-term stability and systematic roll behaviour rather than maximising machining accuracy on the shop floor. Accuracy will be achieved by predictive grinding technology. The technology cannot, however, predict, for example, stress relaxations.

Roll machining accuracy is no longer bound to the accuracy of the machine tool but to the accuracy of the measuring system and the control system. Because of the measuring and control system, the major requirement for the machine tool is now stability, not mechanical accuracy.

The predictive grinding method eliminates the need for dynamic balancing when the run-out is in a reasonable range. Accurate balancing is difficult, especially for rolls with welded ends. Adding mass-balance weight inside a long roll in the middle cross-section is a laborious operation. Dynamic deflection compensation is included in the predictive external grinding geometry. The result is very accurate and can be readjusted at each service grinding if any changes have occurred.

The technology is not limited to the effects of high-speed rotating paper machine rolls; the same method can also be applied to compensate for the uneven thermal expansion or uneven stiffness of the rolls. The technology can also be applied in the steel, plastics, and aluminium industries. The method makes possible the use of rolls in applications which have requirements too high to be met by traditional technology. The economic benefits of this technology are remarkable.

1.7 Author's contribution

The author has developed the technological concept for predictive 3D grinding. The research was carried out under the author's guidance in a paper machines research group, in the Laboratory of Machine Design at Helsinki University of Technology (HUT). The author started the research group in the early '90s and acted at the beginning as project manager and later on as research manager of the group. The author was responsible for the creation and implementation of the research plans in this study. In the experimental research, his contribution was not limited to planning the experimental procedures but he was also, in

some cases, involved with the machining and measurement. The author was also involved in the development of many of the commercial devices used in this study.

2 STATE OF THE ART

Paper machine roll measurement and grinding technology is a narrow branch in the field of manufacturing technology. Roll grinding in larger volumes is carried out in the steel industry, in both hot strip rolling and cold strip rolling. The difference between the rolls used in the steel and paper industries is that in the paper industry rolls are up to 11 metres long and the loads are fairly low. Because of this, the process requirements can be met with rather flexible rolls. Thus, the rolls behave like flexible rotors, i.e. the dynamic behaviour changes as a function of rotational speed. Paper machine rolls are, in most cases, also covered.

There are only a few publications in the area of roll grinding and roll geometry control. Research may have been conducted in companies but the results have not been published. The term 'state of the art' here refers chiefly to the research in paper machine roll technology carried out in the Laboratory of Machine Design at HUT since the early '90s. In addition, similar technologies in other applications are referred to. To get a clear description of the state of the art, the development of roll measurement and machining technology is divided into three generations.

The first-generation technology can measure and compensate for variations in the diameter of the roll in the axial direction. Typically, this error comes from the slideway straightness error of the machine tool. In variations in paper quality, this error can be seen in cross-direction (CD) profiles.

The second-generation technology includes, in addition to the first-generation technology, roundness measurement and compensation technology. By means of this technology, rolls can be machined very accurately to a desired geometry, which is normally cylindrical. All the required measurements are taken in the roll grinding shop.

The third-generation technology not only produces ideal components in the machine shop environment, but also aims to optimise roll function under running conditions on the production line.

Most paper mills have their own roll grinding shops. Roll grinding is a major task in roll maintenance. Traditionally, the target in roll grinding has been to achieve good surface quality and as good a geometry as possible in accordance with the possibilities that exist for measuring roll geometry. The revenue of a typical roll grinding shop is around 2 million euros and there is a tendency to outsource roll grinding in order to save costs. Roll grinding has mainly been seen as a cost, not as a critical production factor.

2.1 First-generation roll machining technology

In the first generation technology, the target is to compensate for slideway errors, which cause systematic diameter variation to the roll in the axial direction. The roll is first machined without a control system and the generated roll diameter variation profile is measured. The compensation machining is carried out according to the measured diameter variation profile.

There are some very novel examples of the implementation of pure mechanical error compensation systems. Figure 2 presents a corrector system for grating transducer systems (McKeown 1989). The same principle of using a correction bar and follower could also be adapted for slideway straightness errors.

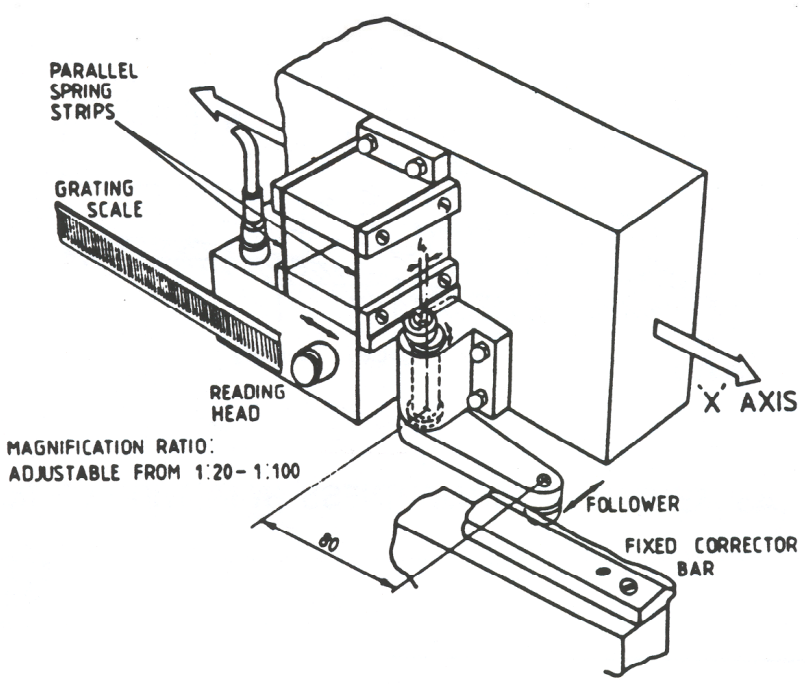

Figure 2 Corrector system for grating transducer systems (McKeown 1989).

Later on, as electronics developed, the compensation was performed by electronic control systems. A common feature of all types of error compensation system is that they provide the revolutionary possibility of machining the workpiece so that it is more accurate than the machine tool itself is. Traditionally, the accuracy of the workpiece was dictated by that of the machine tool.

2.1.1 Factors causing diameter variation in roll machining

The movement of the cutting tool in the sensitive direction of the roll causes, as a function of variations in the Z-axis diameter, a profile which is twice the error of the tool movement in the sensitive direction. The error is caused by the slideway error of the machine tool. Like all rigid

bodies, the carriage of the machine tool has six degrees of freedom, but only one degree of freedom is desirable, i.e. straight movement on the slideway (Figure 3).

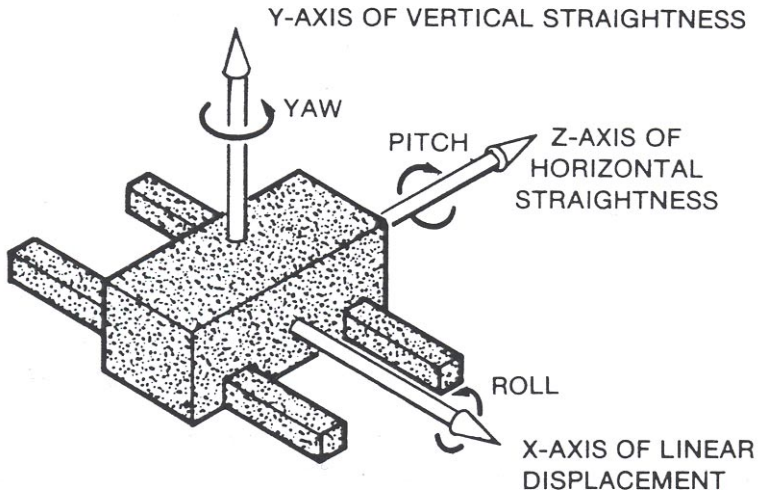

Figure 3 *Six degrees of freedom of a machine carriage (Herreman et al. 1980).*

The five undesirable movements are departure from straightness in the horizontal and vertical directions, yaw, roll, and pitch. In roll grinding and turning, the main error sources affecting the sensitive direction are departure from straightness, roll, and yaw. There are also other important error sources, for example tool wear and thermal deflection. Frank et al. (1999) visualised the thermal effect of ball screws in CNC machines.

The effect of roll and yaw errors on the variations in diameter of the machined roll can be expressed as

$$\Delta D = 2\, d \sin \beta \qquad (1)$$

where ΔD is the diameter change, β is the tilt angle and d is the distance between the tool and the tilt axis.

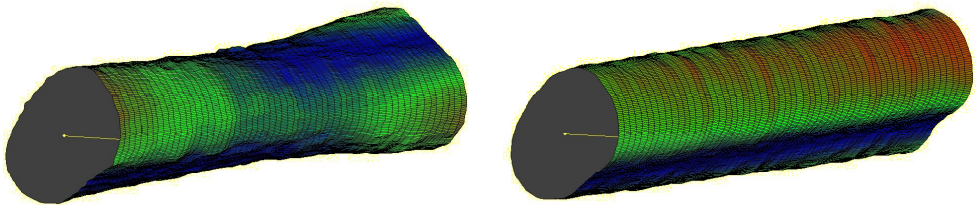

Figure 4 *Two rolls which have nearly the same roundness error, but the error is turned through 90° in the left-hand roll.*

If roundness error is not the same throughout the whole roll length, it may cause diameter variation profile error. This error is illustrated in Figure 4, where the roll was machined twice but, before the second

machining, the conical adapter sleeve was turned through 90°. To be able to measure the same diameter variation profile from the rolls in Figure 4, the left roll should be turned through 90° during measurement.

In practice, the effect of roundness error is avoided by always measuring at the same rotational angle. Of course, this does not remove the roundness error, but the measurements are comparable.

2.1.2 Measurement of roll diameter variation profile

Implementation of a control system for roll machining requires measurement data, according to which the compensation is made. In controlling the CD profiles of a paper machine the CD profile is typically measured by a two-point measuring device where the measuring probes are situated at 180° angles around the roll on the centre line of the measured roll (Figure 5). One of the measuring probes can be replaced by a mechanical contact point if the measuring rig is of the so-called saddle type with free horizontal movement.

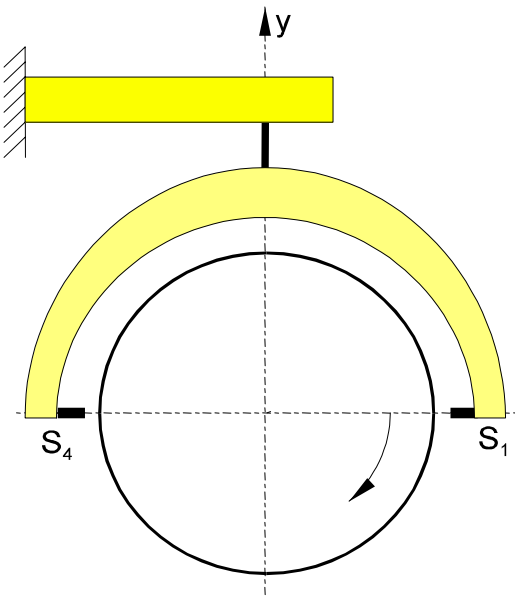

Figure 5 Measuring device for measuring the CD profile of a paper machine roll. S_1 and S_4 are the measuring probes.

2.1.3 Compensation system for roll diameter variation

To compensate for roll diameter variation the roll is first machined without a control system and, after that, the roll diameter variation is measured. The measured data are stored in a control system. The compensation curve is generated from the measured diameter variation profile values by dividing by two. For example, if a 10 µm local diameter expansion is measured after machining without control, the compensation curve will include a 5 µm feed.

If the machine tool is stable as a function of time, the compensation curve can be applied directly to the final machining of a new roll. If

many passes are needed, as in grinding, an intermediate measurement can be taken and the residual error can be taken into account in the compensation curve. This method reduces the machining time and the amount of material removed. The first computer-controlled slideway error compensation systems for roll machining were introduced in the early '90s. A system for compensating for systematic roll diameter variations is illustrated in Figure 6.

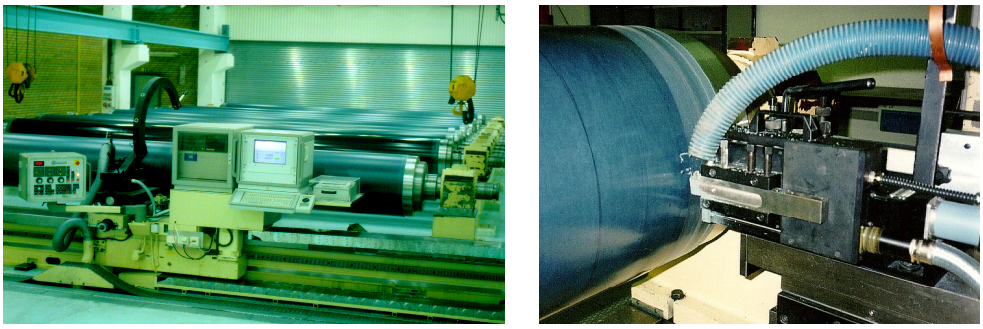

Figure 6 *A system for compensating for systematic roll diameter variations. Measuring frame and the control system with user interface (left) and turning unit for high-precision adjustment of the cutting depth (right).*

Figure 7 illustrates how the control system reduces the variations in diameter of the supercalender fibre roll from 97 µm to 11 µm. In this paper mill, the maximum caliper differences of fibre rolls without error compensation were 90 to 120 µm and, with the control system installed on the lathe, the errors were reduced to 10 to 15 µm.

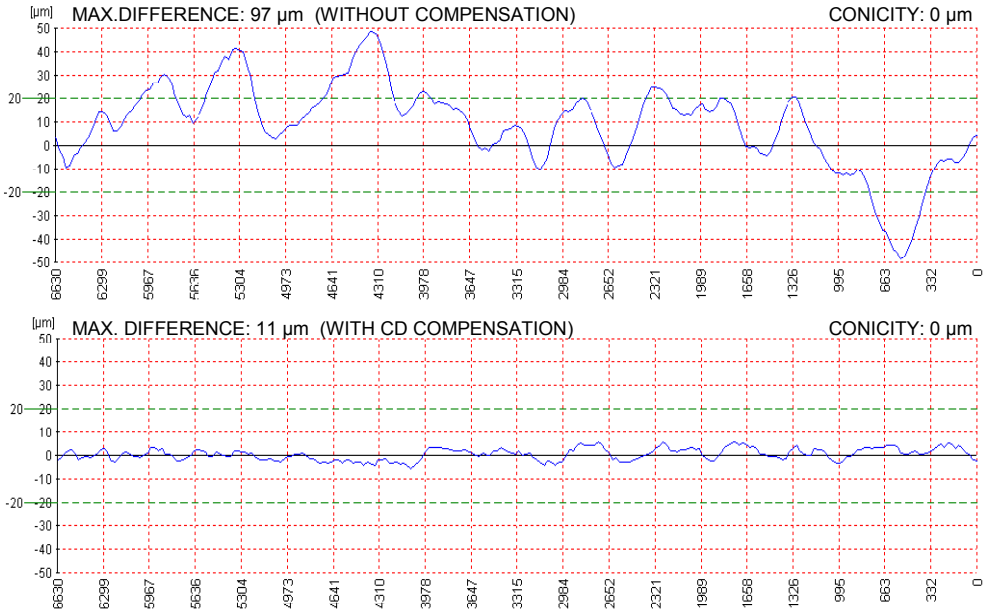

Figure 7 *The upper diameter variation profile is measured in a roll machined without a compensation system. The lower diameter variation profile illustrates the same roll machined using a compensation system.*

The mechanical accuracy of the machine tool is roughly half of the total error (97 µm), because the movement of the tool in the sensitive direction is seen twofold in diameter. It means that in the mill environment the roll is machined, with the compensation system, to a degree of accuracy many times greater than the accuracy of the machine tool itself. The fundamental result of this example is that the accuracy of roll machining is no longer bound to the accuracy of the machine tool but to the accuracy of the measurement system and the control system. Because of the measurement and control systems, the major requirement for the machine tool is now stability, not mechanical accuracy.

2.1.4 Influence of roll diameter variation profile on paper quality

Diameter variations of the rolls normally generate an uneven load in a nip. Those cases where the roll has a deliberate variation in diameter, such as a crown, to compensate for the bending of the roll, are exceptions. It is also possible for rolls to have diameter variation profiles such as mirror image, thus making the load in the nip even. Anyway, in a normal case the variations in diameter of the roll create an uneven load in a nip. The higher the load, the more heat is typically generated. The cover and the body of the roll have a positive thermal expansion coefficient. The diameter of the roll will therefore increase. Thereby we have made a regenerative system, which amplifies the diameter variation error originally generated in machining.

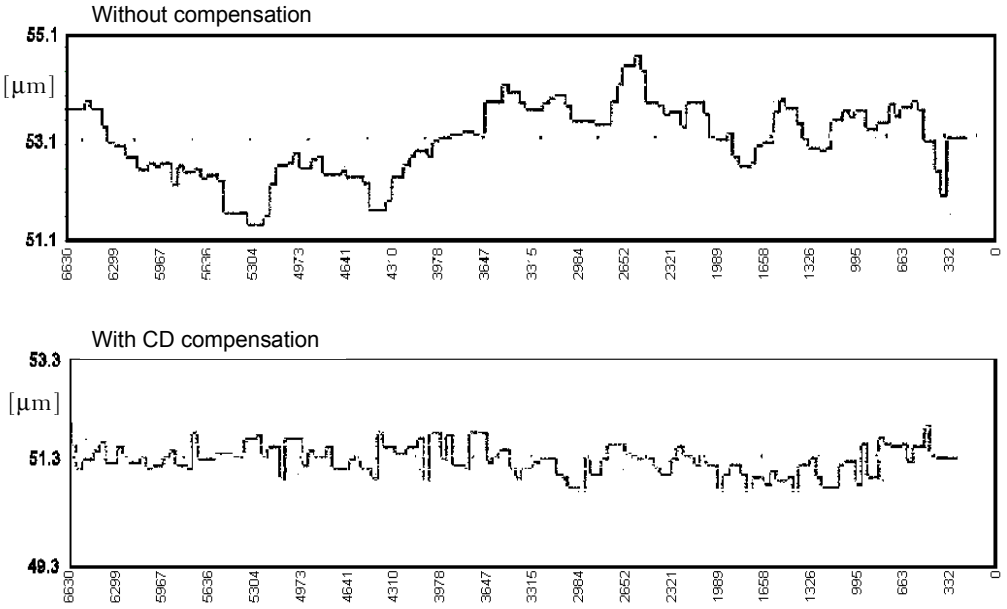

Figure 8 *The effect of variations in fibre roll diameter on the CD caliper profile of supercalendered LWC paper. The diameter variation profiles are according to Figure 7 in all six fibre rolls. The upper CD thickness profile is measured in a paper calendered with fibre rolls machined without a compensation system. In the lower profile, the paper is calendered with compensation control-machined fibre rolls.*

Two different diameter variation profiles of a supercalender fibre roll machined with different methods were illustrated in Figure 7. The effect of roll diameter variation profiles on variations in paper quality was investigated by machining all six fibre rolls of a supercalender, first without any control system, and calendering LWC paper with them. After that, all the fibre rolls were removed from the calender and machined using a control system, and installed back on to the calender. The diameter variation profiles were in accordance with Figure 7 in all six rolls.

The CD thickness profiles of calendered paper shown in Figure 8 are measured by a traversing on-line measuring device. The upper CD thickness profile is measured in a paper calendered with fibre rolls machined without a compensation system. The peak-to-peak value is 3.3 µm. The paper thickness profile is clearly inversely proportional to the diameter variation profile of the fibre rolls. Paper thickness is reduced when nip load is increased (Ehrola et al. 1999).

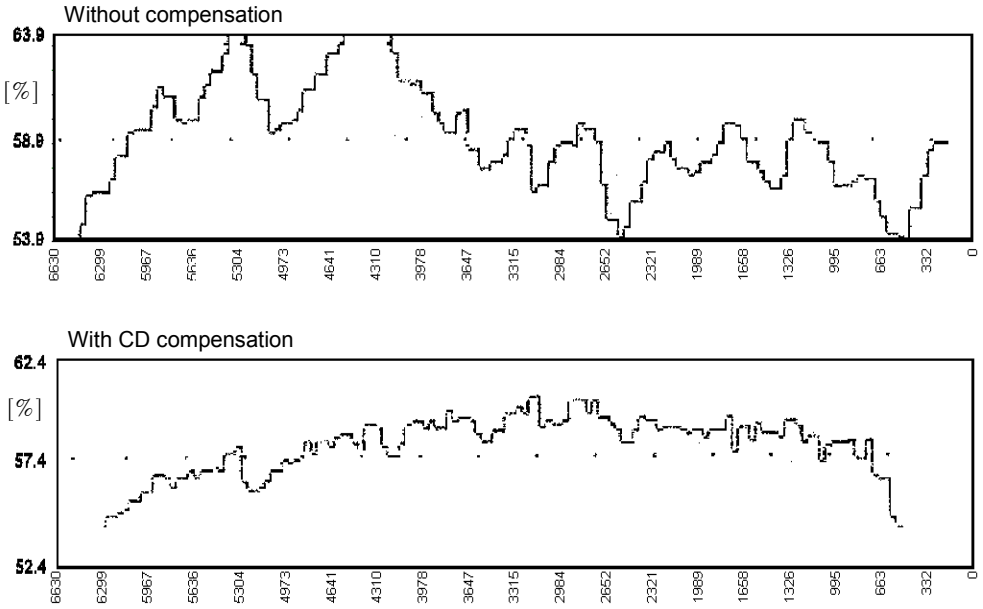

Figure 9 *The effect of variations in fibre roll diameter on the CD gloss profile of supercalendered LWC paper. The diameter variation profiles are according to Figure 7 in all six fibre rolls. The upper CD gloss profile is measured in a paper calendered with fibre rolls machined without a compensation system. In the lower profile, the paper is calendered with compensation control-machined fibre rolls.*

In the lower profile in Figure 8, the paper is calendered with fibre rolls machined with a compensation system. The peak-to-peak value is 1.3 µm. The CD thickness variation is significantly reduced, thanks to the even linear load in the nip. The variation in CD thickness is multiplied in the winding of the customer roll. For example, a roll with a one-metre diameter has about 8500 layers of this paper. The calculated

theoretical diameter variation of the paper roll is 8500·2·0.0033 mm = 28.05 mm. In practice, the paper roll has only little variation in diameter. The effect of variations in paper thickness is mainly seen as variation in the hardness of paper rolls.

The effect of variations in fibre roll diameter on the CD gloss profile of supercalendered LWC paper is illustrated in Figure 9. The upper CD gloss profile is measured on a paper calendered with fibre rolls machined without a compensation system. In the lower profile, the paper is calendered with compensation control-machined fibre rolls. A remarkable difference can be seen between these two gloss profiles. A rule of thumb is that a 5% variation in gloss profile can be seen with the naked eye.

In printing papers, gloss is one of the most important properties of the paper, because it has a direct correlation to the printing quality. The printing quality is most sensitive to variations in paper quality in cases where a large area is printed with a dark colour. Normally, the changes are so smooth that the peak-to-peak gloss variation does not fit on one page. In the case of a double page the difference can be seen particularly clearly, as one page has a different gloss than the other.

2.2 Second-generation roll machining technology

In the second-generation technology, the target is ideal roll geometry after machining. The rolls are manufactured according to manufacturing tolerances which are controlled by measurements taken in the machine shop environment.

The second-generation roll machining technology was developed by the research group to compensate for both variations in roll diameter and roll roundness errors. This makes it possible to machine the whole roll to a precise 3D geometry. The technology was applied first to the turning process of fibre-covered calender rolls (Haikio 1997). After that, the technology was applied to a roll grinding machine, which made it possible to grind different types of rolls to a desired 3D geometry (Kuosmanen 1999).

Few papers have been published in the field of measurement and machining control systems for large rolls because the field is specific and, to some degree, conservative. Until the last ten years, no cheap and sufficiently powerful computers were available. Advanced control technology for compensating for spindle rotational errors (Kim 1983) and, for example, single-point diamond turning (Uda et al. 1996) has been presented. There are also novel applications in manufacturing optical components (Weck 1994). Patzig (2002) presents a non-circular grinding system with an integrated roundness measuring system. In a broader sense, the same kind of technology can be applied in different areas, such as machining pistons for combustion engines (Higuchi et al. 1996 and Schnurr 1998).

2.2.1 Factors causing roundness errors in roll machining

The roundness errors of a roll during the machining process come from the changing distance between the workpiece centre axis and the tool. In machining paper machine rolls, the tool is normally rather steady but the workpiece has a rotational error, which will be copied to roundness error. One of the main causes of rotational errors is the changing flexural stiffness of the flexible rotors. The patent US 5940969 (1999) presents background and useful applications to reduce this harmful effect. Fibre-covered calender rolls used to have two grooves for the driving horn or glue for locking the coating to the roll body. As a consequence of the grooves, the roll exhibited significant variations in its flexural stiffness. This effect caused rotational error in grinding and the result was an oval roundness profile according to the deflection curve. Variations in the flexural stiffness were reduced by milling additional grooves in the roll body (Figure 10). Three or more identical grooves with even circumferential distances produce no variation in the flexural stiffness.

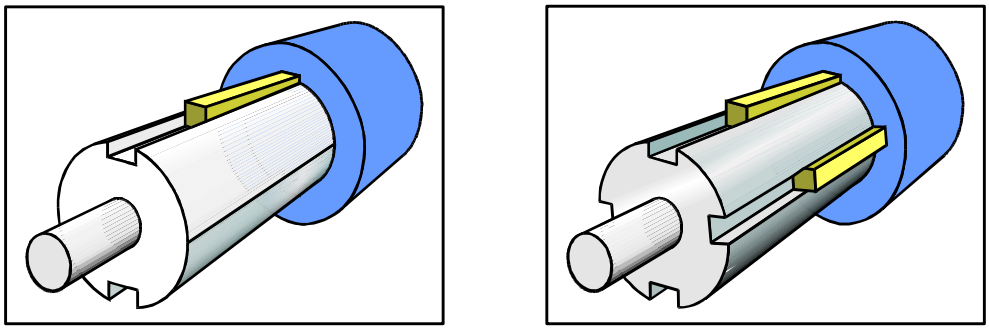

Figure 10 The traditional two grooves for driving horns (left) produce significant variations in the flexural stiffness. The variation can be removed by adding another two grooves.

Another important source of rotational errors is the bearing arrangement. Typically, this type of error derives from the roundness error of the rotating bearing component. In most cases, the inner ring of the bearing is rotating. The roundness of the inner ring is the sum of three components. One source is the roundness error of the shaft. The second source is variation in the thickness of the conical adapter sleeve. The third source is variation in the thickness of the inner ring. The variations in thickness of the inner ring and adapter sleeve are seen as roundness error because they deform by the shaft in tight fit when assembled. Figure 11 illustrates measurements of all these three components. The example is of a backing roll of a coating station. The roundness error of the shaft is 14 µm and the variation in thickness of the adapter sleeve is 10 µm. The inner ring has a variation in thickness of 43 µm. The calculated sum profile of the measurements is plotted in the same picture as the measured roundness profile of the roller race. The calculated sum roundness of 46 µm and measured roller race roundness of 36 µm are rather close to each other and the roundness profiles have a similar form.

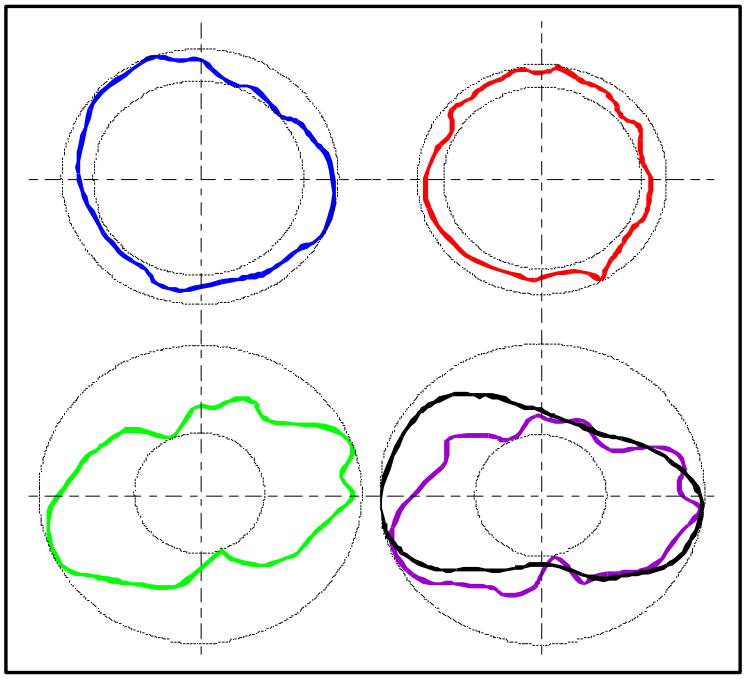

Figure 11 *Measurement of bearing components and the roundness of the roller race. Above left is the measured roundness of the shaft. Above right is the measured variation in thickness of the adapter sleeve. Below left is the variation in thickness of the inner ring. Below right are the calculated (violet) and measured (black) roundness profiles of the roller race.*

The measured movement of the rotational axis during one roll revolution and the achieved roundness profile are presented in Figure 12. In practice, the roundness profile is a copy of the horizontal movement of the roll during the machining process.

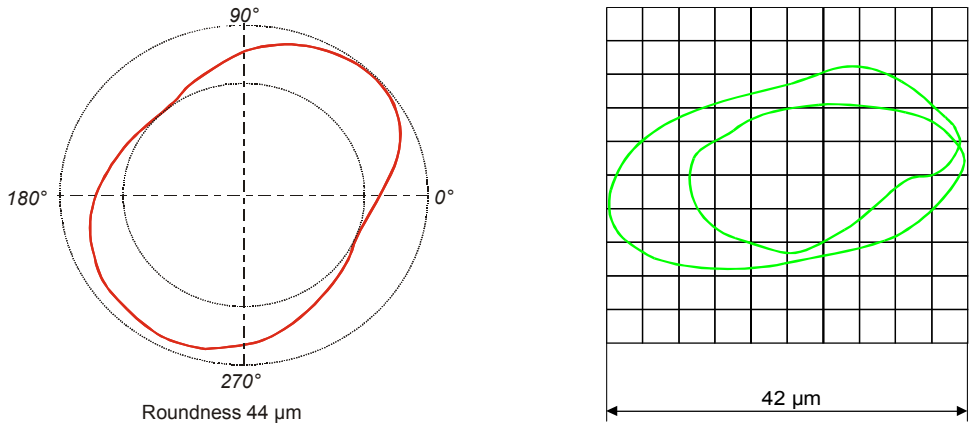

Figure 12 *Roundness profile (left) and movement of the centre point (right) of a roll with rotational error coming from bearings.*

Roundness errors can also derive from workpiece vibrations, which are synchronous with the rotation. Vibrations which are not synchronous

with the rotation of the workpiece reduce the quality of the surface but they do not affect the roundness directly.

2.2.2 Measurement of roundness

Roundness is defined in, for example, the ANSI B 89.3.1 (1972) standard. The roundness profile can give different roundness values, depending on the method applied. A very common method for the definition of roundness is the least squares method (LSC). The centre point of the measured cross-section profile (= weight centre) is calculated by the LSC. Two concentric circles are selected in and outside the profile so that the radial distance is minimum and the centre points are equal to the centre of the cross-section profile. The radial distances from the centre point show the roundness profile. The roundness is the difference between the maximum and minimum of the radial distances.

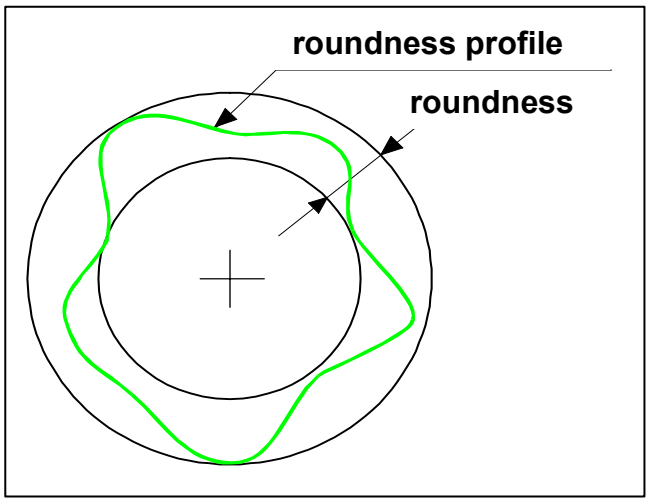

Figure 13 Roundness profile with definition of roundness.

Measuring the roundness and, thus, the cylindricity of a large rotating cylinder has traditionally been difficult because of the movement of the axes of rotation, which can be equated with the spindle error of a standard roundness-measuring machine. To measure roundness, separation of the axes of rotation and the roundness profile is necessary. In measuring the run-out signal, one cannot know if the signal derives from the movement of the object or from the roundness profile. In a standard roundness-measuring machine, the problem is avoided by using a very accurate spindle.

For roll measurement purposes, a measuring device has been developed at HUT, based on the multipoint measurement method. Four sensors are used as a combination of a two-point method and a three-point method. Several attempts to generate this kind of hybrid method had earlier been made by, for example, Barth (1984) and Sonozaki (1989). With this multipoint measurement method, both the roundness profile and movement of the workpiece can be measured simultaneously. In

addition, the measuring probes situated 180 ° from each other make the measurement of variation in diameter accurate.

2.2.3 Compensation system for roll roundness error and diameter variation

The first second-generation grinding control system was put into use at Myllykoski Paper Inc. in 1999. The system was built as part of a research project to perform a full-scale grinding test with paper machine rolls. The roundness error compensation soon became the company standard. In the beginning, the main task for the 3D grinding control technology was grinding the polymer-covered calender rolls to a very round shape with low diameter variation. Figure 14 illustrates the same polymer-covered calender roll ground in the traditional way and with the 3D grinding control technology.

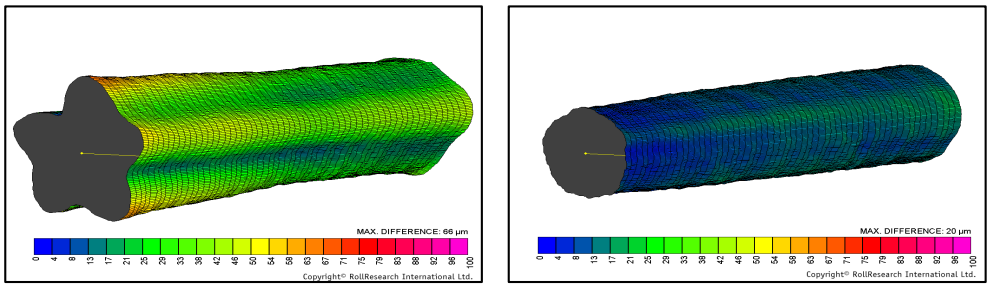

Figure 14 Polymer-covered supercalender roll ground in the traditional way (left) and with the 3D grinding control technology.

Figure 15 Modernised roll grinding machine of Fortek Oy. The machine is situated at the Stora Enso Corp. Oulu Paper Mill. The control system includes 3D grinding control technology. The fully-automatic 3D measuring device is based on the four-point measuring method.

The use of roll roundness error compensation systems has increased rapidly in recent years, especially in the grinding of high-speed and wide paper machines (Figure 15). Väänänen (1993) verified that the sensor angles of 0°, 38°, 67°, and 180° proposed by Kato (1991) give the minimum error propagation rate and are useful in measuring roundness profiles with less than 35 lobes.

2.2.4 Significance of roll roundness errors in papermaking

In addition to a clear correlation with the runnability and vibration level of a paper machine, the roundness errors of the rolls have also proved to have a clear correlation with variations in MD paper quality (Kuosmanen et al. 1998).

Before accurate roll roundness measuring devices, the rolls were considered as round after grinding and variations in the thickness of the paper web were regarded as the main reason for calender barring. Chen and Boos (1975) pointed out the importance of the paper web's longitudinal uniformity of compressibility, moisture, thickness, and basis weight. They considered uneven basis weight to be the main source of excitation.

Roll roundness tolerance is just one number and does not include all the necessary information. In vibration problems, the frequency of excitation is very important. Even very low-amplitude excitation, at or close to the specific frequency of the system, can create a high response. In future, the frequency and amplitude of each component in the roundness profile spectrum should be considered individually according to the requirements of the specific installation. When the roll tolerances are being defined, these should be compared with the tolerances of the paper web.

2.3 Third-generation roll machining technology

The third-generation roll machining technology optimises the roll geometry to the production environment so that the roll has the optimum geometry to carry out its specific process task. It means that we are no longer limited to ideal round and straight shapes during the grinding process. The rolls may be machined to oval and curved shapes or some other desired geometry. Anyway, in the production environment these rolls achieve an ideal geometry and manage the process task better than rolls machined in the traditional way.

2.3.1 Need for production environment-optimised roll geometry

The needs for predictive 3D roll machining can be divided into the following categories:

1. Changes in roll behaviour between the machine shop environment and the production environment.

2. Deviations from the ideal production environment, for example uneven temperature distribution.

3. Needs for profiling in the MD or CD direction.

Changes in geometry between the roll machining shop environment and the production environment are typical of rolls with a large diameter and low wall thickness. The most important factors to take into account are speed, temperature, and load. The roll shell may have variations in thickness as a result of inaccuracies in internal machining, and at a higher speed the uneven mass distribution generates uneven centrifugal force distribution, which causes shell deformation (Figure 17). Moreover, the shell of a cast iron roll in particular may consist of material layers with different module of elasticity and thermal expansion coefficients. In that case even an ideal geometry after grinding would feature shell deformation. The influence of this uneven stiffness distribution can be seen more clearly when the roll is loaded. The uneven distribution of the thermal coefficient of the roll material makes the roll deflect as the temperature changes.

The roll is not always in an environment that provides an even temperature. Normally, the middle of the roll is warmer than the ends of the roll, because of convection. In the case of peripherally bored thermorolls, the temperature distribution may vary considerably in the circumferential direction, too (Figure 16).

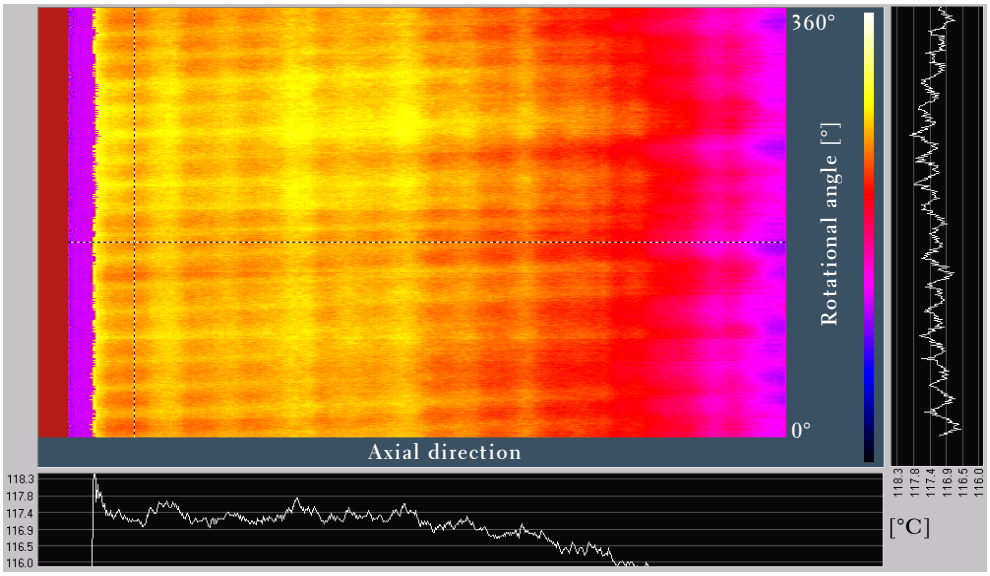

Figure 16 Temperature distribution in the drive end of a soft calender's thermoroll. The curves are from dotted lines.

A roundness and deflection measuring system for high-speed rotating rolls has been built at Helsinki University of Technology. It can measure roll dynamic behaviour as a function of rotational speed. A third-generation grinding control system has also been developed. The system is an alternative and supplementary method for the verification of roll deformations. The rolls are loaded in the process with a radial nip load.

In addition, the internal centrifugal force is radial. The shell deformation can be calculated with the finite element method (FEM) or analytically with a Fourier double series (Girkmann 1963). In practice, the accuracy of the calculations is not adequate, because the raw data needed for the calculations are not accurate enough. For example, it is very difficult to measure the wall thickness of a roll accurately enough.

In this case, third-generation predictive 3D machining is applied to optimise the roll geometry to the production running speed. The system was tested in the laboratory with the backing roll (length 8 m, diameter 1500 mm, and shell thickness 40 mm) of a coating machine. Figure 17 illustrates the deformation of the roll shell as a function of running speed. The deformation at a running speed of 1600 m/min was minimised by third-generation predictive 3D grinding.

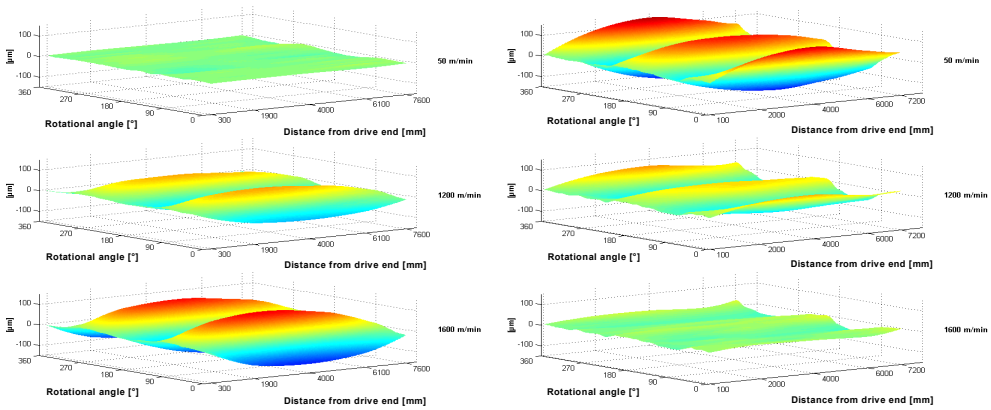

Figure 17 The deformation (µm) of the backing roll shell at running speeds of 50, 1200, and 1600 m/min. On the left, the roll is machined in the traditional way. On the right, the roll is machined using third-generation predictive 3D grinding.

2.3.2 Variations in paper quality in the machine direction

The level of variations in paper quality is the most important feedback information in applying the third-generation roll machining technology. The efforts in studying variations in paper quality are mainly focused on cross-direction (CD) variations but several studies have also considered machine-direction (MD) variations. Cutshall (1990) documented the scale, direction, and sources of variability of fundamental paper properties. He introduces a statistical approach to variation. He also argues that reducing variation makes it possible to reduce the target value, which usually means lower manufacturing costs.

Korpela (1994) presents a case example of MD variations in a coating machine. The paper analysis showed that the problem is in the backing rolls. Since the backing rolls had slightly different (0.006 Hz) rotational frequencies (4.972 vs. 4.966 Hz), a long (over 4000 m) MD sample was needed to separate the variation contributions of each backing roll. The

peak-to-peak basis weight variation fluctuated from 2 - 7 g/m^2 depending on the phase between the rolls.

Jaehn (1985) classified MD variation into four categories:

1. Long-term: longer than 200 s
2. Medium-term: 200 to 1 s
3. Short-term: 1 s to 100 mm
4. Formation: less than 100 mm.

The change from seconds to millimetres is intended to make it easier to visualise the wavelength. For example, 1 second at a running speed of 1100 m/min is equivalent to a wavelength of 18.3 metres. A wavelength of 100 mm is equivalent to a time period of 0.005 seconds. In this study, the wavelength of the backing roll is included in short-term variation, because the circumference of the roll is around 3 metres and the second harmonic is 1.5 metres. At a running speed of 1100 m/min, the times used for one wavelength are 0.16 s and 0.08 s respectively.

Erho et al. (2002) summarise the effects of variations in paper quality on printing. Variations make it more difficult to find the correct print conditions to achieve the correct print density and the correct print colours. This may prolong the start-up time. In addition, the variations may affect the raw material and energy costs. For example, in printing the amount of ink must be adjusted according to the poorest spot in order to meet the quality criteria. In other spots, too much ink is applied to no purpose. The ink must be dried and extra energy is used in most parts of the printing. Excessive drying may lead to quality problems and increase the amount of misprinted paper. Because of variations in strength and tension, the probability of web breaks increases.

The same principles can be applied to coating. Extra energy is used to dry an uneven layer of wet coating material. If drying capacity limits the process, this coating variation may lead to speed reduction. The areas with less coating material will be overdried, which reduces strength properties.

MD variation also affects the cross-direction (CD) profile, because MD variation can confuse the traversing on-line scanners. The CD control system may draw false conclusions and control the CD profile in the wrong direction (Fu and Nuyan 2002).

3 EXPERIMENTS

The aim of experiments is to verify how the predictive 3D grinding method works when applied to the grinding of the backing rolls of a coating machine. The improved roll behaviour at running speed in the production environment should improve the coating film evenness of the coated paper.

The system consists of measuring systems and a grinding system. The roll dynamic measuring system measures roll roundness and rotational accuracy at different rotational speeds. The 3D grinding system controls the grinding process according to the information gained from measurements. A roll measuring device, which measures roll geometry at low speeds with contacting sensors, is installed in the grinding machine.

The specimens were two backing rolls of coating stations. The experiments were carried out at a paper mill, on a medium-weight coated (MWC) paper production line. The paper was analysed before and after the predictive 3D grinding by a paper analyser.

3.1 Measurement of the dynamic 3D geometry and run-out of the rolls

Increasing the running speed of paper machine rolls also requires development of the dynamic behaviour of the rolls. The standard balancing machine does not give adequate information about the dynamic behaviour of the roll because it was developed for balancing only. Balancing machines normally have a run-out measuring sensor, but the measurement system filters away all the information except the first harmonic, which is essential information for balancing. The first harmonic component of the horizontal forces in the supporting units and of one run-out signal do not meet today's requirements.

The roll dynamic measuring device was developed in a research project at HUT to provide information for the development and production of high-speed rolls. Now the measuring device is commercially available and is being further developed under the trade name Hybrid DynaTest (RollResearch 2003).

3.1.1 Equipment

The roll dynamic measuring device consists of four laser sensors, a digital signal processing unit, and a system for rotating the workpiece at different speeds. Matsushita NAIS LM 300 reflective laser sensors measure the position of reflective light intensity maximum. A rotational pulse encoder with 1024 pulses per revolution is used to measure the angular position of the roll. The rotating system can be a traditional balancing machine or a specific arrangement for rotating the roll. In this study, the roll was rotated in a grinding machine with a separate belt drive unit. The surface speed range with paper machine rolls is up to 2500 m/min. The sensors are attached to a C-frame, which is available in

a range of diameters from 200-2000 mm. The C-frame is made of carbon fibre to avoid thermal expansion.

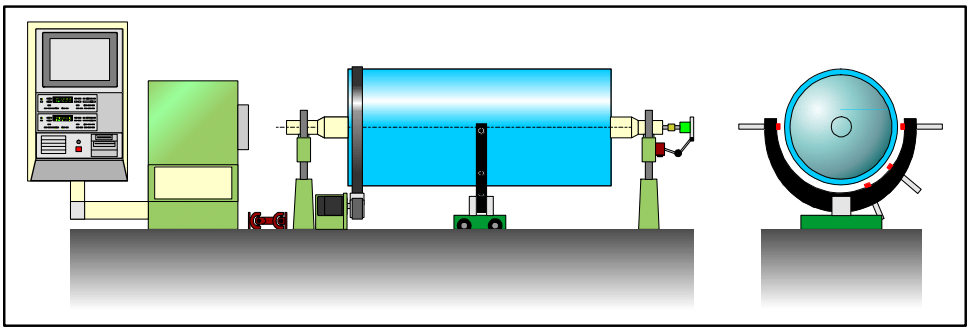

Figure 18 Roll dynamic measuring device.

The measuring device can calculate the run-out spectrum of the roll in any direction, because the run-out is a combination of the known roundness profile and the centre axis movement. The run-out tolerances can be set to the measuring system. The device can also measure resonance vibrations at subcritical speeds. The run-out and resonance vibration measurements are used in the detection of runnability problems. In this study, the run-out measurements of the backing rolls are used to predict the variations in paper quality caused by the rolls.

The measurement of dynamic deflection indicates how the roll behaves at different speeds. The dynamic deflection can be compensated for by balancing the flexible rotor in several planes according to advice given in the ISO 11342 (1994) standard. 3-plane balancing with counterweights is simple and the most common method. To minimise balancing masses inside the roll, the axis of rotation and the centre axis of mass should be adjusted coaxially. This adjustment can be performed from the chucks according to roll dynamic measurements. The third method of balancing is the removal of material from the outer surface. In this research, deflection compensation is carried out by 3D grinding. This technology can be applied to both roll manufacturing and servicing.

The roll dynamic measuring device gives information about roll roundness at different rotational speeds. Changes in roundness profile are typical of high-speed rolls with a large diameter. There are several ways to use the information gained from measurements to reduce the dynamic deformation of the roundness profile. One is to reduce the variations in thickness by internal machining. Another is adding mass to compensate for an uneven mass distribution. The third method is to increase the circumferential stiffness by adding sleeves inside the roll. In this study, the geometry compensation is performed by 3D grinding. There is a data transfer interface between the roll dynamic measuring device and the 3D grinding system.

The rotational error motion of a bearing is one of the biggest sources of inaccuracies in high-precision rolls. The bearing excitations and

geometric errors of roller path and shaft error motion can be detected by the measuring device. Because of the importance of bearing assembly accuracy, the rolls should always be measured, and even balanced, with the bearings assembled.

3.1.2 Method

The measuring method is based on the four-point measuring method. The algorithm is the same as is used in the roll measuring device with contacting sensors introduced by Kuosmanen and Väänänen (1996).

3.1.3 Accuracy of the measuring system

The traceability and accuracy of the measuring system were verified with a reference disc, which was measured by a Taylor-Hobson K510-21 roundness measuring device at the Centre for Metrology and Accreditation in Finland. In the reference measurement, both the roundness and the undulation components of the roundness profile were verified. The diameter of the disc is 250 mm, ground with a geometry consisting of undulations from two to nine per revolution. The disc is black nitrated and the surface roughness Ra is 1.4 µm. The uncertainty of the reference roundness measurement is ±0.2 µm at a 95% level of confidence.

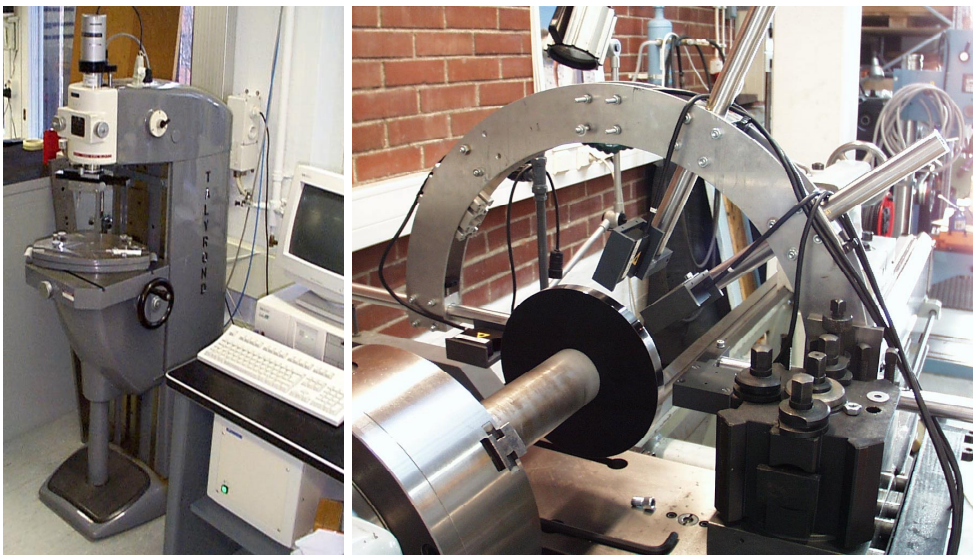

Figure 19 Taylor-Hobson K510-21 roundness measuring device at the Centre for Metrology and Accreditation in Finland (left) and the setup of the roll dynamic measuring device for disc measurement in the laboratory (right).

With the roll dynamic measuring device, the reference disc was measured in the laboratory at different rotational speeds. The measured values were compared to the measurement results of the Taylor-Hobson K510-21 roundness measuring device. In the laboratory measurement setup, the disc was attached to the shaft. The shaft was centred to the chuck of a lathe with an accuracy of 0.01 mm. The sensors were

assembled on to the measuring frame, which was attached to the tool holder with an accuracy of ±0.5 mm in respect to the centre of the reference disc. The laser sensors were assembled to follow the same track with an accuracy of ±0.5 mm. The accuracy of the sensor angles was ±1°. The measurement was repeated ten times at each rotating speed of 0.2, 1.6, 6.3, and 9 Hz. Each measurement is the value of synchronised time averaging during a hundred rotations. The low-pass filter was adjusted to twenty undulations per revolution. (Pullinen 2001.)

Results

The roundness of the reference disc measured by the Taylor-Hobson measuring device was 107.0 ±0.2 µm. Taylor-Hobson measures at low speed with a contacting sensor. With a roll dynamic measuring system, the disc is measured at different speeds. The assumption is that the roundness of the disc does not change over the speed range applied. Figure 20 illustrates the reference disc roundness profile measured by the roll dynamic measuring device at the lowest speed, 0.2 Hz. The roundness profile measured by Taylor-Hobson is illustrated in the same figure.

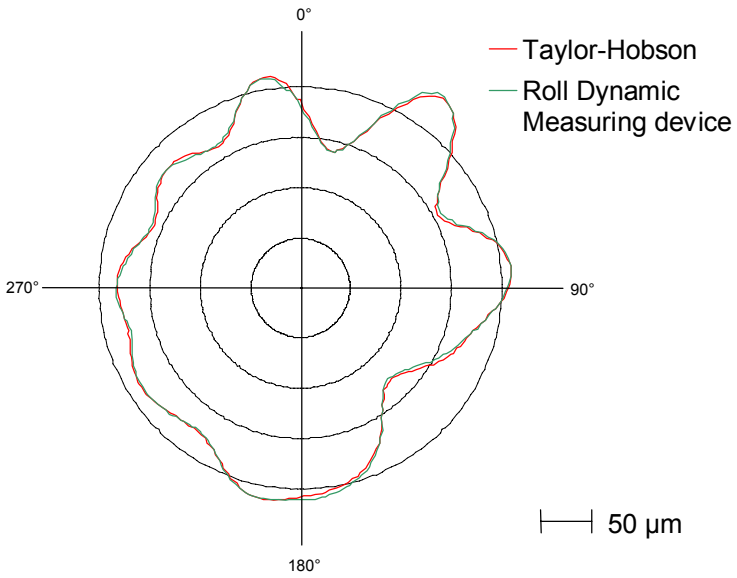

Figure 20 Roundness profile of the reference disc measured with the Taylor-Hobson roundness measurement device (red profile) and with a roll dynamic measuring device at an 0.2 Hz rotating speed (green profile).

The roundness measured by the roll dynamic measuring device at an 0.2 Hz rotating speed was 110.2 µm. The deviation of the roundness value from the reference measurement was 3.2 µm. At other speeds, the deviation was smaller (Table 1).

Table 1 *Roundness values of the reference disc measured with the roll dynamic measuring device at different speeds.*

Rotating speed (Hz)	*Roundness (μm)*
0.2	*110.2*
1.6	*106.9*
6.3	*105.7*
9	*109.9*

The roundness profile can be divided into undulations, which are amplitude terms of the Fourier series of the roundness profile. Table 2 presents the amplitudes of different undulations measured by the roll dynamic measuring device at different speeds. The results from the reference measurement are also included in the table.

Table 2 *Amplitude of the roundness profile components of the reference disc at different rotating speeds.*

Lobes	*Reference (μm)*	*Roll dynamic measuring system (μm)*			
		0.2 Hz	*1.6 Hz*	*6.3 Hz*	*9 Hz*
2	*14.7*	*15.1*	*15.0*	*15.0*	*15.2*
3	*11.4*	*12.6*	*12.2*	*12.0*	*12.7*
4	*10.8*	*11.1*	*10.9*	*10.9*	*11.2*
5	*11.4*	*11.7*	*11.5*	*11.5*	*11.4*
6	*10.7*	*11.1*	*10.8*	*10.5*	*11.0*
7	*11.1*	*11.0*	*10.8*	*10.8*	*11.0*
8	*10.4*	*10.2*	*10.0*	*9.9*	*10.1*
9	*11.5*	*10.8*	*10.1*	*9.8*	*10.9*
10	*0.8*	*0.8*	*0.6*	*0.6*	*0.8*
11	*0.9*	*0.8*	*1.1*	*1.1*	*0.2*
12	*0.5*	*0.2*	*0.3*	*0.3*	*0.4*
13	*0.3*	*0.2*	*0.7*	*0.8*	*0.3*
14	*0.4*	*0.3*	*0.4*	*0.5*	*0.2*
15	*0.1*	*0.6*	*0.6*	*0.5*	*0.6*
16	*0.3*	*0.6*	*0.7*	*0.7*	*0.5*
17	*0.5*	*0.8*	*0.7*	*0.6*	*0.7*
18	*0.2*	*0.2*	*0.1*	*0.2*	*0.2*
19	*0.2*	*0.2*	*0.3*	*0.2*	*0.3*

The biggest difference between the measured and reference values is 1.7 µm in nine undulations per revolution at a 6.3 Hz rotating speed. Nine undulations per revolution also showed high deviation at other speeds, as did three undulations per revolution (Figure 21).

In addition to the dynamic deflection, two and three undulations per revolution are the main roundness errors of the experimental rolls at running speed. Therefore, the higher frequencies are negligible in the case of backing roll measurement. The dynamic roll measurement aims not to measure the absolute roundness but the changes in roundness profile as a function of speed.

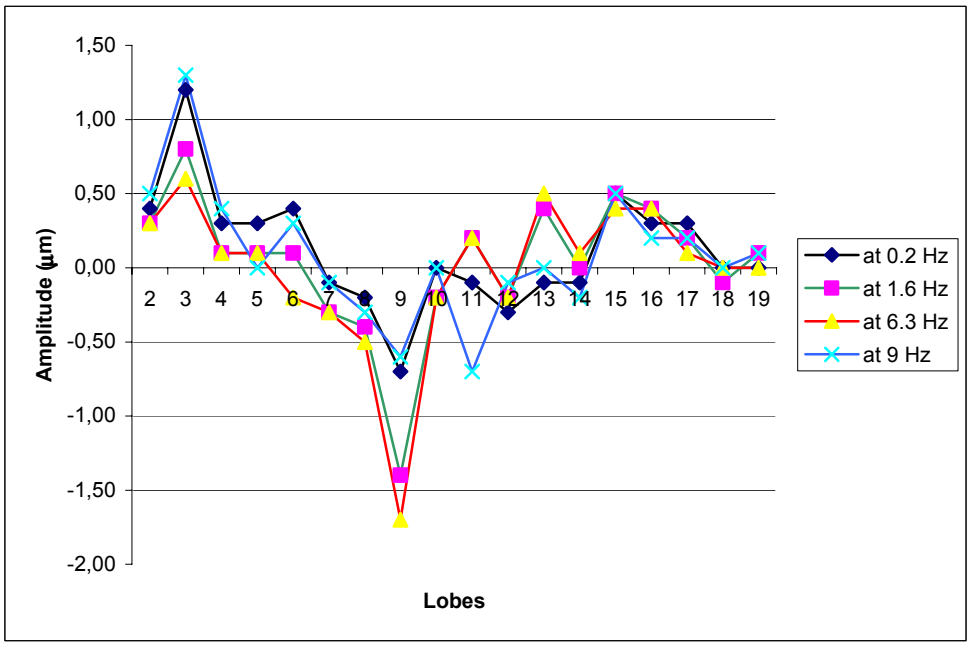

Figure 21 Deviation of the measured undulation component amplitudes from the reference values.

The uncertainty of the measurement

There are several methods that can be used to calculate the roundness value. In this research, the roundness is calculated with the least square method (LSC) (Whitehouse 1994). In addition, the signals measured with the Taylor-Hobson K510-21 reference measuring machine are calculated with the same method so as to make the results comparable. The roundness value is dependent on the ability to find the centre point of the profile. Regardless, the calculation methods do not change the roundness profile.

Systematic errors in calibration measuring are:

- True sensor angles deviate from those used in the calculation algorithm

- Inaccuracy of the roundness profile calculation algorithm

- Adjustment of the measuring frame in respect to the centre of the reference disc

- Movement of the measuring frame during measurement

- Each measurement sensor follows different paths

- Variation in the surface quality of the reference disc – surface roughness influences optical properties

Systematic errors are involved in estimating the uncertainty of the measurement. The estimation is based on statistical methods. The estimate of the measurement result is obtained from the arithmetical mean of independent determinations. The expanded uncertainty is obtained by multiplying the combined standard uncertainty by a coverage factor, which has a value of two at a 95% level of confidence (International Organisation for Standardization 1993). The overall uncertainty of the measurement is ±3.5 µm.

3.2 Roll grinding system

The grinding system is based on a standard WST II b 60·10000 roll-grinding machine manufactured by Waldrich Siegen in 1978. The grinding machine is designed for rolls with a maximum length of 10 metres and weight of 60 tons. The machine was upgraded to a 3D grinding machine by replacing the measuring device with a four-point roundness measurement device and upgrading the control system to a 3D grinding control system with the trade name Hybrid GrindControl 3D. The main mechanical changes in the upgrade were in the measurement rig, which was replaced by a carbon fibre rig with places for four measuring sensors. The traditional mechanical camber control grinding carriage was replaced by a precision positioning unit. The precision positioning unit attends to the crown and high feed precision in noncircular grinding.

Figure 22 Four-point measuring device (left) and high-precision positioning unit (right) installed in an old roll grinding machine.

The 3D grinding system controls the grinding process according to the information provided by measurements. A roll measuring device is installed in the grinding machine, as in Figure 22, which measures roll geometry at low speeds with contacting sensors. The roll dynamic measuring system measures roll roundness and rotational accuracy at different rotational speeds.

The grinding process with a control system differs from the manual grinding machine. If the roughing is started without measurement of the roll, an old basic curve may be used for bed error compensation. Alternatively, grinding can be started with constant current grinding, which provides a constant material removal rate without major changes in geometry. Naturally, roughing can also be done fully manually.

Either current or position grinding is used in finishing. Current grinding is mainly used for hard rolls and position grinding for rolls covered with soft material. The compensation curve is achieved through roll measurement. There are also functions for the superfinishing and grinding of the roll's chamfers and conical axes. There are also sharpening functions for straight wheels, crowned wheels, and conical wheels for grinding cones. The roll measurements are carried out with the four-point measuring device.

3.2.1 Grinding control system

The grinding control system is based on a standard NC controller and a separate NC unit for 3D grinding (Figure 23). The measuring device, encoders, motors, and operator's panel are interconnected via Ethernet TCP/IP (transmission control protocol/Internet protocol) or Profibus.

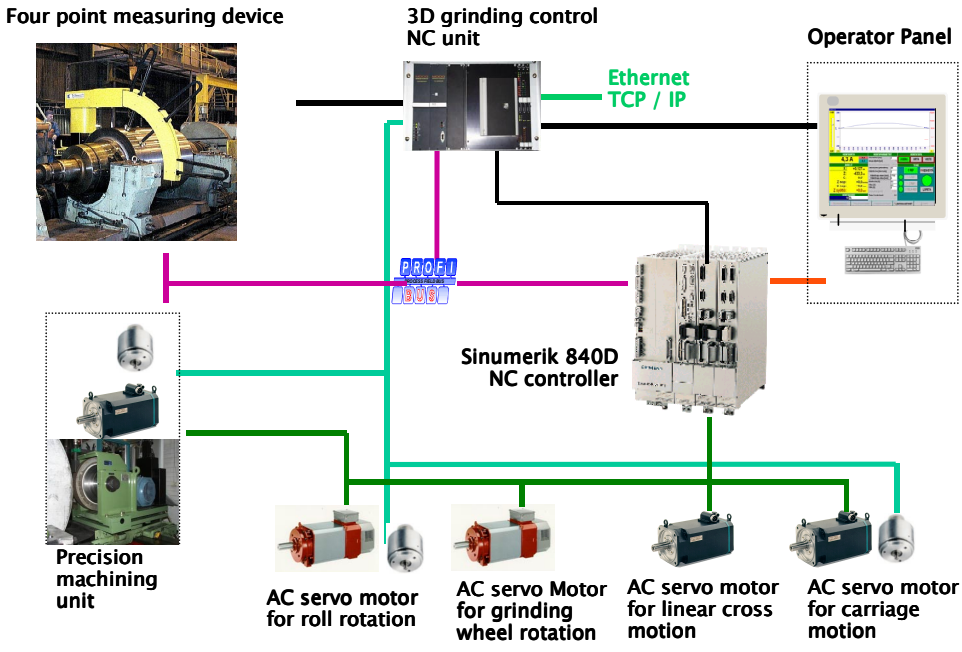

Figure 23 The basic 3D grinding control system arrangement.

The control system has many features to help the operator. For example, the program suggests how many grinding passes are needed and the user may change the number of passes while grinding. There is an automatic infeed at the roll ends [µm] and continuous infeed [µm/min] for compensating for grinding stone wear, as well as programmable turn-around points. Grinding with pitch can be selected either as relative to rotation [mm/r] or as a constant speed [mm/min]. Beside the roll's rotation speed, feed and carriage speed can also be adjusted during the grinding.

At the start, the grinding stone approaches and contacts the roll automatically. Interval wobble of roll speed reduces chatter vibrations with flexible rolls. There is an electrical handwheel for the manual control of the U-, X-, and Z-axes.

3.2.2 Accuracy of the grinding system

The accuracy of the grinding process is heavily dependent on the accuracy of the control system, which gets the feedback from the information gained through the measurements. The manufacturer of the grinding control system has announced accuracy values both for soft and hard rolls (Table 3).

Table 3. Accuracy of grinding control system

	CD compensation (caliper variation)	*MD compensation (roundness profile):*
Hard rolls	± 2.5 µm	± 2 µm
Soft rolls	± 5 µm	± 5 µm

There are prerequisites for the proper grinding conditions to achieve grinding accuracy. The most important one is that the environment and coolant temperature is 20 ±0.5°C and there is no direct sunlight or great temperature differences. Before grinding, the temperature of the roll and grinding machine must be stabilised. For example, no coolant should be put on the roll surface when the grinding process is not under way. The surface roughness of the roll should be Ra 3.2 or better. During the roll measurement, the roll must be clean and no grinding dust or liquid are allowed on the roll surface. The speed of the roll and carriages must be even and systematic. The grinding wheel must be well balanced.

3.3 Paper analyzer

The Tapio Analyzator, manufactured by Tapio Technologies Inc. is used for paper analysis. In this research, the analyser was used to measure basis weight, thickness, gloss, and ash. The Tapio Analyzator is a laboratory device which can measure both MD and CD paper samples.

Hilden and Perento (2000) presented a summary of the functions and sensors currently available. Basis weight was measured with an aperture 5 mm in diameter. The source of radiation is Promethium PM-147. The gloss was measured on both sides with a 4 mm · 4 mm aperture. A 5 mm aperture size and an iron source (Fe 55) which is semiconductor-based were used in ash measurement. The thickness was measured by measuring heads with a 0.3 mm diameter contact area located on both sides of the web. The measuring heads are provided with detectors employed to measure the distances of the measuring heads from the respective surfaces of the web (Makkonen 1988).

The Tapio Analyzator includes a paper feed mechanism, sensors, and measuring and control electronics. The sensors are synchronised to measure the same position even if the sensors are situated sequentially. The Tapio Analyzator can handle paper rolls with a maximum diameter of 700 mm and a maximum width of 250 mm. The measuring speed is 2.4 - 120 m/min (Figure 24).). The analysing software includes a frequency spectrum, time signal, CD spectrum, variance component analysis, correlation, and analysis for separating original signals (Perento 1999).

Figure 24 Tapio Analyzator for the time domain and frequency analysis of paper samples (Tapio Analyzator 2003).

The Tapio Analyzator can perform analyses both in the time and frequency domains. In MD analyses, the sample lengths have to be in the range of 3000 - 5000 m for high-frequency resolution. High resolution is needed to separate the effects of rolls which have very small differences in rotational frequency, i.e. the rolls have nearly the same diameter.

Ghosh et al. (2001) showed in case studies how the Tapio Analyzator can be used in improving variability in paper properties. Regular audits

of paper uniformity using off-line measurements offer a tool for the optimisation of the paper machine, coater, and supercalender.

Erho et al. (2002) used the Tapio Analyzator to verify correlations between different measurements of the coated paper and the print. The measurements were paper and print gloss, basis weight, ash content, and printability index values.

The manufacturer of the Tapio Analyzator has verified the accuracy of the instrument. The manufacturer guarantees the repeatability of the measurements in test procedures, where an 8 m long cross-direction test paper sample is measured ten times. The standard deviations in measurements are given in Table 4.

Table 4 Standard deviation of the Tapio Analyzator measurements.

Measurement	*Standard deviation*
Basis weight [g/m^2]	< 0.12
Ash [g/m^2]	< 0.12
Gloss [%]	< 0.5
Thickness [µm]	< 0.2

3.4 Coating machine

The coating machine is situated in a paper mill owned by Myllykoski Paper Inc. The width of the trim is 5420 mm and the annual production is 160,000 tons of medium-weight coated (MWC) printing paper. The production line started working in 1984.

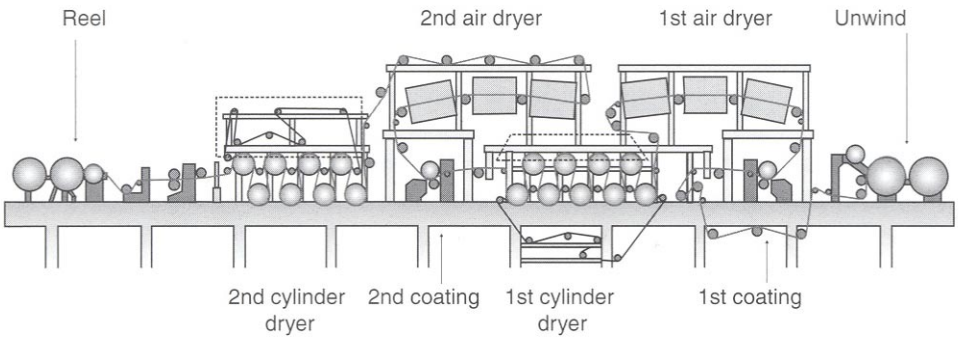

Figure 25 Layout of the coating machine used for coating tests (Lehtinen 2000).

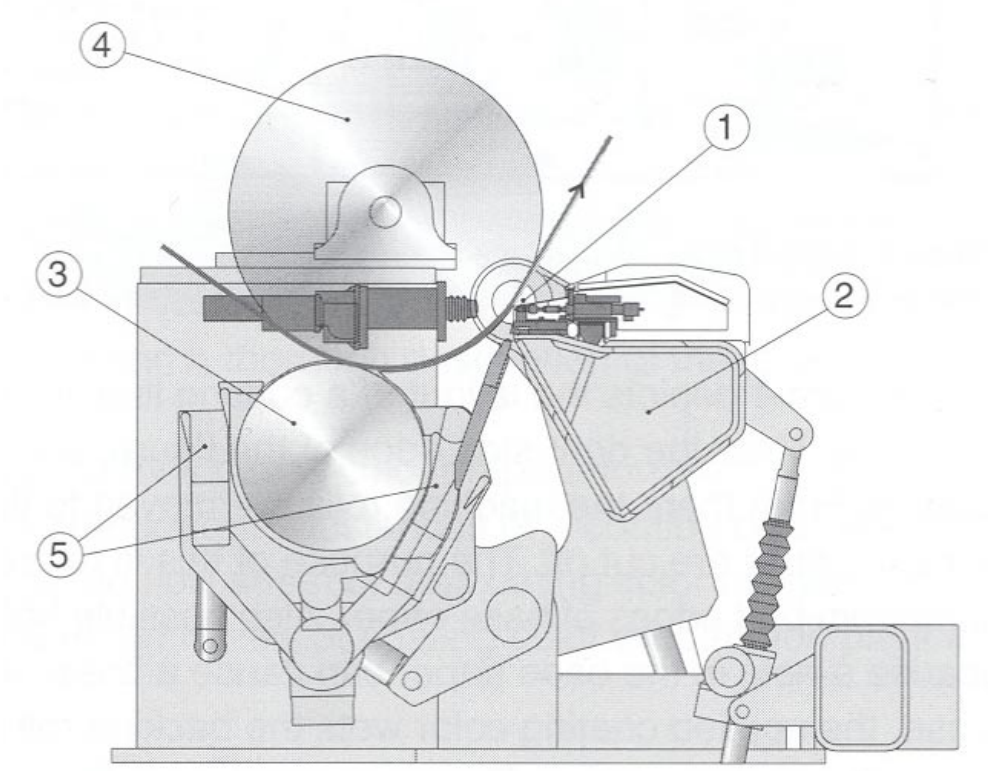

Figure 26 A blade coating station of the coating machine: (1) metering blade, (2) support beam of the blade, (3) applicator roll, (4) backing roll, and (5) collectors of colour overflow from applicator and back circulation from blade (Lehtinen 2000).

3.5 Backing rolls

The specimens were backing rolls of the coating machine (Figure 27). The roll bodies were of a welded steel structure. The nominal diameter of the rolls was 965 mm and the mass 5410 kg.

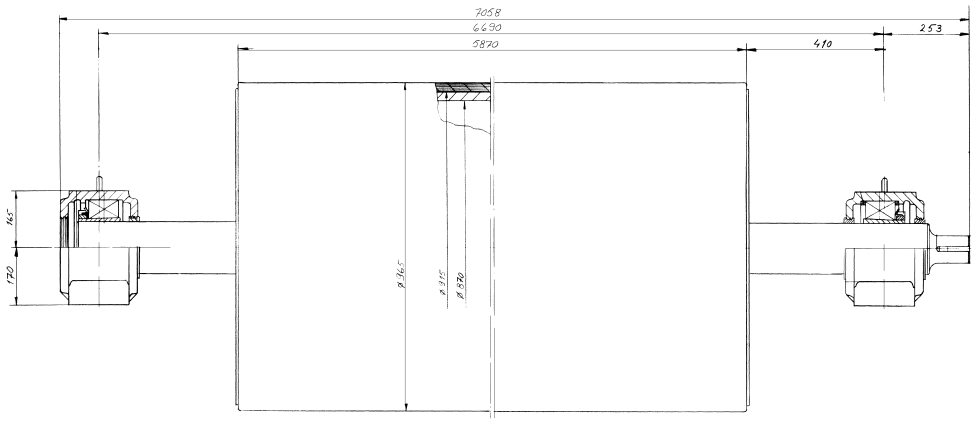

Figure 27 Backing roll of a coating station.

The rolls are covered with rubber with an initial thickness of 25 mm, which is reduced by regrinding. The rolls are provided with SKF 23134

CK/W33+ H3134 roller bearings. The bearings and bearing housings are not removed during grinding or dynamic measurements. The universal shaft is attached to the drive end of the roll.

3.6 Experimental procedure

The following procedure was applied.

1. An MD paper sample is taken from the middle of the calendered paper web.

2. The paper sample is analysed with the Tapio Analyzator.

3. The backing rolls are removed from the coating machine.

4. The measurements of the dynamic behavior of the backing rolls are carried out in the roll dynamic measuring device at speeds of 50 and 1120 m/m (production speed) in nine cross-sections.

5. The roundness and deflection changes are analysed as a function of the rotational speed of the roll.

6. The control curve for the 3D machining system is calculated to optimise the roll roundness and deflection at a running speed of 1120 m/min.

7. The rolls are ground with the calculated compensation curve.

8. The dynamic behaviour of the backing rolls is measured after 3D grinding.

9. If residual geometry error over the allowed tolerance exists, the correction curve to compensate for residual error is calculated.

10. The correction curve to compensate for residual error is added to the original correction curve. Stages 7-8 are repeated until the grinding is ready.

11. The rolls are mounted in the same positions where they were when the paper analysed was taken.

12. The MD paper sample is taken under equivalent conditions to those in Stage 1.

13. The paper is analysed with the Tapio Analyzator as in Stage 2.

4 RESULTS

4.1 Influence of predictive 3D grinding on roll roundness

The roundness profiles of the backing rolls were measured after traditional grinding and after predictive grinding. The measurements were carried out with a roll dynamic measuring device at speeds between 50 and 1120 m/min in nine cross-sections. A 3D contour was generated through the roundness profiles.

4.1.1 Roundness of the backing roll of the first coating station

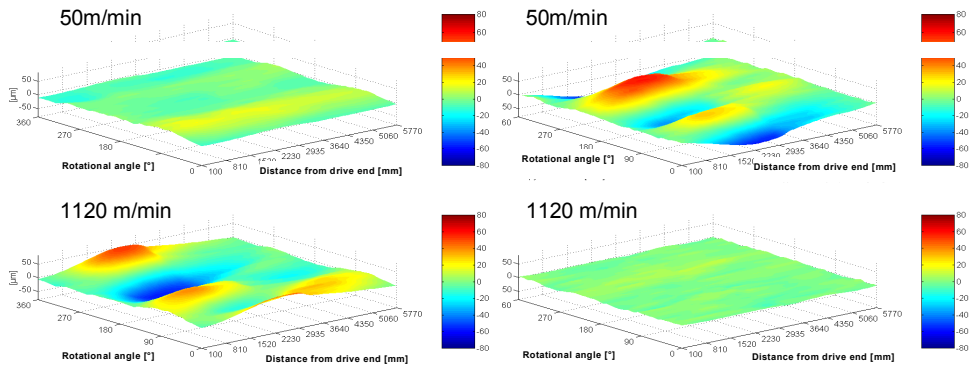

Figure 28 3D geometry of the backing roll of the first coating station at a low running speed of 50 m/min and at the production speed of 1120 m/min. The roll is ground without a control system (left) and with predictive 3D grinding (right).

Traditional grinding gives rather good roundness at low speed. Rolls have a roundness error of less than 10 µm, alternating smoothly between the ends. When the running speed is increased to 1120 m/min, the roundness profiles change, as shown below left in Figure 28. This shell deformation turns out to be highly asymmetrical. The maximum roundness error of 76 µm is closer to the drive end.

Above right in Figure 28 is the same roll machined with predictive 3D grinding. The roll roundness error is rather high at low speed but at production speed the roundness is improved to the level of high-precision rolls. Predictive 3D grinding reduces the maximum roundness at a running speed of 1120 m/m to 13 µm (Figure 30). Before predictive 3D grinding, the out-of-roundness is 41 µm in the cross-section 810 mm from the drive end. At the same distance from the open end, the roundness is smaller (25 µm). After predictive 3D grinding the out-of-roundness figures are 11 µm and 8 µm respectively.

Figure 29 illustrates the roundness profiles in three cross-sections. Ovality (54 µm) is the dominating out-of-roundness component in the

middle cross-section before predictive 3D grinding. Predictive 3D grinding reduced the ovality to 9 µm.

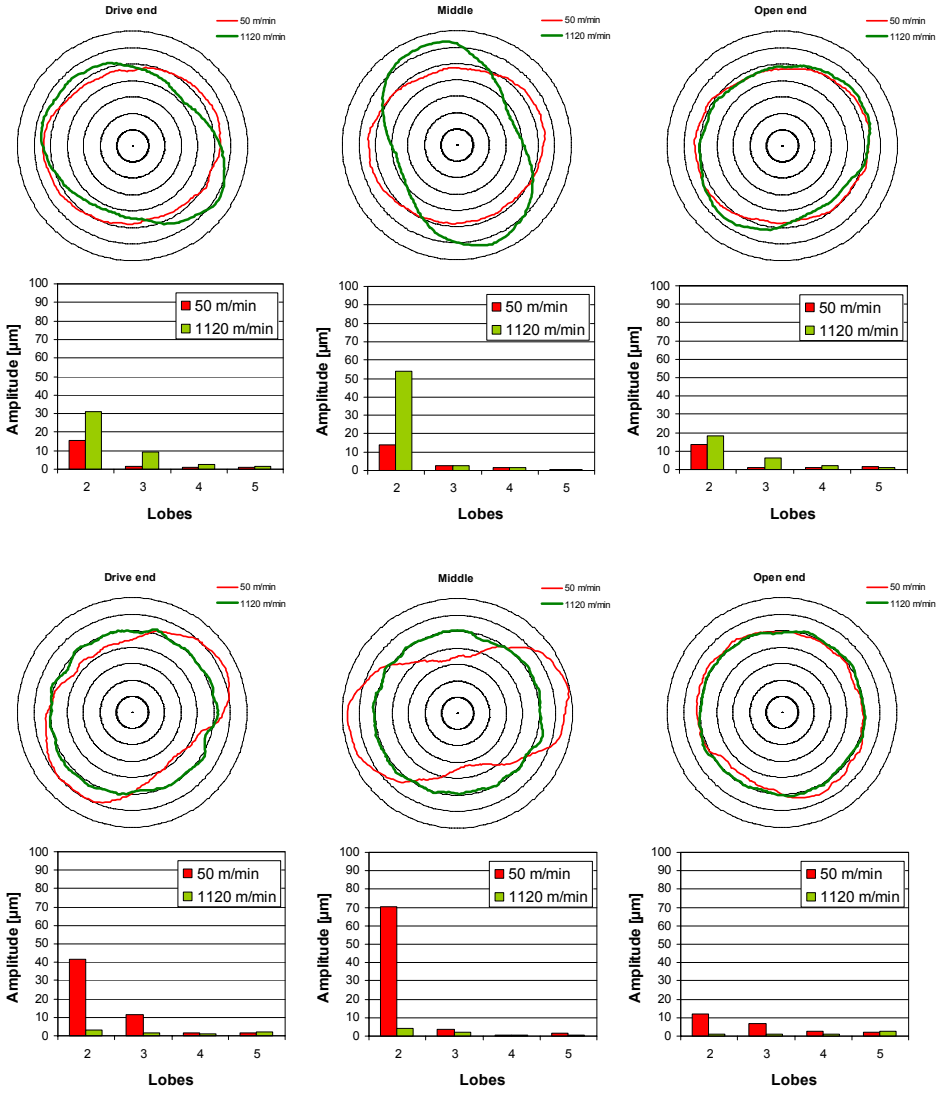

Figure 29 *Roundness profiles of the backing roll of the first coating station ground without a control system (above) and after predictive 3D grinding (below) 810 mm from both ends and the middle. Roundness profiles are illustrated at a low running speed of 50 m/min (red) and at the production speed of 1120 m/min (green). The grid is 20 µm. The distribution of lobes is presented below each roundness profile.*

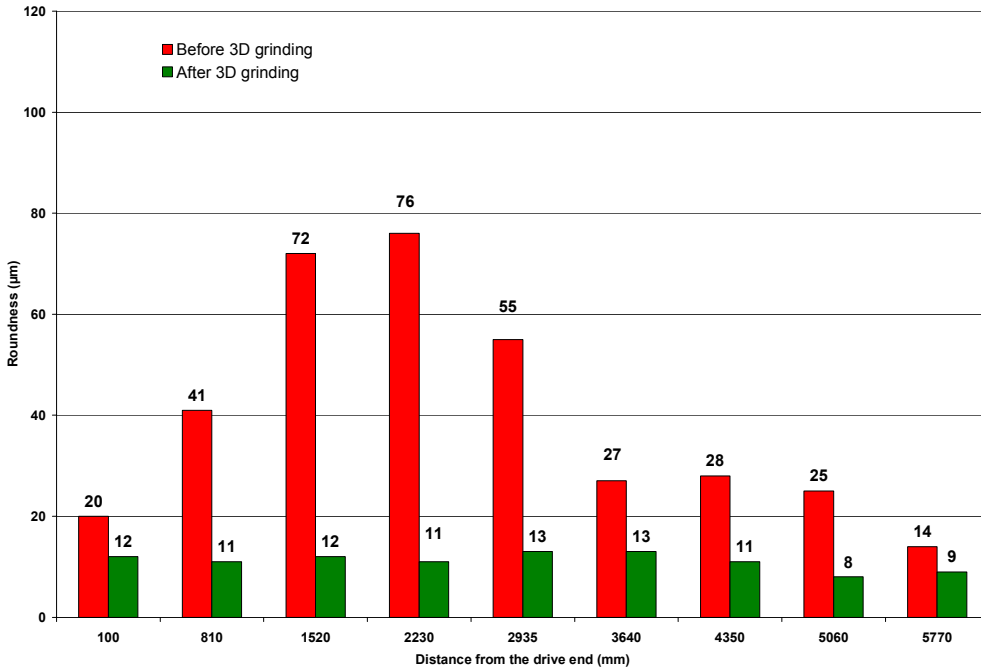

Figure 30 *Roundness of the backing roll of the first coating station at the production speed of 1120 m/min ground without a control system (red bars) and after predictive 3D grinding (green bars).*

4.1.2 Roundness of the backing roll of the second coating station

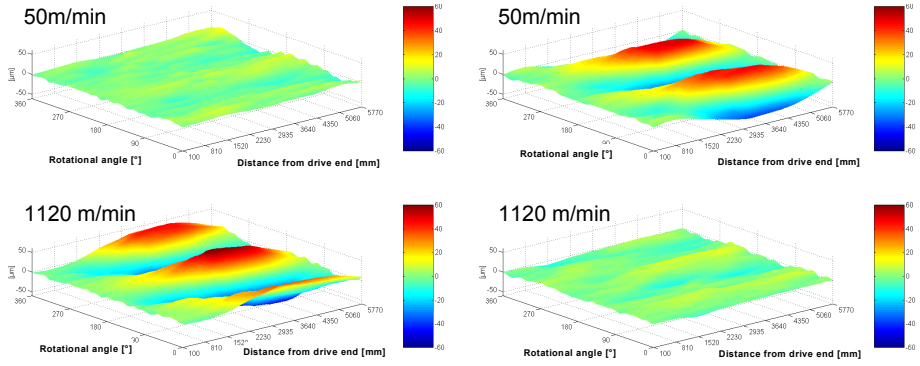

Figure 31 *3D geometry of the backing roll of the second coating station at a low running speed of 50 m/min and at the production speed of 1120 m/min. The roll is ground without a control system (left) and with predictive 3D grinding (right).*

Figure 31 shows that the geometry of the backing roll of the second coating station changes significantly when the speed is increased to the production speed of 1120 m/min. This roll also shows a strong asymmetric shell deformation. The roll reaches its maximum roundness error of 117 µm close to the open end. The manufacturing method is comparable to the first backing roll.

On the right in Figure 31, the same roll is machined with predictive 3D grinding. The roll roundness is poor at low speed but at the production running speed, the roundness error is very low. Predictive 3D grinding reduces the maximum roundness at a running speed of 1120 m/m to 22 µm (Figure 33). Before predictive 3D grinding, the out-of-roundness is rather low (25 µm) in the cross-section 810 mm from the drive end. At the same distance from the open end, the roundness is clearly higher (66 µm). After predictive 3D grinding the out-of-roundness figures are 11 µm and 22 µm respectively.

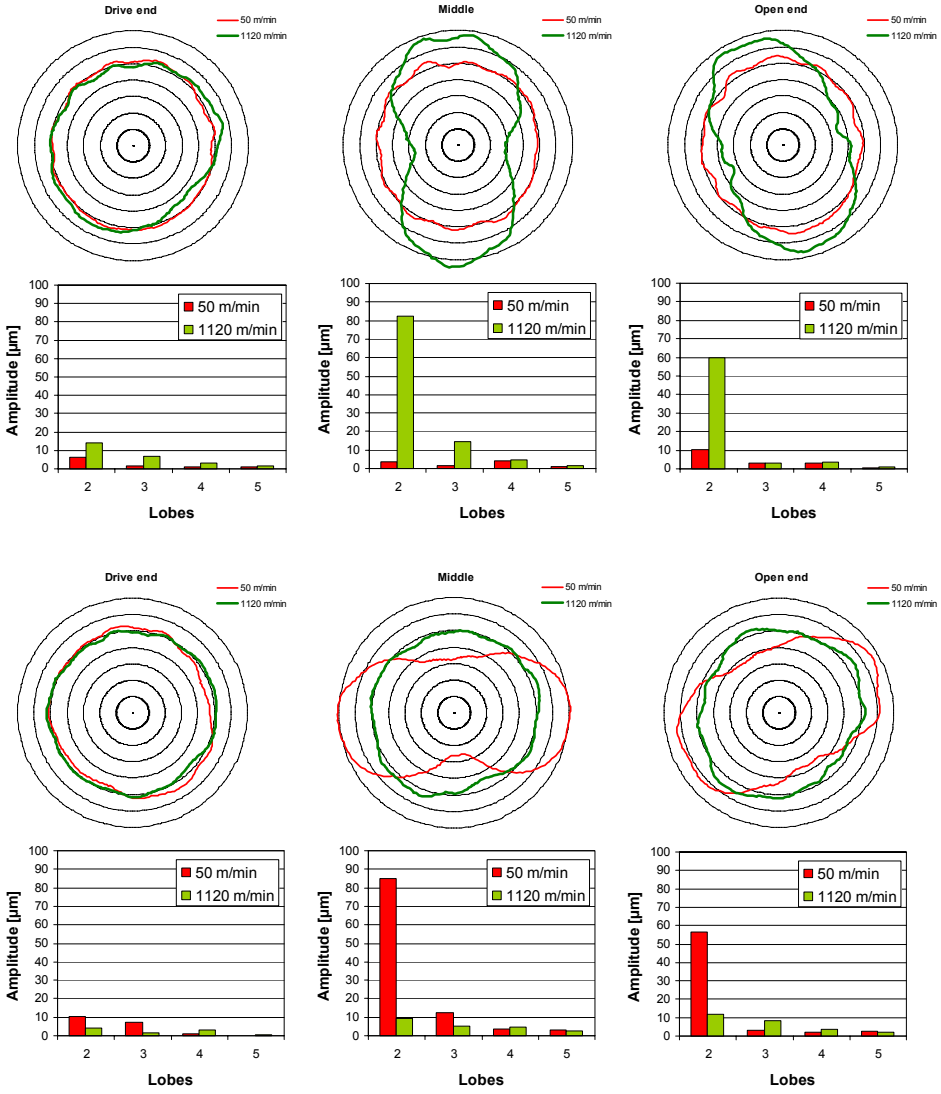

Figure 32 Roundness profiles of the backing roll of the second coating station ground without a control system (above) and after predictive 3D grinding (below) 810 mm from both ends and the middle. Roundness profiles are illustrated at a low running speed of 50 m/min (red) and at the production speed of 1120 m/min (green). The grid is 20 µm. The distribution of lobes is presented below each roundness profile.

Figure 32 illustrates the roundness profiles in three cross-sections. Ovality (82 µm) is the major out-of-roundness component in the middle cross-section before predictive 3D grinding. Predictive 3D grinding reduced the ovality to 9 µm.

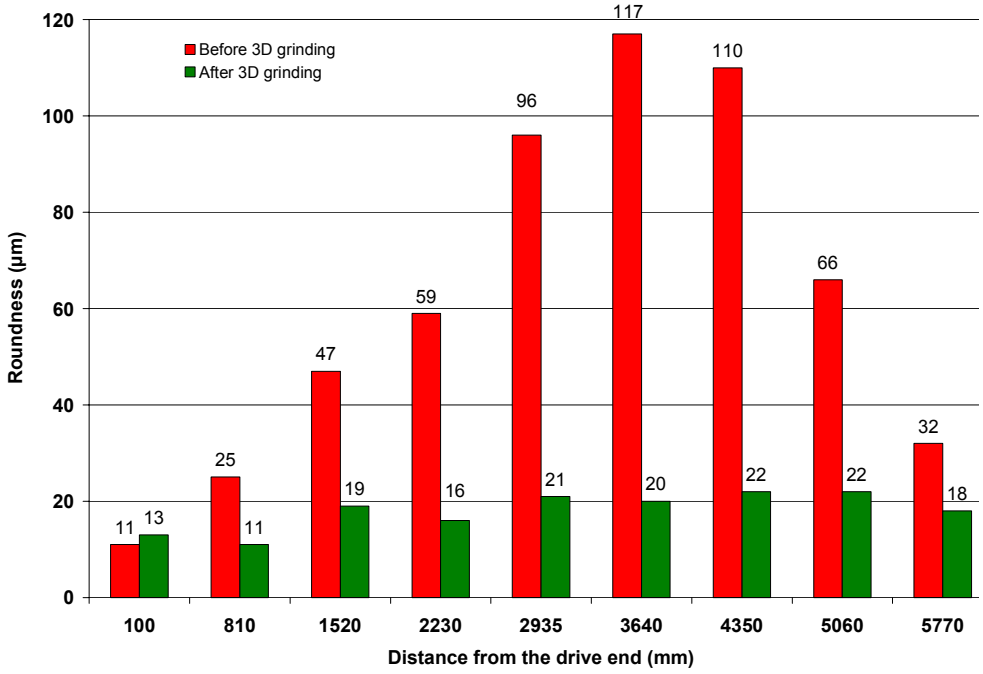

Figure 33 Roundness of the backing roll of the second coating station ground without a control system (red bars) and with predictive 3D grinding (green bars) at the production speed of 1120 m/min.

4.2 Influence of predictive 3D grinding on run-out

The run-out of the backing rolls was measured after traditional grinding and after predictive grinding. The measurements were carried out in nine cross-sections with a roll dynamic measuring device. Before predictive 3D grinding the rolls were measured at several speeds between 50 and 1120 m/min. After predictive 3D grinding the speeds were between 50 and 1200 m/min. The dynamic measuring device can calculate the run-out signal in a desired direction. In this study, the run-out signals are introduced in the direction of the metering blade, which is the sensitive direction in the coating process.

4.2.1 Run-out of the backing roll of the first coating station

The backing roll of the first coating station machined without a control system had its maximum (109 µm) run-out in the direction of the metering blade at a running speed of 1120 m/min (Figure 34). The run-out is distributed asymmetrically, as is the out-of-roundness. The run-out also changes smoothly and the maximum run-out is closer to the drive end.

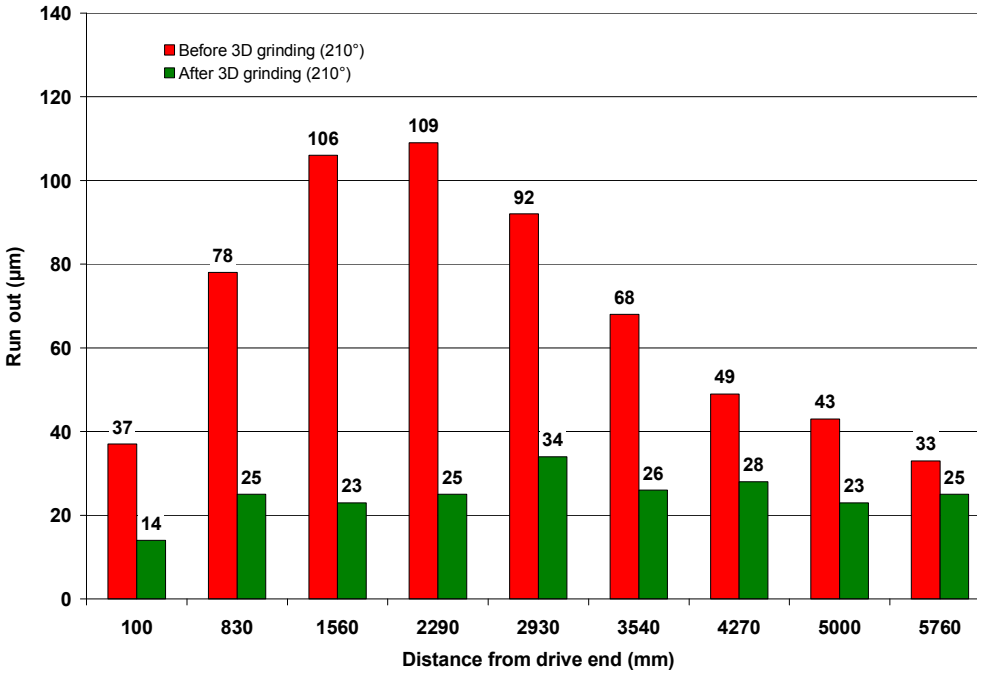

Figure 34 Run-out at the production speed of 1120 m/min of the backing roll of the first coating station ground without a control system (red bars) and with predictive 3D grinding (green bars).

With predictive 3D grinding the maximum run-out was 34 µm, without any remarkable changes in the axial direction. The values were between 14 and 34 µm in all cross-sections (Figure 34).

There is a inconsistence between the Figure 34 and 35 concerning the run-out values at the production speed of 1120 m/min in the middle cross-section with predictive 3D grinding. In Figure 34 the run-out is 34 µm and in Figure 35 the run-out is 28 µm. The measurements in Figure 34 were carried out by moving the measuring frame to axial positions and the roll was rotating with constant speed. After that the run-out in the middle cross-section was measured at different running speeds (Figure 35). The positioning accuracy of the measuring frame is around 0.1 mm and the spot size of the laser beam is 0.03·0.05 mm. As a result of this, different cross-sections were measured. Anyway, the difference is inside the overall uncertainty of the measurement. In measurement of the backing roll of the second coating station, the procedure was changed so that the measurements at different running speeds are carried out in each cross-section.

Figure 35 shows the run-out in the direction of the metering blade and its lowest harmonics at different running speeds in the middle cross-section of the backing roll of the first coating station. The run-out of the backing roll ground without a control system consists mainly of the first (once per revolution) and second harmonic (twice per revolution) components. The run-out is 49 µm at a running speed of 50 m/min and diminishes to the local minimum (46 µm) at a running speed of

200 m/min. The first harmonic also reaches its minimum (34 µm) at the same running speed. Correspondingly, the second harmonic reaches its minimum (15 µm) at a running speed of 600 m/min. Despite the local minimum, the run-out has a clear tendency to grow with an increased running speed. At a running speed of 1120 m/min, the run-out has already increased to 92 µm.

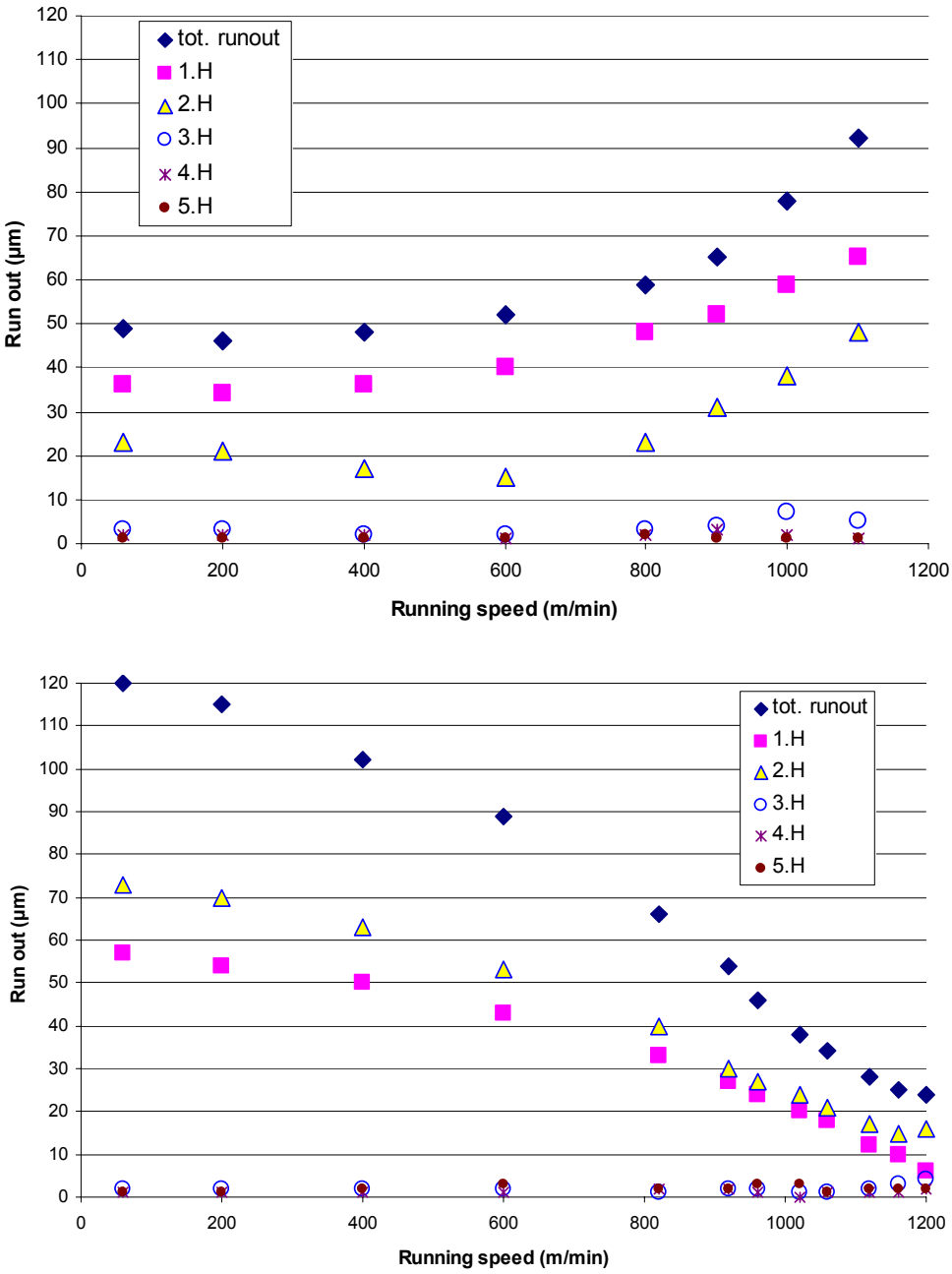

Figure 35 *Run-out and its harmonics at different running speeds in the middle cross-section of the first coating station's backing roll ground without a control system (above) and with predictive 3D grinding (below).*

The run-out after predictive 3D grinding also consists mainly of the first and second harmonic components. The run-out is 120 µm at a running

speed of 50 m/min and diminishes to 28 µm at a running speed of 1120 m/min. The first harmonic reaches its minimum (6 µm) at a running speed of 1200 m/min. The second harmonic reaches its minimum (15 µm) at a running speed of 1160 m/min.

4.2.2 Run-out of the backing roll of the second coating station

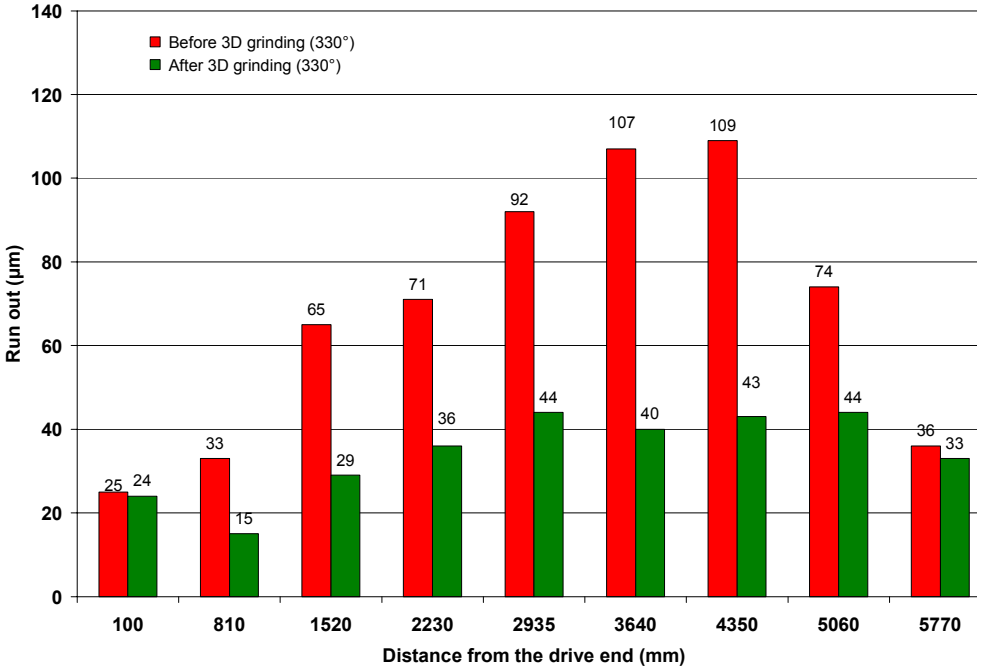

Figure 36 Run-out at the production speed of 1120 m/min of the backing roll of the second coating station ground without a control system (red bars) and with predictive 3D grinding (green bars).

Without a control system, the machined roll has a maximum run-out of 109 µm and with predictive 3D machining, the maximum run-out is 44 µm (Figure 36).

Figure 37 shows the run-out and its lowest harmonics at different running speeds in the middle cross-sections of the first coating station backing roll before and after predictive 3D grinding in the direction of the metering blade. The run-out before predictive 3D grinding is 23 µm at a running speed of 50 m/min and increases with running speed up to 92 µm at 1120 m/min. The run-out consists mainly of the second harmonic (twice per revolution) component, which increases from 3 µm at 50 m/min to 79 µm at 1120 m/min. The first and third harmonic components are less than 20 µm at all running speeds.

The run-out after predictive 3D grinding has the same dominant second harmonic component as before predictive 3D grinding. The run-out is 92 µm at a running speed of 50 m/min and diminishes to 40 µm at 1000 m/min. At the production running speed of 1120 m/min, the run-out is 44 µm. The second harmonic reaches its minimum (16 µm) at a

running speed of 1120 m/min. The first and third harmonics reach their minimums (10 µm and 8 µm) at 900 m/min.

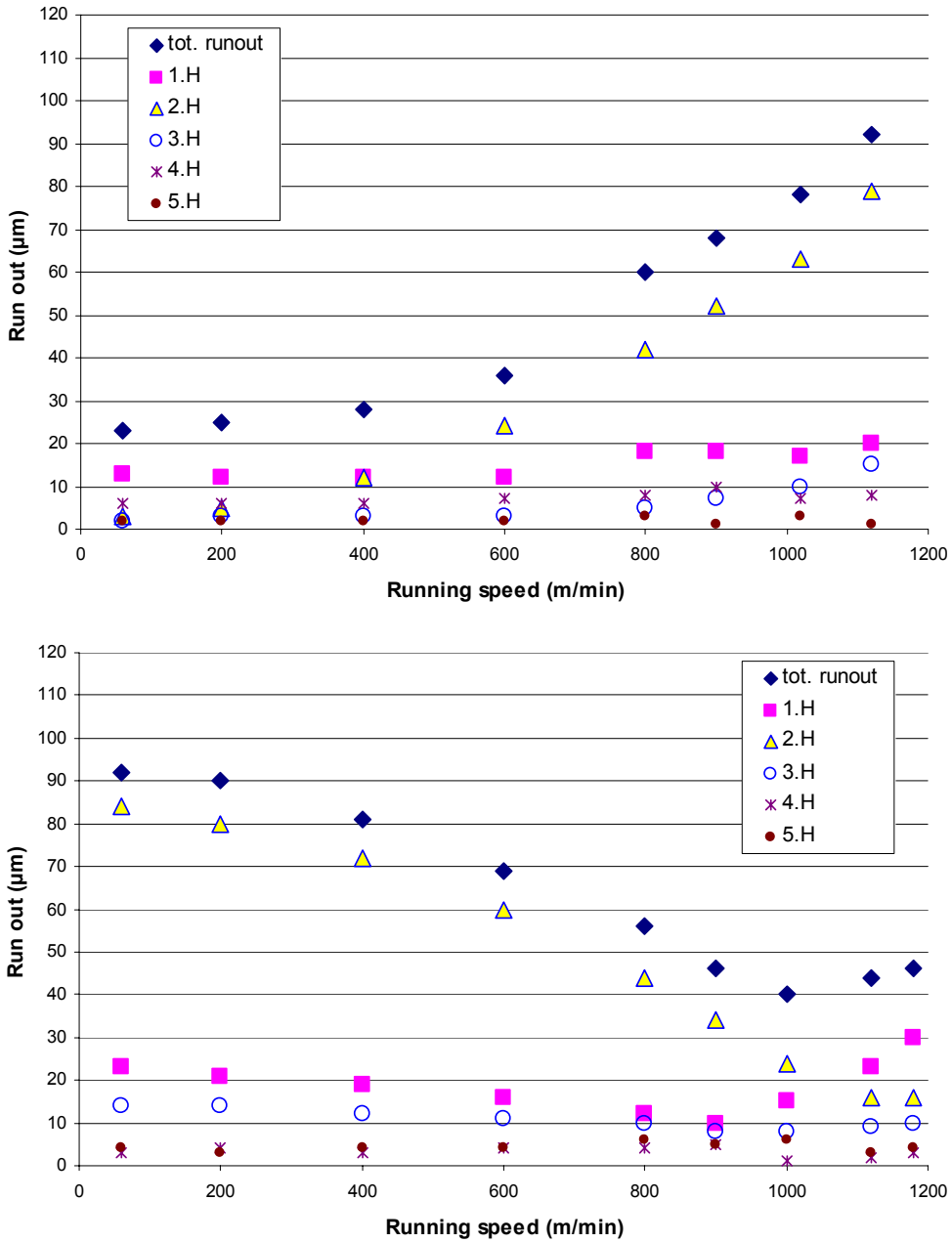

Figure 37 Run-out and its harmonics at different running speeds in the middle cross-section of the second coating station's backing roll ground without a control system (above) and with predictive 3D grinding (below).

4.3 Influence of predictive 3D grinding on variations in paper quality in machine direction

To facilitate the comparability of the results, the conditions under which tests were carried out at different times were standardised. The

paper grade produced was almost the same in both samples. The running speed was almost exactly the same and the backing rolls were in the same positions. The length of the MD paper sample was 4000 m in both cases.

The first paper analysis was of coated paper and was performed before the 3D ground rolls were added to the coating stations. The paper grade was MWC with 13 g/m^2 coating on both sides. Thus, the base paper basis weight was 44 g/m^2. The production speed was 1100 m/min.

The second paper analysis was of coated paper and was performed after the 3D ground rolls were added to the coating stations. This time the paper grade was 80 g/m^2 LWC with 13.5 g/m^2 coating on both sides. Thus, the base paper basis weight was 53 g/m^2. The production speed was 1103 m/min.

Table 5 presents the results for the paper characteristics before the 3D grinding of the backing rolls. Table 6 presents the results for the paper characteristics after the 3D grinding of the backing rolls. In both tables, the values are based on time domain signals of a 100 m paper sample period starting from 1000 m.

Table 5 Results of the time domain paper analysis before 3D grinding. Low-pass filtering is 20 Hz.

	Ash [g/m^2]	*Basis weight [g/m^2]*	*Thickness [μm]*	*Gloss Station 1 [%]*	*Gloss Station 2 [%]*
Average	*22.0*	*70.1*	*57.2*	*62.4*	*61.6*
Std. Dev.	*0.9*	*1.1*	*0.4*	*2.2*	*1.8*
Max	*24.0*	*72.7*	*58.5*	*66.8*	*65.5*
Min	*20.1*	*67.5*	*56.1*	*57.9*	*57.6*
Max-min	*3.9*	*5.2*	*2.4*	*8.9*	*7.9*

Table 6 Results of the time domain paper analysis after 3D grinding. Low-pass filtering is 20 Hz.

	Ash [g/m²]	*Basis weight [g/m²]*	*Thickness [µm]*	*Gloss Station 1 [%]*	*Gloss Station 2 [%]*
Average	24.7	81.0	67.0	62.1	63.0
Std. Dev.	0.3	0.4	0.4	0.6	0.5
Max	25.7	82.2	68.1	64.1	64.4
Min	24.2	79.8	66.0	60.6	61.5
Max-min	1.5	2.4	2.1	3.5	2.9

Table 7 presents variations in paper characteristics, synchronised to the rotating frequency and the harmonics of the backing rolls. The results after traditional grinding and after predictive 3D grinding are presented. The values are based on the spectral analysis of the total length of 400 m long samples.

Table 7 Influence of predictive 3D grinding of the backing rolls on variations in paper quality. The numbers are peak-to-peak values. Low-pass filtering is 358 Hz.

	Coating station 1		*Coating station 2*	
	Traditional grinding	*3D grinding*	*Traditional grinding*	*3D grinding*
Ash (g/m²)	2.0	0.7	3.2	0.4
Basis weight (g/m²)	2.5	0.8	3.8	0.6
Thickness (µm)	1.3	0.4	1.4	0.3
Gloss Station 1 (%)	5.3	0.7	4.7	1.1

4.3.1 Ash variation in machine direction

Ash variation has a clear correlation to coating variation, because base paper contains little ash. In this study, the ash content of base paper of 80 g/m² MWC is around 5 g/m². The ash content of base paper of 70 g/m² MWC is around 3 g/m². In addition, the distribution of the ash in base paper is different from that in coating. For example, there are no rolls of the same diameter as the backing rolls of the coating machine.

The paper analysis shows a clear reduction in ash variation after predictive 3D grinding. In a 100 m time domain the signal starting from 1000 m shows that the peak-to-peak value has diminished from 3.9 g/m² to 1.5 g/m² (Figure 38).

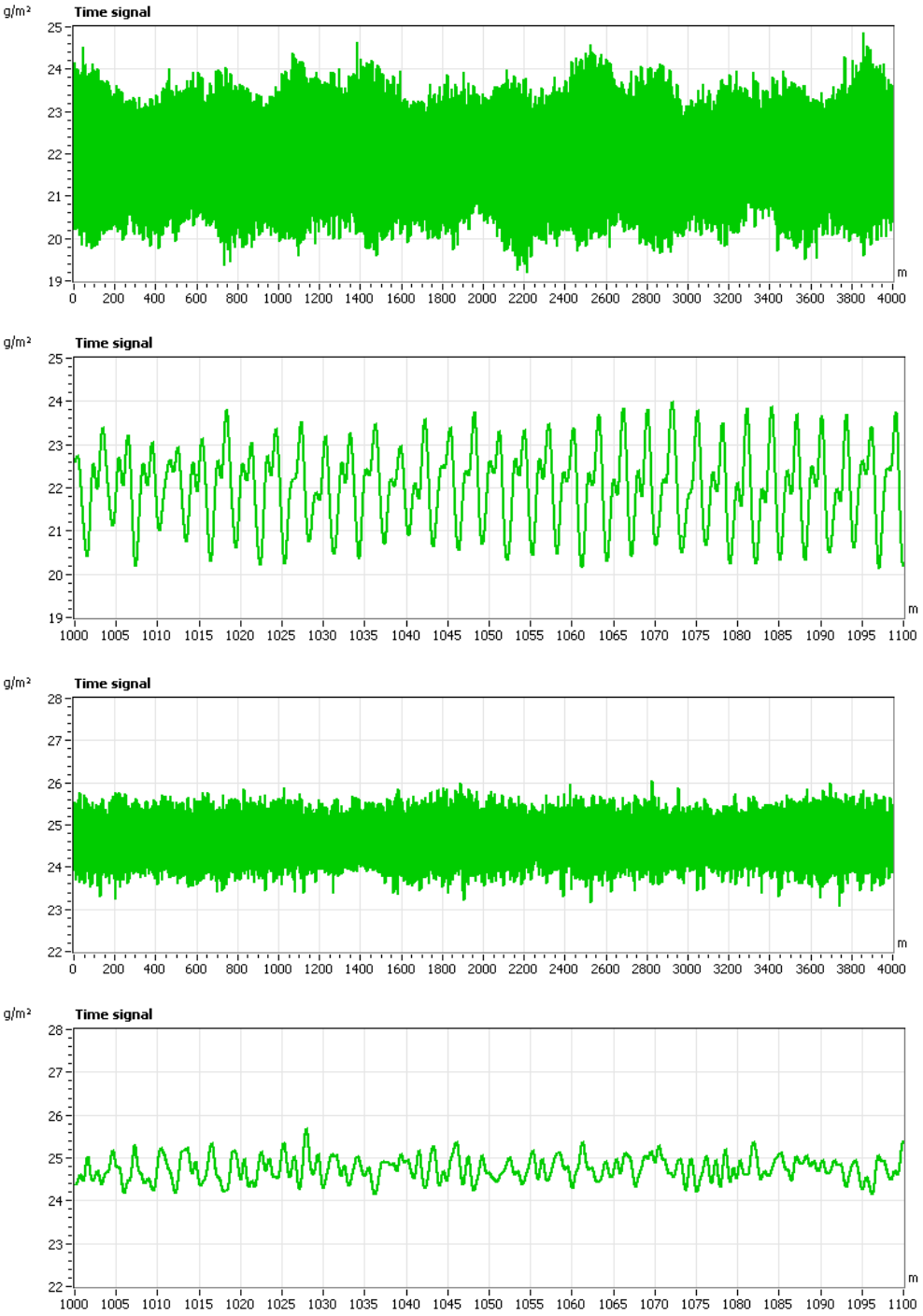

Figure 38 Ash variation of the coated paper in the time domain in MD before (upper two frames) and after (lower two frames) predictive 3D machining.

In the frequency domain (Figure 39), the harmonic components corresponding to roll rotation frequency are marked. The backing roll of the first coating station caused a 2.0 g/m^2 peak-to-peak ash variation before predictive 3D grinding. Predictive 3D grinding reduced the ash variation to 0.7 g/m^2.

The backing roll of the second coating station caused a 3.2 g/m^2 peak-to-peak ash variation before predictive 3D grinding. Predictive 3D grinding reduced the ash variation to 0.4 g/m^2 (Figure 40).

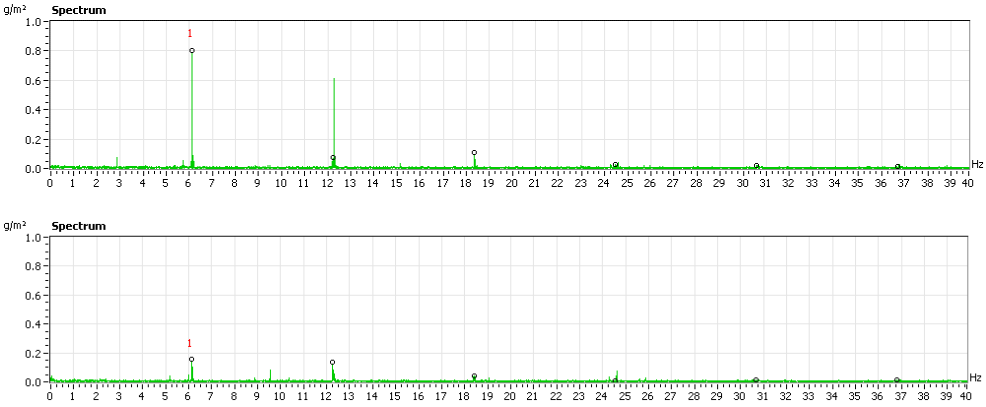

Figure 39 *Ash variation of the coated paper in MD caused by the backing roll of the first coating station before (above) and after (below) predictive 3D machining.*

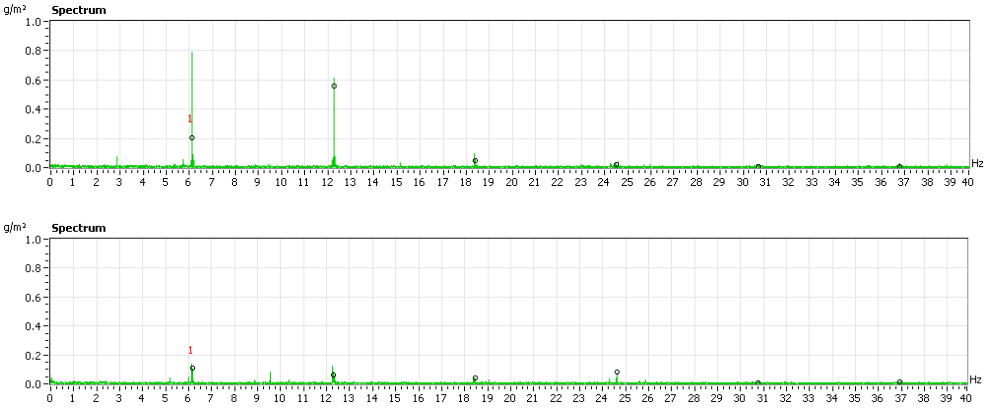

Figure 40 *Ash variation of the coated paper in MD caused by the backing roll of the second coating station before (above) and after (below) predictive 3D machining.*

In Figure 41 the spectrum is generated as an average of 55 individual spectra. Each individual spectrum is calculated from a paper sample period around 210 m long. The sample is moved one-third between each individual spectrum. The spectral stability analysis frame shows these 55 spectra plotted in a plane figure.

The spectral stability analysis shows a clear reduction in ash variation after predictive 3D grinding. The spectra show nearly the same results as the spectrum of the long sample in Figure 39 and in Figure 40. Before

predictive 3D grinding the stability frame shows the interference of the backing rolls, with diameters close to each other. In particular, the second harmonic at 12.2 Hz displays clear waviness in ash variation. After predictive 3D grinding, the variation has almost disappeared. Only light spectral lines are visible but even these include waviness.

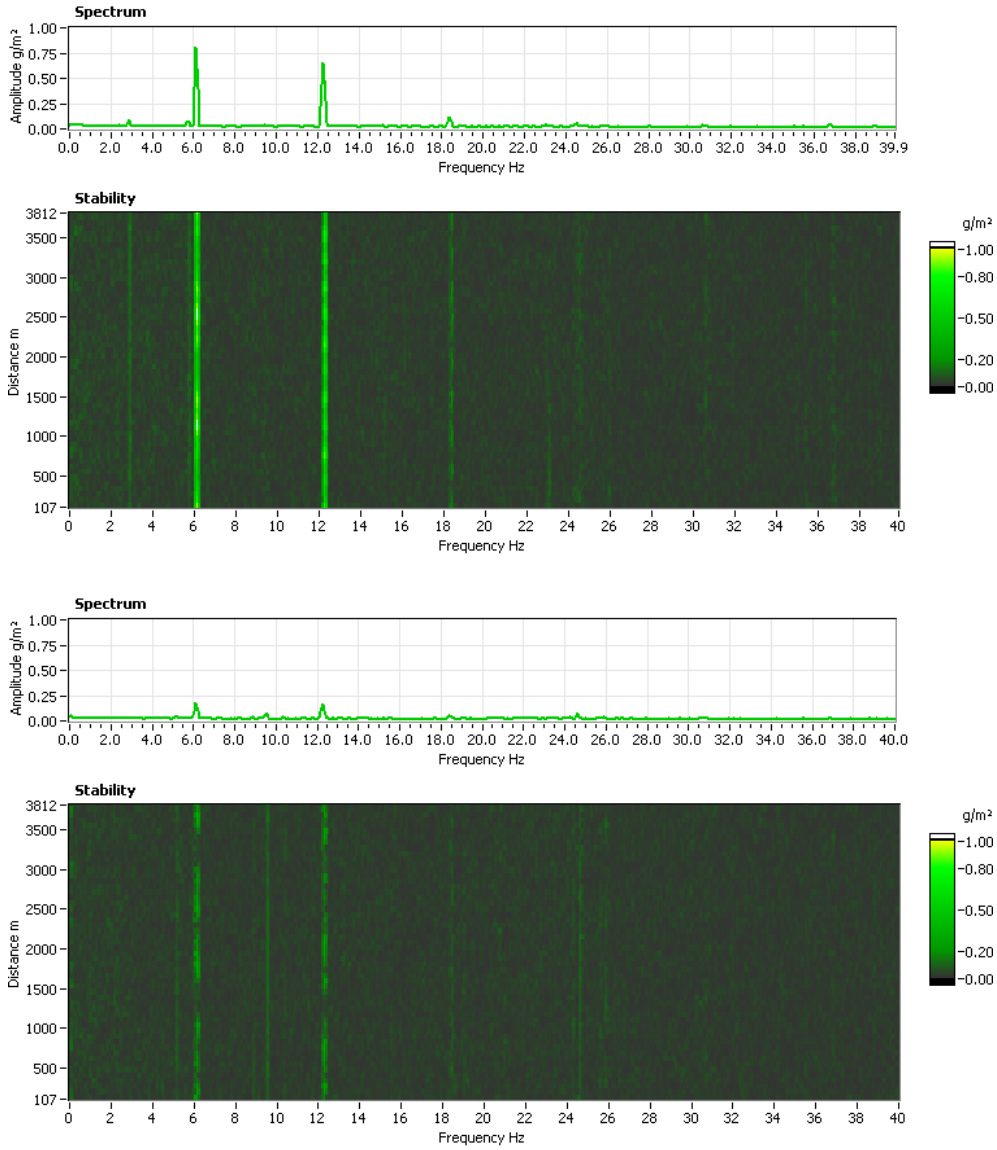

Figure 41 Spectral stability analysis of ash variation before (above) and after (below) predictive 3D machining.

4.3.2 Basis weight variation in machine direction

The paper analysis shows a clear reduction in basis weight variation after predictive 3D grinding. In a 100 m time domain the signal starting from 1000 m shows that the peak-to-peak variation has diminished from 5.2 g/m^2 to 2.4 g/m^2 (Figure 42).

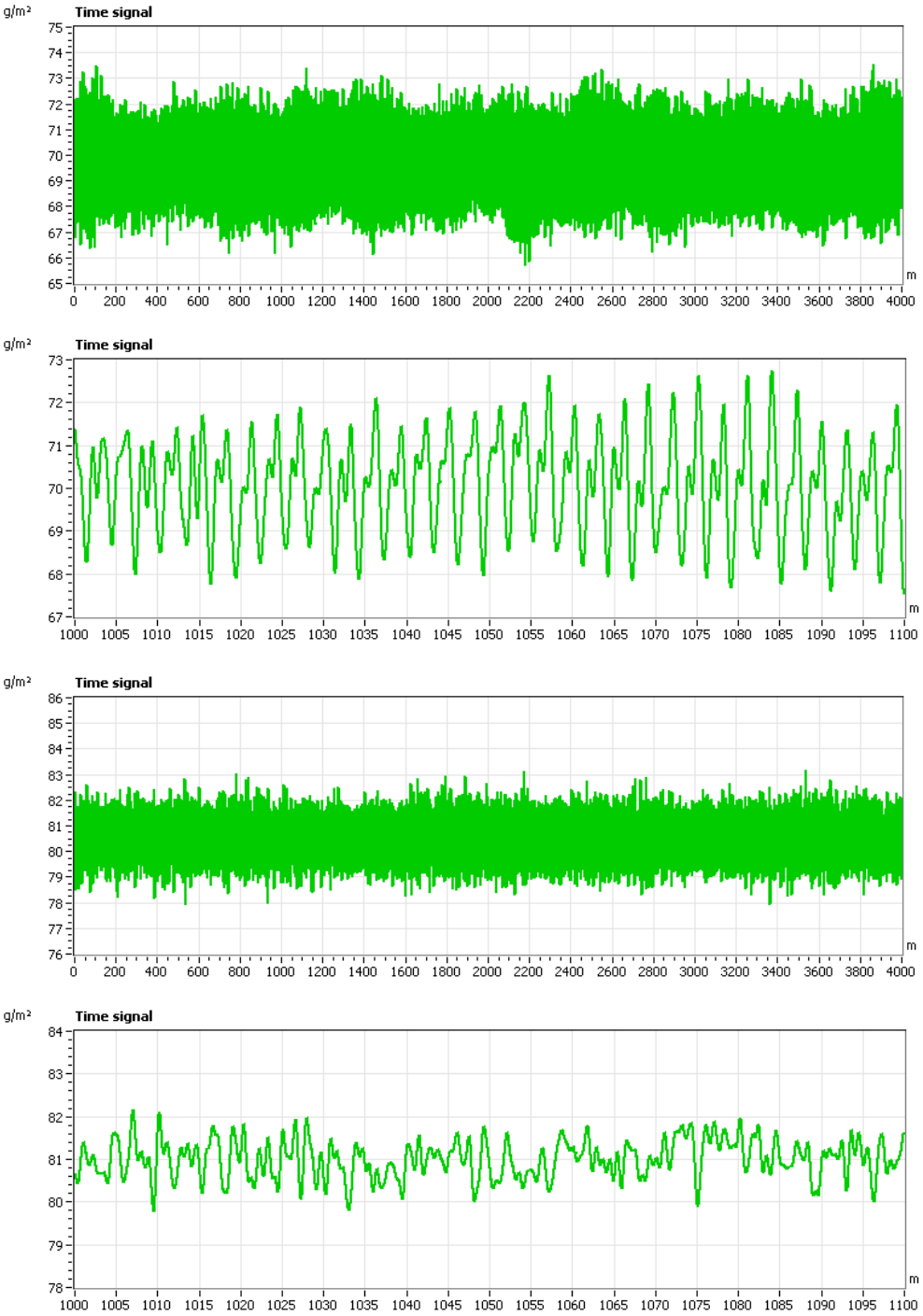

Figure 42 Basis weight variation in the time domain of the coated paper in MD before (above) and after (below) predictive 3D machining.

The backing roll of the first coating station caused a 2.5 g/m^2 peak-to-peak basis weight variation before predictive 3D grinding. Predictive 3D grinding reduced the basis weight variation to 0.8 g/m^2 (Figure 43).

The backing roll of the second coating station caused a 3.8 g/m^2 peak-to-peak basis weight variation before predictive 3D grinding. Predictive 3D grinding reduced the basis weight variation to 0.6 g/m^2 (Figure 44).

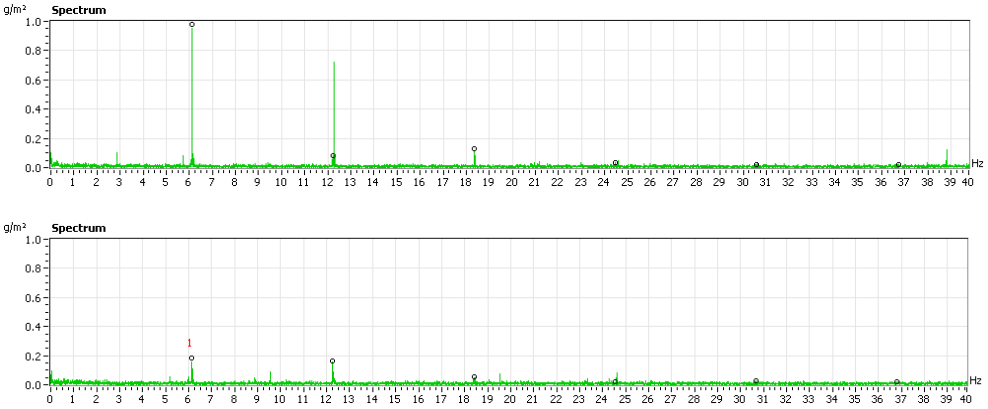

Figure 43 Basis weight variation of the coated paper in MD caused by the backing roll of the first coating station before (above) and after (below) predictive 3D machining

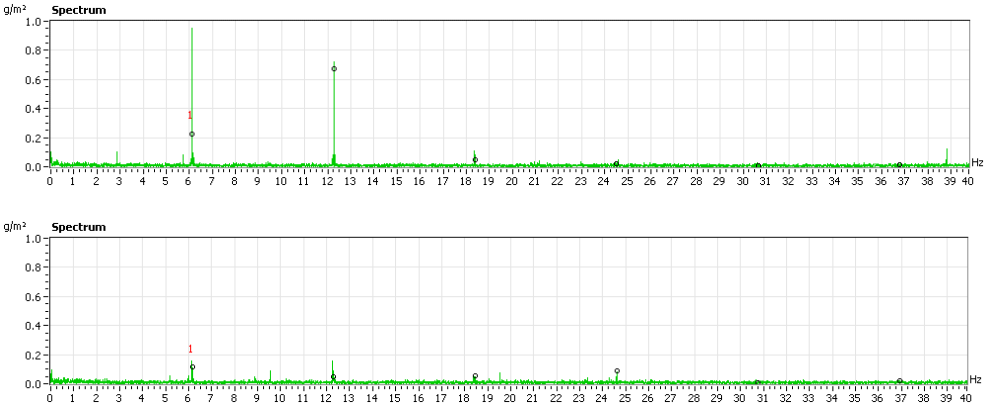

Figure 44 Basis weight variation of the coated paper in MD caused by the backing roll of the second coating station before (above) and after (below) predictive 3D machining.

The spectral stability analysis shows a clear reduction in basis weight variation after predictive 3D grinding, as was the case in ash variation. Before predictive 3D grinding the stability frame shows interference from the backing rolls, with diameters close to each other. In particular, the second harmonic at 12.2 Hz displays clear waviness in basis weight variation. After predictive 3D grinding the variation has almost disappeared. Only light spectral lines are visible but even these include waviness.

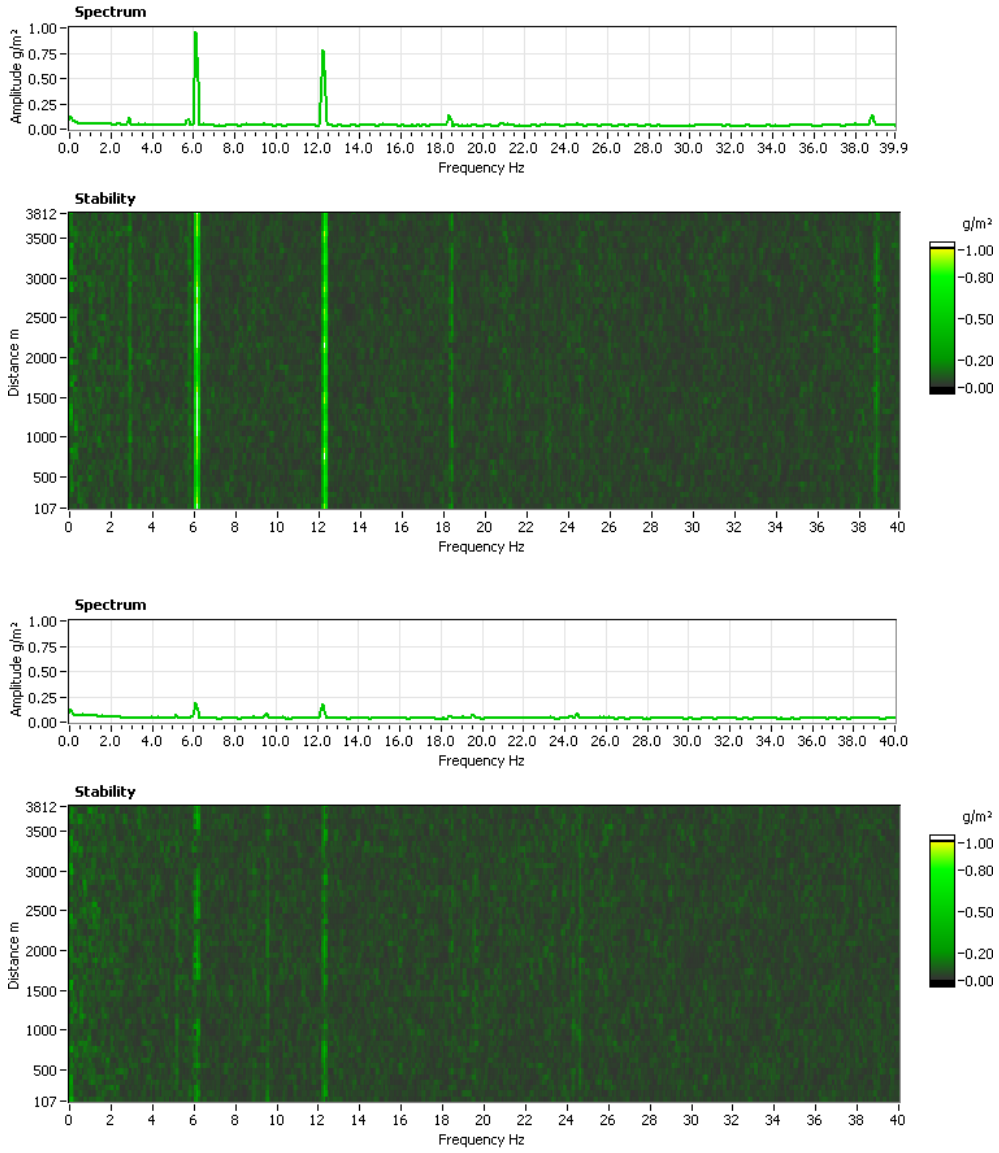

Figure 45 Spectral stability analysis of basis weight variation before (above) and after (below) predictive 3D machining.

4.3.3 Thickness variation in machine direction

The paper analysis shows only scant reduction in thickness variation after predictive 3D grinding. In a 100 m time domain the signal starting from 1000 m shows that the peak-to-peak variation has diminished from 2.4 µm to 2.1 µm (Figure 46).

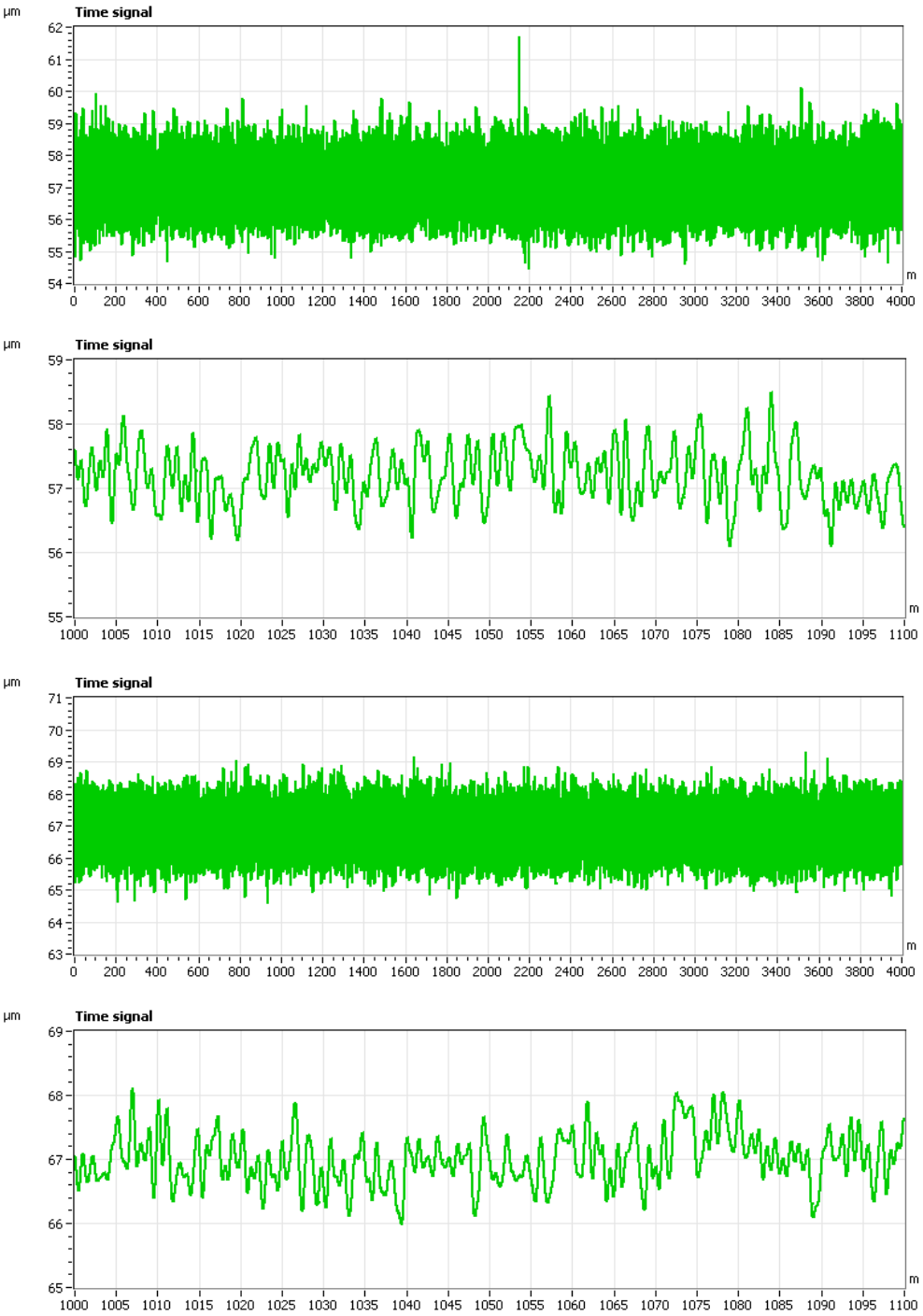

Figure 46 Thickness variation of the coated paper in MD before (above) and after (below) predictive 3D machining.

The backing roll of the first coating station caused a 1.3 µm peak-to-peak thickness variation before predictive 3D grinding. Predictive 3D grinding reduced the thickness variation to 0.4 µm (Figure 47).

The backing roll of the second coating station caused a 1.4 µm peak-to-peak thickness variation before predictive 3D grinding. Predictive 3D grinding reduced the thickness variation to 0.3 µm (Figure 48).

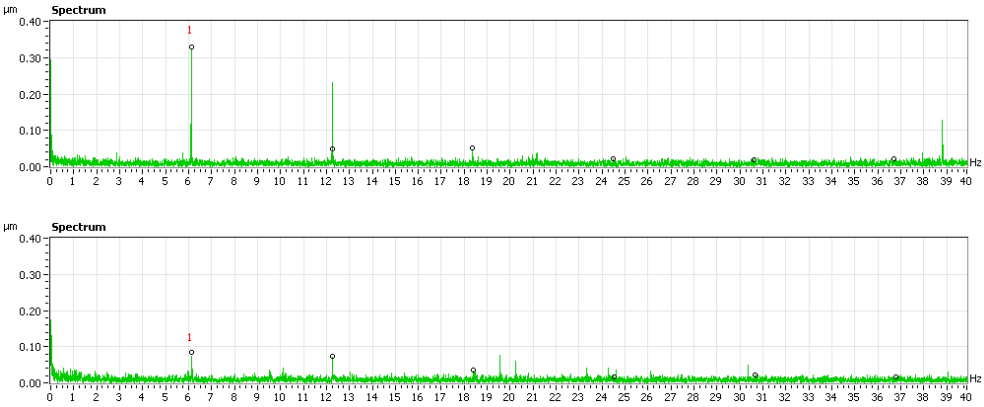

Figure 47 Thickness variation of the coated paper in MD caused by the backing roll of the first coating station before (above) and after (below) predictive 3D machining.

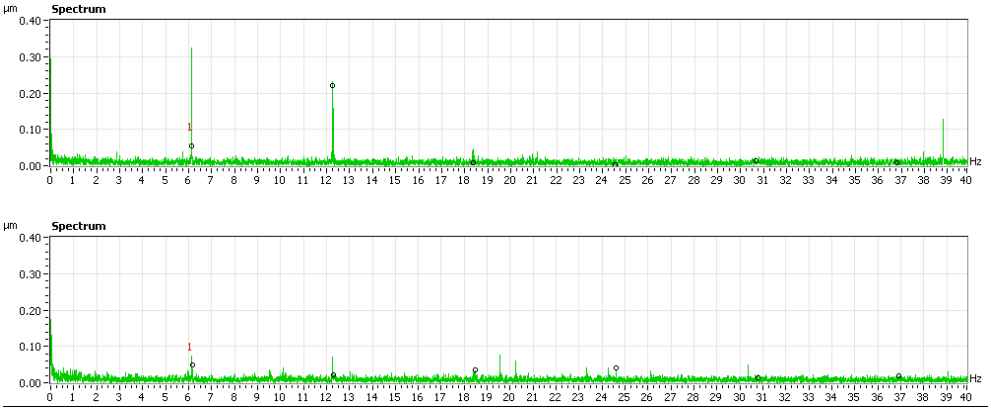

Figure 48 Thickness variation of the coated paper in MD caused by the backing roll of the second coating station before (above) and after (below) predictive 3D machining.

The spectral stability analysis shows a clear reduction in thickness variation after predictive 3D grinding. Before predictive 3D grinding the stability frame shows clear spectral lines of the first and second harmonics. After predictive 3D grinding these spectral lines have almost disappeared.

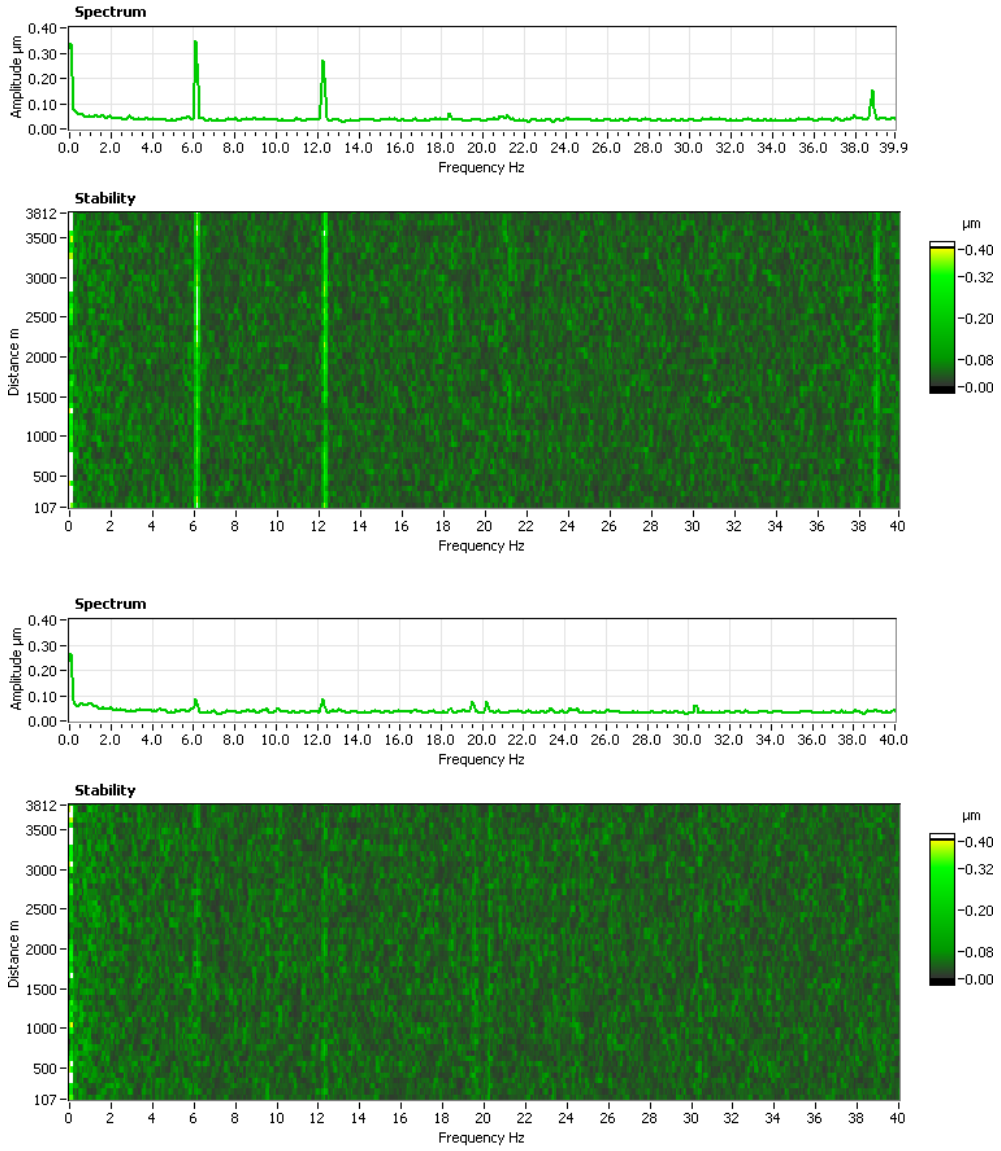

Figure 49 Spectral stability analysis of thickness variation before (above) and after (below) predictive 3D machining.

4.3.4 Gloss variation in machine direction

The paper analysis shows a clear reduction in gloss variation caused by the backing roll of the first coating station after predictive 3D grinding. In a 100 m time domain the signal starting from 1000 m shows that the peak-to-peak variation has diminished from 8.9% to 3.5% (Figure 50).

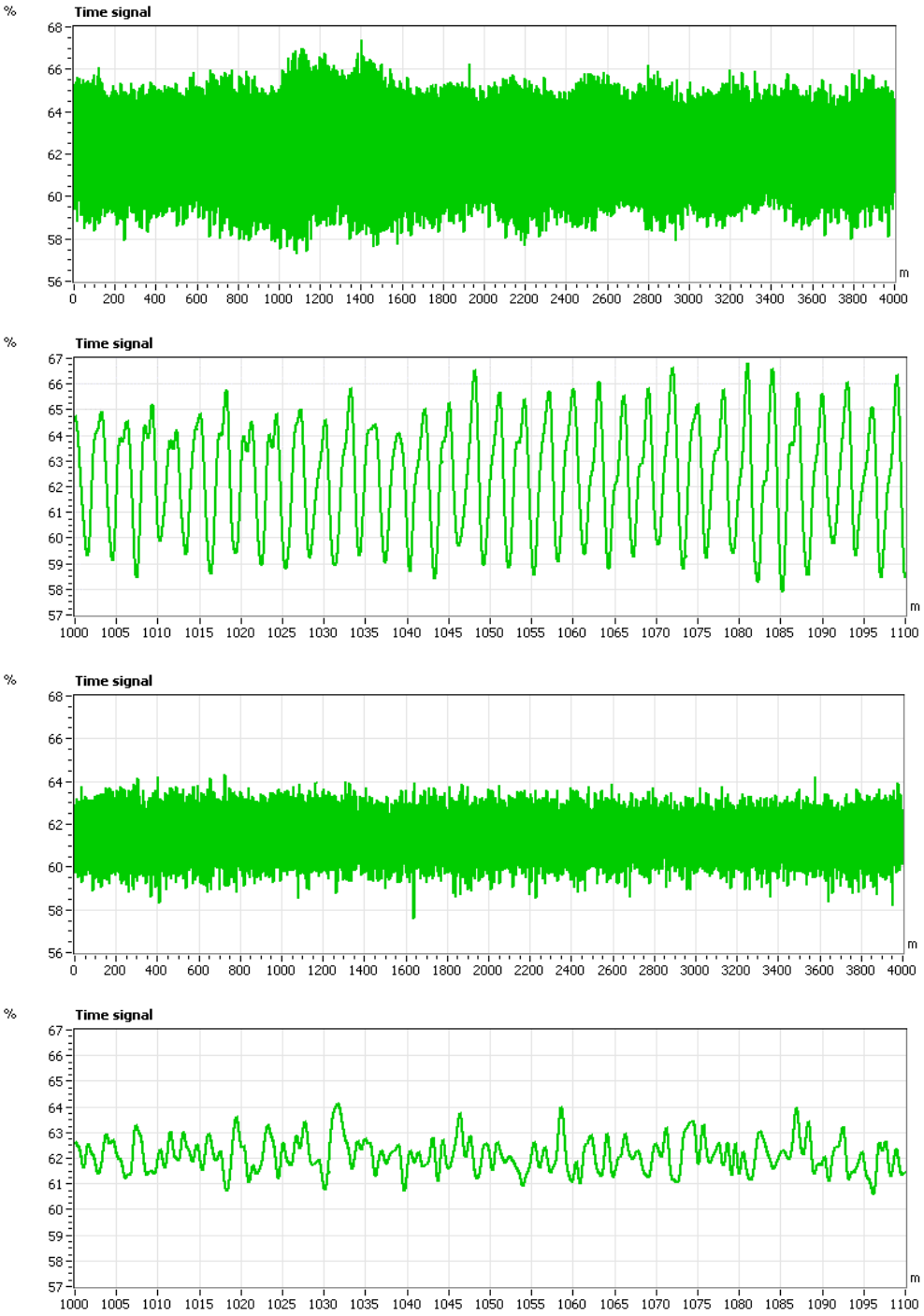

Figure 50 Gloss variation of the coated paper in MD caused by the backing roll of the first coating station before (above) and after (below) predictive 3D machining.

The backing roll of the first coating station caused a 5.3% peak-to-peak gloss variation before predictive 3D grinding. Predictive 3D grinding reduced the gloss variation to 0.7% (Figure 51).

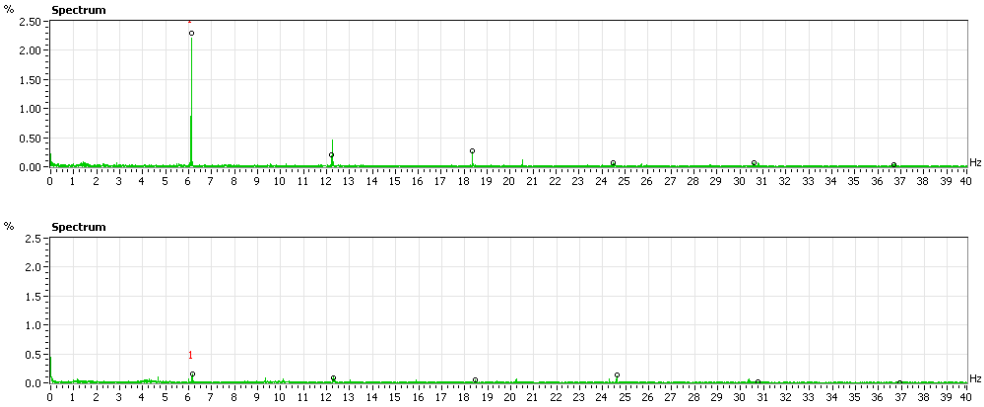

Figure 51 Gloss variation of the coated paper in MD caused by the backing roll of the first coating station before (above) and after (below) predictive 3D machining.

The spectral stability analysis shows a clear reduction in gloss variation caused by the backing roll of the first coating station after predictive 3D grinding. Before predictive 3D grinding the stability frame shows clear spectral lines caused by the first and second harmonics. After predictive 3D grinding these spectral lines have almost disappeared (Figure 52).

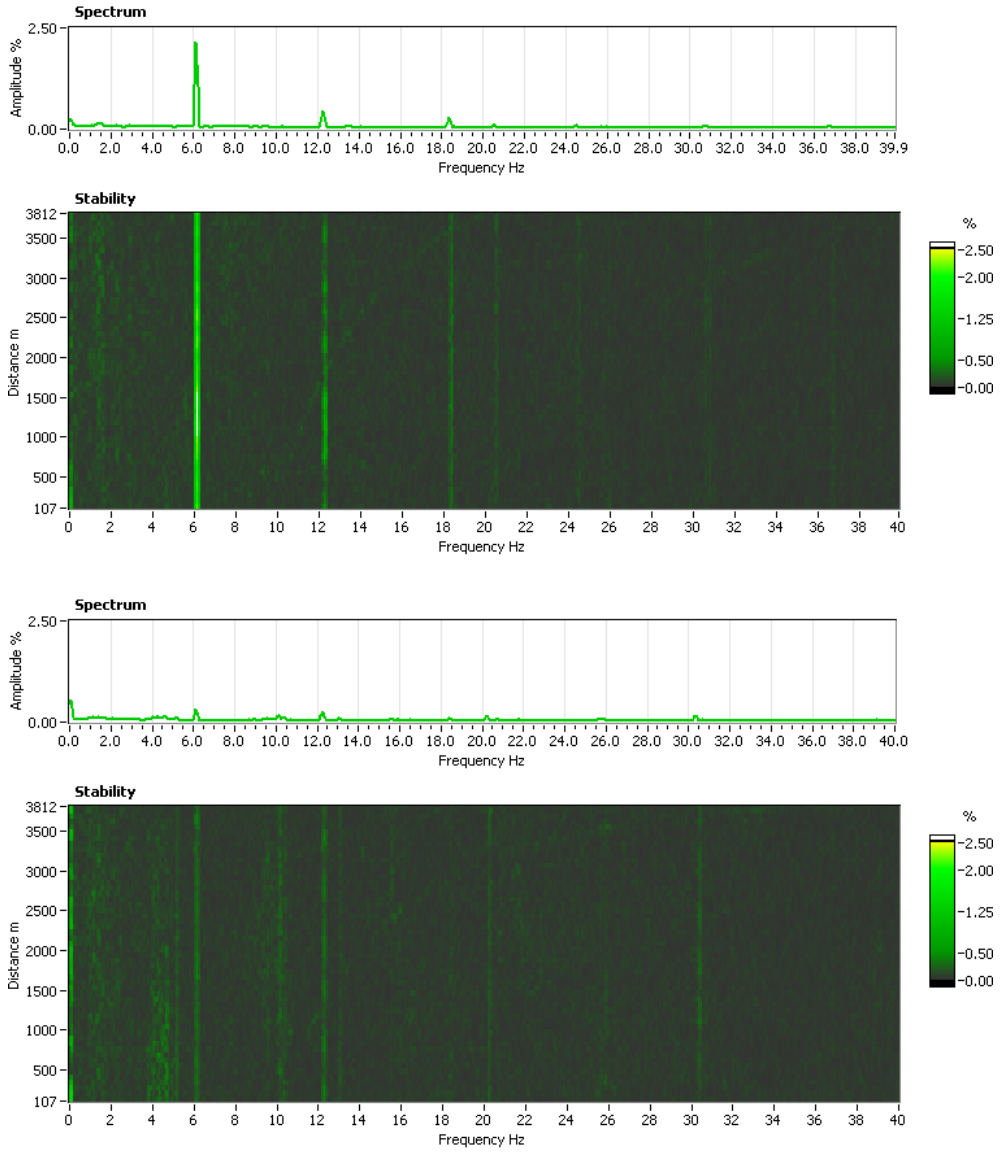

Figure 52 Spectral stability analysis of gloss variation caused by the backing roll of the first coating station before (above) and after (below) predictive 3D machining.

The paper analysis shows a clear reduction in gloss variation caused by the backing roll of the second coating station after predictive 3D grinding. In a 100 m time domain the signal starting from 1000 m shows that the peak-to-peak variation has diminished from 7.9% to 2.9% (Figure 53).

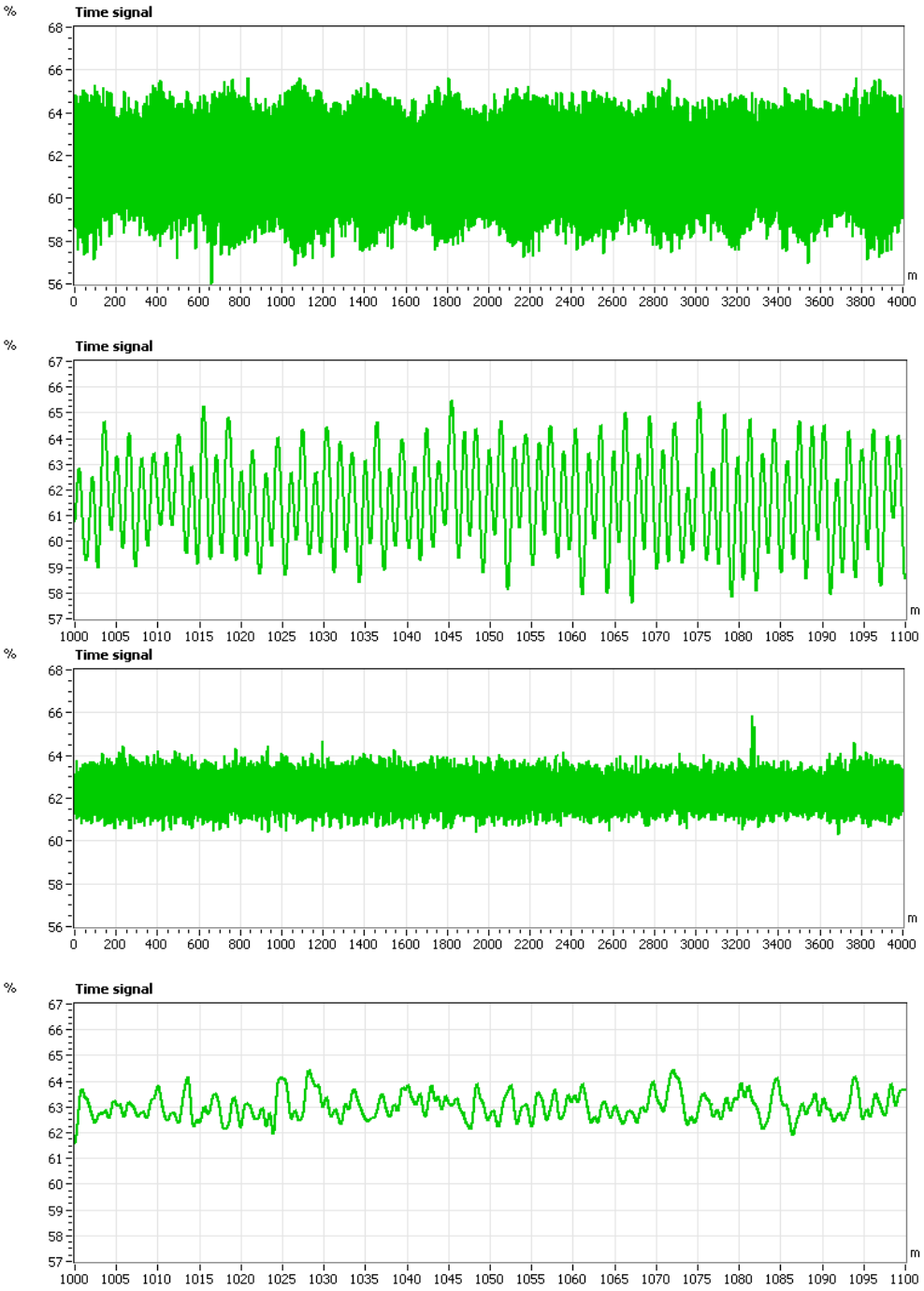

Figure 53 Gloss variation of the coated paper in MD caused by the backing roll of the second coating station before (above) and after (below) predictive 3D machining.

The backing roll of the second coating station caused a 4.7% peak-to-peak gloss variation before predictive 3D grinding. Predictive 3D grinding reduced the gloss variation to 1.1% (Figure 54).

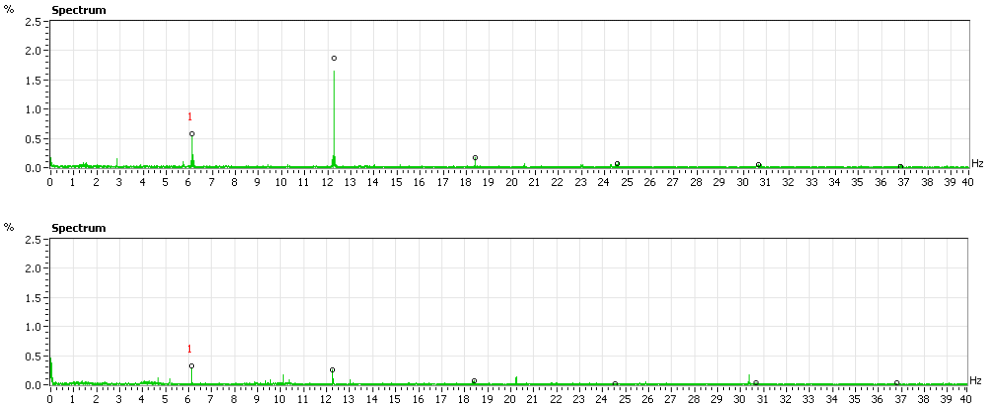

Figure 54 Gloss variation of the coated paper in MD caused by the backing roll of the second coating station before (above) and after (below) predictive 3D machining.

The spectral stability analysis shows a clear reduction in gloss variation caused by the backing roll of the second coating station after predictive 3D grinding. Before predictive 3D grinding the stability frame shows clear spectral lines, especially caused by the second harmonic. After predictive 3D grinding this spectral line has disappeared.

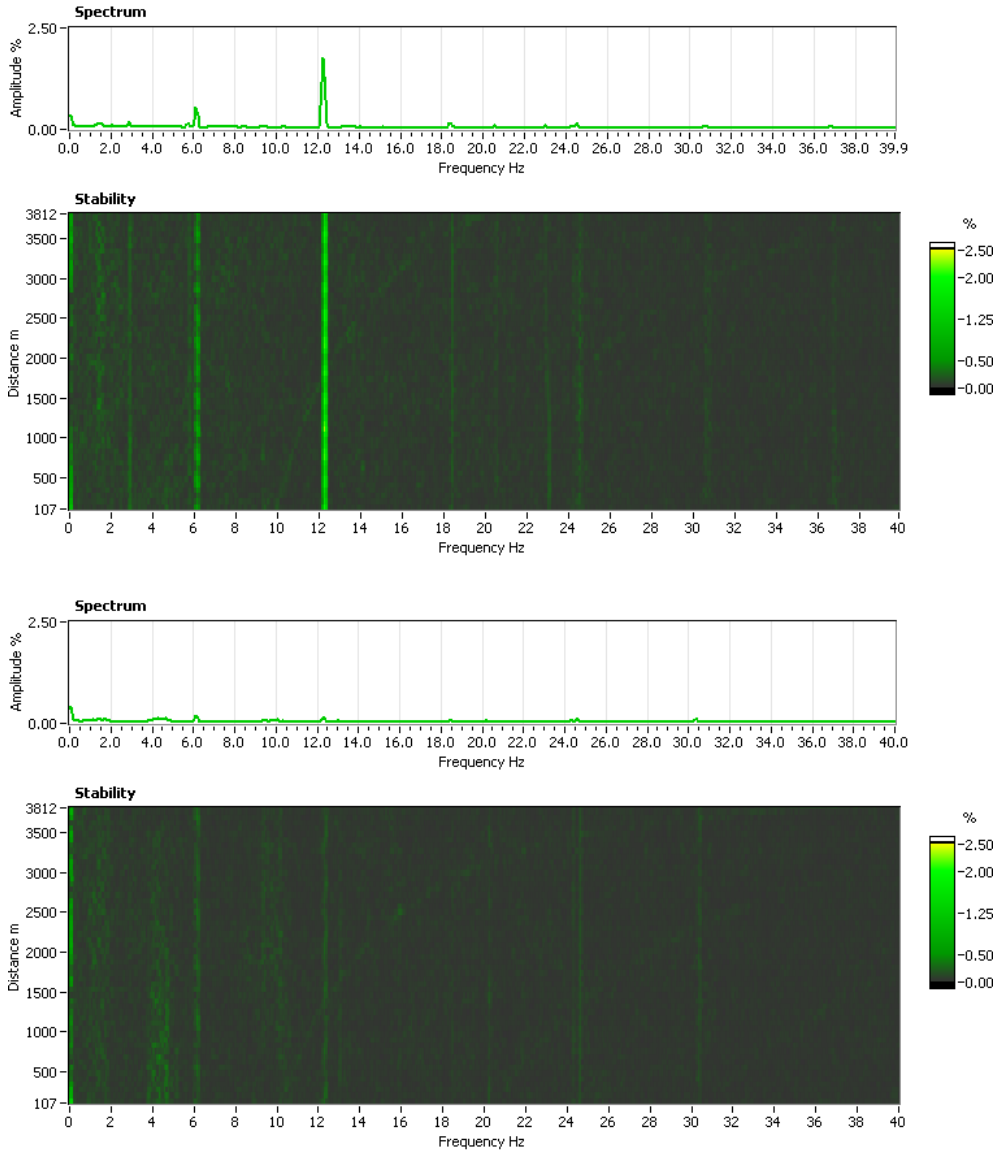

Figure 55 Spectral stability analysis of gloss variation caused by the backing roll of the second coating station before (above) and after (below) predictive 3D machining.

5 DISCUSSION

This study applies an experimental approach to measure roundness and run-out directly. Another possibility is to model a roll and calculate the dynamic behaviour according to the available information, such as roll thickness and material stiffness. The main problem in modelling is the inaccuracy of the source data; the calculated results cannot reach a useful degree of accuracy. For example, the thickness of a roll shell can be measured with an ultrasonic probe (Figure 56). The measurement is based on the delay between the sent and reflected ultrasonic pulses.

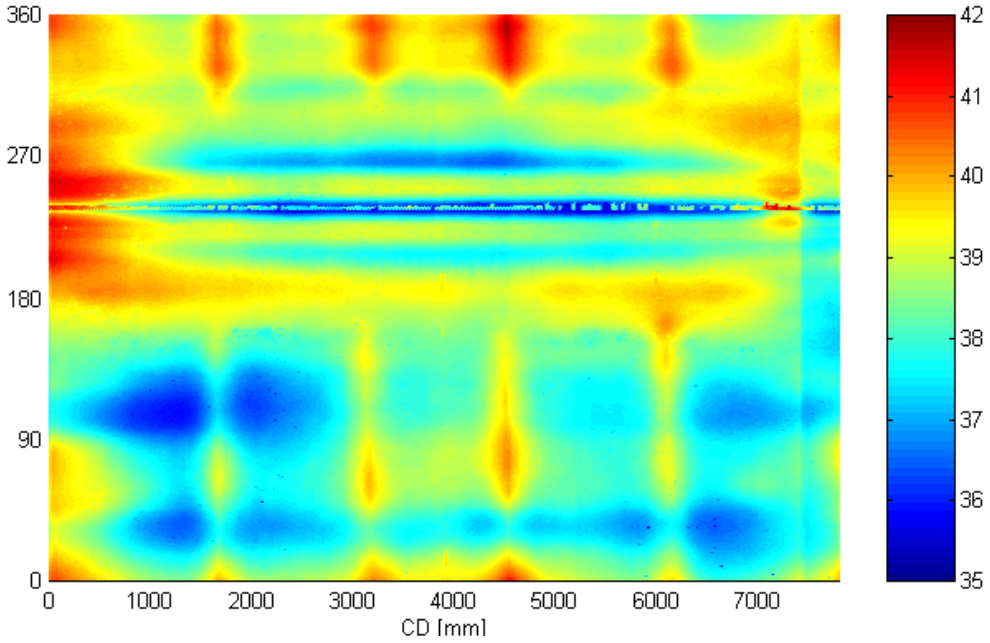

Figure 56 *Shell thickness of a backing roll made of rolled iron sheet. The scale is in millimetres. Welding can be seen in the axial direction at an angle of 230 °.*

In rolled sheet iron the ultrasonic method works well, with an accuracy as great as ±10 µm (Savolainen 1996). In practice such high accuracy can very seldom be reached, as, for example, the welds disturb the ultrasonic pulse. The rolls are often covered or the roll shell is made of cast iron. In these cases the thickness cannot be measured or the accuracy is much poorer. Furthermore, the thickness of the roll shell is only one important parameter in calculating the dynamic behaviour of the roll. The stiffness and temperature distribution of the material, initial bending of the roll body, rotational accuracy and stiffness of the bearings etc. should also be known with high accuracy in order to be able to calculate the real dynamic behaviour. This modelling work is very important and gives information concerning the parameters influencing roll behaviour. The experimental research supplements model development. A roll dynamic measuring device is an excellent tool in verifying the models.

5.1 Influence of predictive 3D grinding on roundness and run-out

Both test rolls exhibited remarkable asymmetric deformation as a function of running speed (Figure 28 and Figure 31). This can be explained by the roll manufacturing process. The roll is welded together from two pieces of different lengths, which is a typical design for large cylinders. Both parts have different mass distribution and stiffness, which leads to asymmetric deformation under high centrifugal force.

Predictive 3D grinding improved the roll roundness by an average of 77%, from 76 µm to 17 µm at the production running speed in the middle cross-section. At the ends, the roundness was already very good after traditional machining and the roll roundness only improved by 32%, from 19 µm to 13 µm. At the ends the stiffness of the end plates minimises the deformation. The remaining error derives from the rotational error from the bearings, which is copied in grinding to roundness error. With the 3D grinding technology the roundness of the rolls was better at the running speed than with traditional grinding at a low speed.

The run-out is a sum of out-of-roundness and the movement of the rotational axis. In flexible rotors eccentricity is normally the main component of run-out. Backing rolls with a large diameter and thin cylinder wall are exceptional because they may exhibit high shell deformation at a high running speed. Both test rolls had a strong second harmonic, which derives from an oval roundness profile at running speed. The backing roll of the second coating station actually had the second harmonic as the major run-out component.

Predictive 3D grinding improved the roll run-out by an average of 58%, from 92 µm to 39 µm at production running speed in the middle cross-section. At the ends, the run-out was already very good after traditional machining and the roll run-out only improved by 27%, from 33 µm to 24 µm.

5.2 Comparison of the results with other high-precision roll manufacturing methods

Besides the method presented, the run-out of the backing rolls can be reduced by alternative means. Traditionally, the existing roll is replaced by a new and more precisely manufactured roll. The other existing possibility is the mechanical renewal process of the existing roll by the methods presented by Pullinen et al. (1997). Both alternatives imply expensive investment.

5.2.1 Comparison with new high-precision backing rolls

Roll manufacturers market new high-precision backing rolls with a run-out accuracy of 50 µm at the running speed of the paper machine. This

has become possible with the roll dynamic measuring devices that have been developed, which give more information about the manufacturing process. The effects of the improvements in the manufacturing process can be measured in roll dynamic behaviour.

In this study, the run-out in the middle cross-section was reduced to 34 µm and 44 µm on the old backing rolls by means of predictive 3D grinding. The run-out achieved at running speed can be considered as at least as good as that which the new high-precision backing rolls can provide.

5.2.2 Comparison with renovated backing rolls

The mechanical renovation process of the existing roll is presented by Pullinen et al. (1997) and Kuosmanen et al. (1998). Roll manufacturers have developed their own slightly differing methods for the renovation process. The renovation process is very close to manufacturing a new roll. Only the shell and probably the ends of the roll are re-used. The shell deformation is normally the result of uneven mass distribution. It can be reduced by inside machining or adding mass symmetrically. Stiffness in the circumferential direction can be increased by welding circular rings inside. The same accuracy can be achieved with the renovation process as by manufacturing a new precision roll.

5.2.3 Effect on the balance of the roll

The dynamic deflection is the first harmonic component of the run-out signal measured in the middle cross-section. The asymmetrical removal of material in respect to the axis of rotation changes the balance of the roll. The balance remains unaltered only in compensating for symmetrical deformations with symmetrical geometric compensation. The method presented can be used for dynamic balancing if the ground geometry includes eccentricity. The benefit of this method is that the addition of mass inside the roll is avoided. The method also provides an opportunity to improve the balance simultaneously with geometric correction.

Figure 57 shows the effect of 3D grinding on the dynamic deflection of the backing roll of the first coating station. The geometry was optimised to a running speed of 1120 m/min but the first harmonic of the run-out reached its minimum above 1200 m/min.

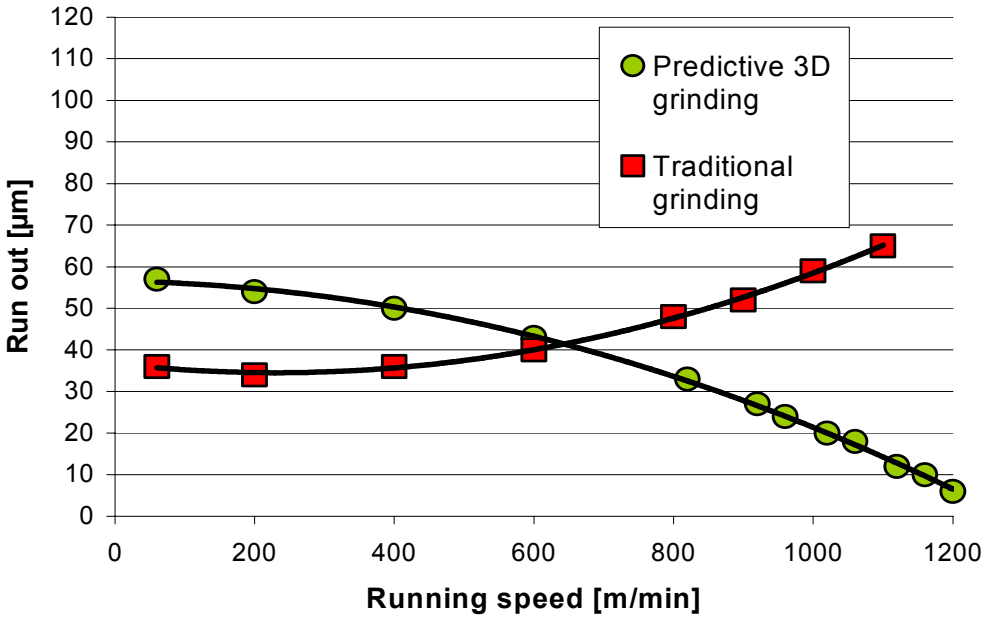

Figure 57 Effect of predictive 3D grinding on the dynamic deflection of the backing roll of the first coating station.

5.2.4 Cost-effectiveness

The price of a new backing roll is approximately 150,000 euros. A two-station coating machine needs four rolls. Two are in use and both stations need a backup roll, which is undergoing service grinding in the interim period. Thus the total cost of new rolls is about 600,000 euros.

The renovation process is very cost-effective when compared with investment in new rolls The investment in the mechanical renovation process of the existing roll is, depending on the method used, roughly one third of the cost of a new roll.

The investment in 3D control and measuring technology starts from 300,000 euros. The use of this technology is not limited to the backing rolls; the accuracy of all rolls can be improved. The method developed reduces the need to invest in new rolls. After the investment in control and measuring technology, the rolls can be ground with predictive 3D grinding without additional costs. The grinding time has been proven actually to be shorter than with the traditional methods. The reason for the time-saving in the grinding process is not in the increased material removal rate, but the fact that the control system avoids some unnecessary actions performed in the case of manual control. Naturally, the dynamic measurement takes some time and thus the overall time span is not shorter than in traditional grinding.

5.2.5 Stability of the rolls

The stability of old rolls can be considered as better when compared with that of new rolls. Despite thermal treatment, new rolls may have high internal stresses, which can relax during transportation or in use. The stability of a renovated roll is comparable to that of a new roll.

The predictive grinding method does not change the internal stresses of the roll. The grinding is normally performed on the roll cover. Soft covers normally have a low coefficient of elasticity, and thus the grinding process has little effect on the stiffness of the roll.

As the roll is re-covered, the old cover is removed mechanically, the roll surface is sandblasted, and the new cover may be vulcanised at a high temperature. In this process, the relaxation of stresses may occur. After disassembly and assembly, the bearings will have a different path of rotation. The roll is considered as a new roll, with high stresses close to the surface, and the rotational accuracy of the roll is reduced.

With predictive 3D machining, the new dynamic behaviour is first measured and the grinding is performed according to the measured data. This is a remarkable advantage over the traditional method, where the roll loses its accuracy during its lifetime and especially during servicing processes such as re-covering. The developed method makes it possible to optimise the behaviour of old rolls the production environment every time the roll is reground.

5.2.6 Applicability to changing environment

Is the predictive 3D grinding method useful if the running speed is not constant? Is there a risk that the roll will work even more poorly than would be the case without predictive 3D grinding? The answer is that in traditional grinding the optimisation is performed at the speed of the grinding process, i.e. 5 rpm. The closer to the actual running speed the optimisation is performed, the better. If the running conditions change between the grinding periods, the geometry can be optimised, for example to the critical running conditions or to the most common running conditions. The optimisation can be updated in the next grinding.

The measurements of the rolls have shown that the rolls have individual dynamic behaviours.

Figure 58 shows the dynamic deflection of three different fictional rolls at different speeds. The dashed lines show the roll run-out in traditional machining and the solid line shows the behaviour after predictive 3D grinding. In practice, traditional machining cannot reach a zero run-out at low speeds. The optimisation is performed to the assumed production speed of 1600 m/min. If the maximum accepted run-out is set to 50 µm, after traditional grinding Roll C exceeds the tolerance at a running speed of 850 m/min and Roll A exceeds the tolerance at 1500 m/min, which is clearly below the production speed.

Roll C needs strong geometry compensation to be optimal at a running speed of 1600 m/min. Roll A needs the least geometry compensation to reach a zero run-out at the running speed of 1600 m/min. The difference between Rolls A and C is in the usable running speed range. If the maximum accepted run-out is set to 50 µm, Roll C has a usable working speed range from 1400 to 1800 m/min. Roll A has a usable working speed range from 700 to 2350 m/min. The usable speed range describes the mechanical quality of the roll.

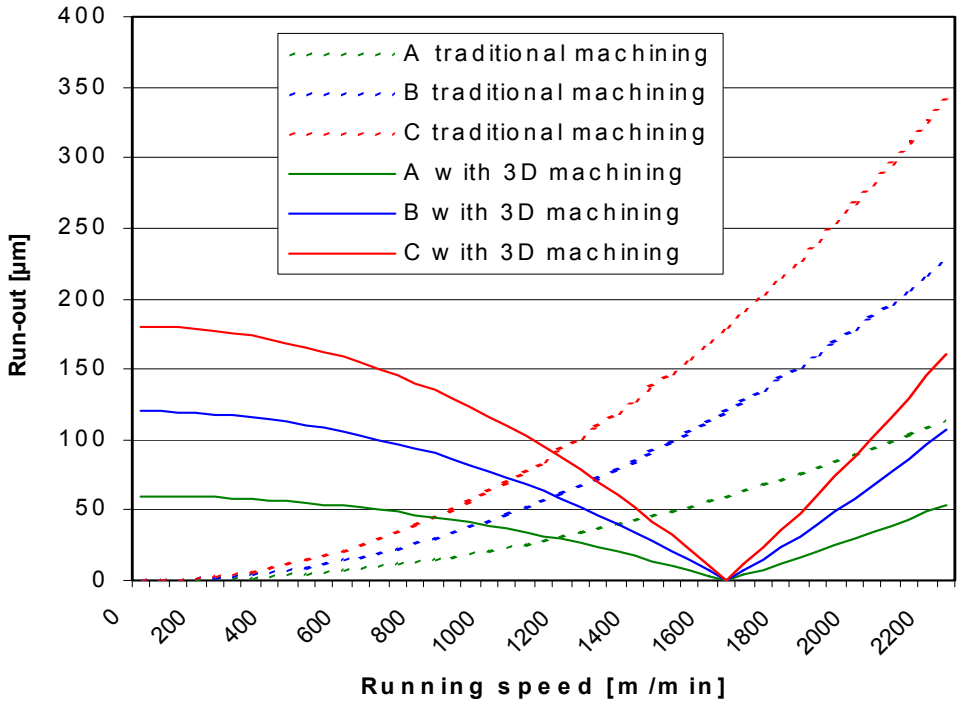

Figure 58 Theoretical run-out of three different paper machine rolls with traditional machining and with 3D machining. The speed range where the run-out is less than the 50 µm tolerance is considered the usable production speed range.

In fact, the principle of predictive geometry compensation is close to the continuous balancing of flexible rotors. The optimisation must be performed to the right production speed. Optimisation to speeds that are too high or too low reduces the quality of the process.

5.3 Influence of predictive 3D grinding on paper quality variations in machine direction

Although the improvement of roll dynamic behaviour is very important, it is not very interesting if it does not have a correlation to the quality of the end product, which was, in this study, paper. The covariance was calculated according to Equation 2. The distribution is expressed with ordered pairs of numbers $(x_1, y_1), (x_2, y_2), \ldots, (x_n, y_n)$.

$$s_{xy} = \frac{\sum_{i=1}^{n}(x_i - \bar{x})(y_i - \bar{y})}{n} \quad (2)$$

where $\bar{x}$ and $\bar{y}$ are mean values.

The correlation factor r is calculated with Equation 3.

$$r = \frac{\sum_{i=1}^{n}(x_i - \bar{x})(y_i - \bar{y})}{\sqrt{\sum_{i=1}^{n}(x_i - \bar{x})^2 \sum_{i=1}^{n}(y_i - \bar{y})^2}} \quad (3)$$

If the correlation factor $r = \pm 1$, then x and y are linearly dependent on each other.

Table 8 Interpretation of the correlation coefficient.

Correlation	$\lvert r \rvert$
Negligible	$0 < r \leq 0.3$
Moderate	$0.3 < r \leq 0.6$
Substantial	$0.6 < r \leq 0.8$
Strong	$0.8 < r < 1$

The calculation needs ordered pairs of numbers. If the frequencies of the signals are not exactly the same, the correlation decreases when the number of pairs is increased. To avoid this, the measured data are analysed as follows. A frequency close to the rotational frequency of the roll is manually selected from the frequency domain signal of a paper characteristic. There are several reasons why the wavelength of the backing roll in the paper web is not exactly known. First, the circumference of the roll is measured to an accuracy of ±0.2 mm. This measurement is taken at the roll shop temperature and the temperature is easily 50°C higher in the process, which increases the diameter of the backing roll by roughly 0.5 mm. In addition, the paper web may have relative motion in proportion to the roll surface. Paper also stretches during the process and the sample is taken from a customer roll ready for packing. After the first harmonic is selected, the actual amplitude and phase of the other harmonics are calculated. These harmonics are transformed to a time domain signal, which has a length of 256 points and is equivalent to the perimeter of the roll. To adjust the rotational angle of the backing roll to the paper sample, the correlations are calculated by shifting the signal by one point and repeating the calculation of the correlation. The phase between signals is locked to the position where ash variation and roll run-out have the highest negative correlation. The pairs of numbers and correlation line are plotted in an xy-diagram.

5.3.1 Ash variation in machine direction

The machine-direction (MD) coating variation caused by the backing rolls diminished by an average of 76% when the backing rolls were ground with predictive 3D grinding. The paper grade was not exactly the same in both samples. The paper had more coating in the latter test (13.5 g/m^2 vs. 13 g/m^2 per side), where the backing rolls were ground with predictive 3D grinding. Normally, a greater thickness increases the variation in thickness. The experiments would have shown even greater improvements with the same paper grade.

The ash variation caused by the backing roll of the first coating station is presented in Figure 39. The time domain signals of run-out (left) and ash variation during one roll rotation before and after predictive 3D grinding are presented in Figure 59.

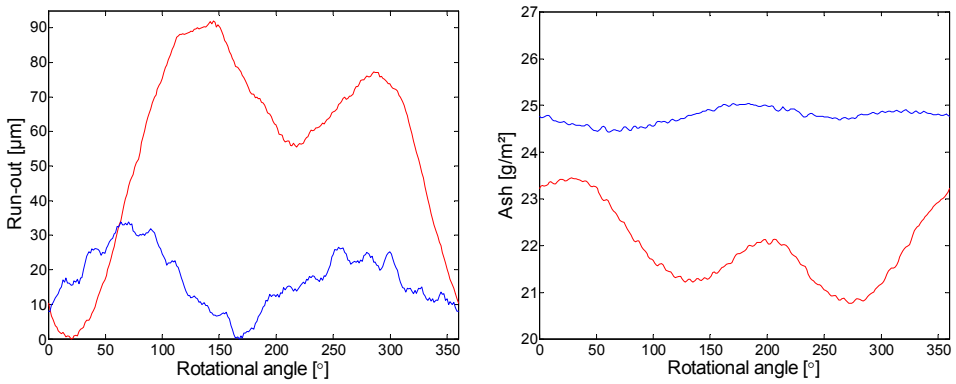

Figure 59 *Run-out of the backing roll of the first coating station during one roll rotation in the direction of the metering blade (left) and ash caused by the first coating station of the same period (right). Curves in both figures are measured before (red) and after (blue) predictive 3D machining.*

Figure 60 shows the correlation between ash and run-out of the first coating station backing roll before and after predictive 3D machining. The correlation reduced slightly from 0.92 to 0.81 which is still strong correlation. These results show that strong correlation between run-out and ash variation remains although the amplitudes are reduced.

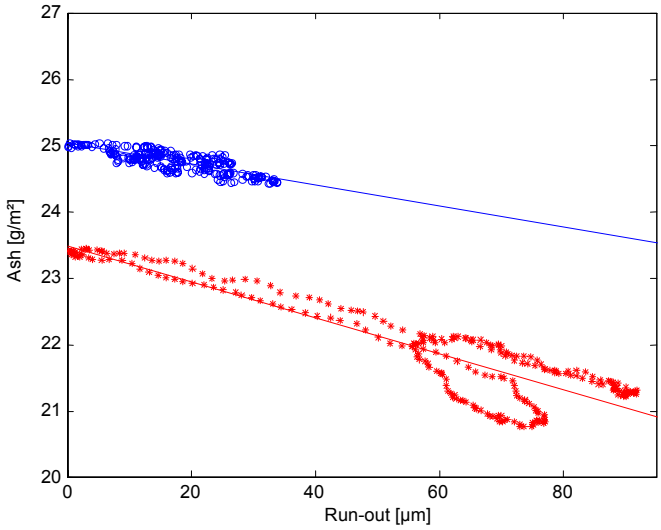

Figure 60 *The correlation between ash and run-out of the first coating station backing roll before (red stars) and after (blue circles) predictive 3D machining.*

The ash variation caused by the backing roll of the second coating station is presented in Figure 40. The time domain signals of run-out (left) and ash variation during one roll rotation before and after predictive 3D grinding are shown in Figure 61.

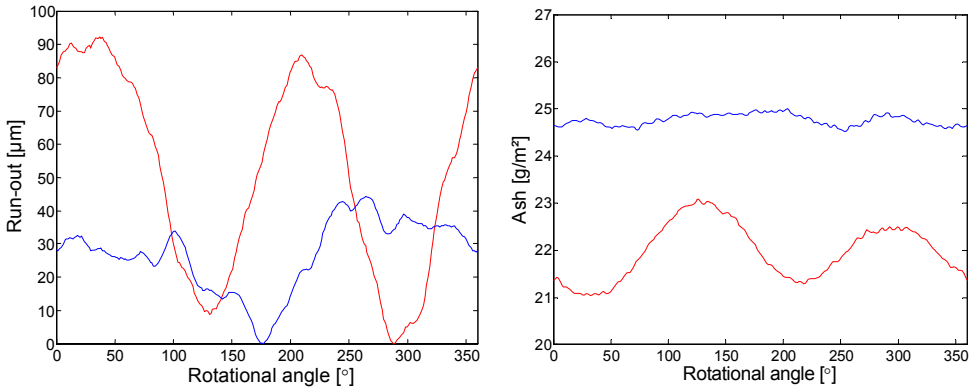

Figure 61 *Run-out of the backing roll of the second coating station during one roll rotation in the direction of the metering blade (left) and ash caused by the first coating station of the same period (right). Curves in both figures are measured before (red) and after (blue) predictive 3D machining.*

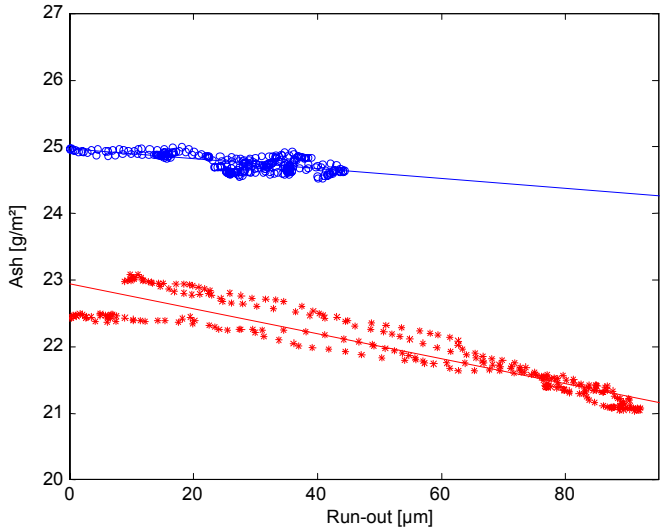

Figure 62 *The correlation between ash and run-out of the second coating station backing roll before (red stars) and after (blue circles) predictive 3D machining.*

Figure 62 shows the correlation between ash and run-out of the second coating station backing roll before and after predictive 3D machining. The correlation reduced from strong (0.93) to substantial (0.66). The reduction in correlation is more clear than in case of the first coating station backing roll.

5.3.2 Gloss variation in machine direction

As a result of a more even coating film, the MD gloss variation was reduced by 79%. The gloss variation caused by the backing roll of the first coating station is presented in Figure 51. The run-out signal of the backing roll is presented in Figure 35. The time domain signals are presented in Figure 63.

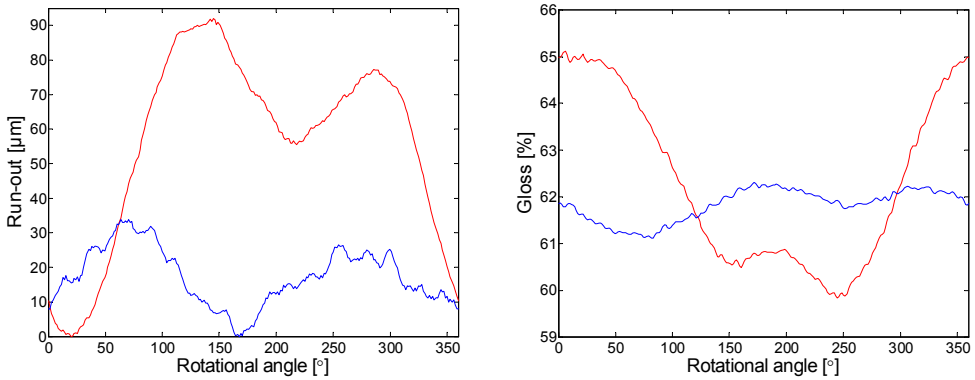

Figure 63 *Run-out of the backing roll of the first coating station during one roll rotation in the direction of the metering blade (left) and gloss of the same period (right). Curves in both figures are measured before (above) and after (below) predictive 3D machining.*

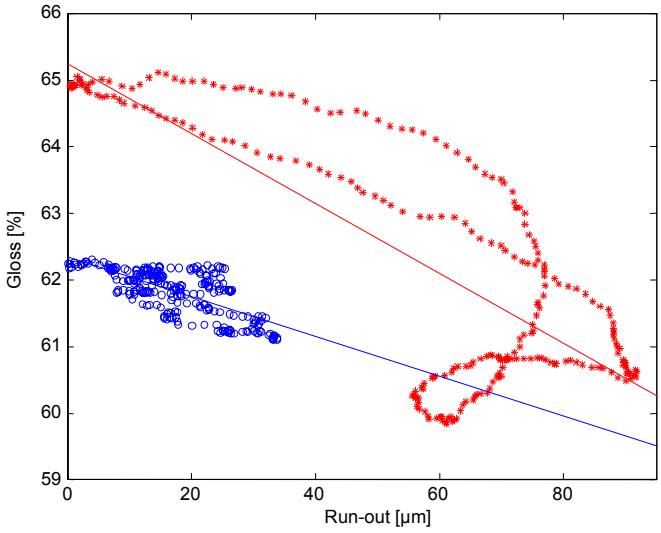

Figure 64 *The correlation between gloss and run-out of the first coating station backing roll before (red stars) and after (blue circles) predictive 3D machining.*

The peak close to the second harmonic in the gloss signal before 3D grinding Figure 51 was not exactly the second harmonic and was not taken into account in the correlation calculation. With that second harmonic, Figure 64 would not have that clear loop at the bottom. The correlation would also have been better. The peak disappeared after 3D grinding.

The gloss variation caused by the backing roll of the second coating station is presented in Figure 54. The run-out signal of the backing roll is presented in Figure 37. The time domain signals are presented in Figure 65.

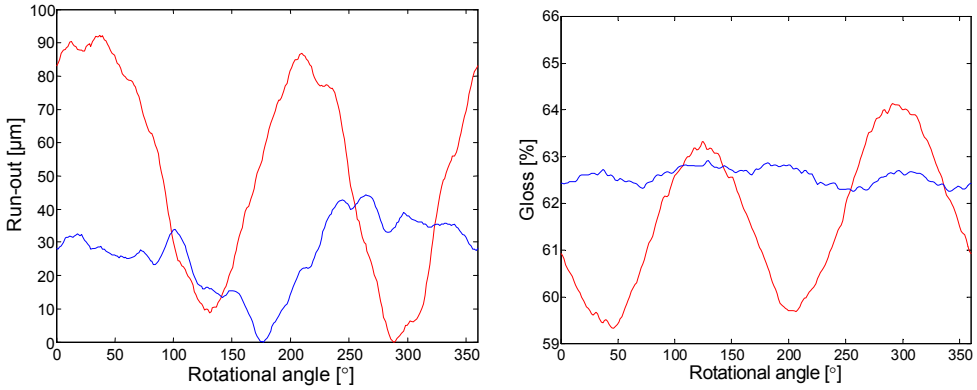

Figure 65 *Run-out of the backing roll of the second coating station during one roll rotation in the direction of the metering blade (left) and gloss of the same period (right). Curves in both figures are measured before (above) and after (below) predictive 3D machining.*

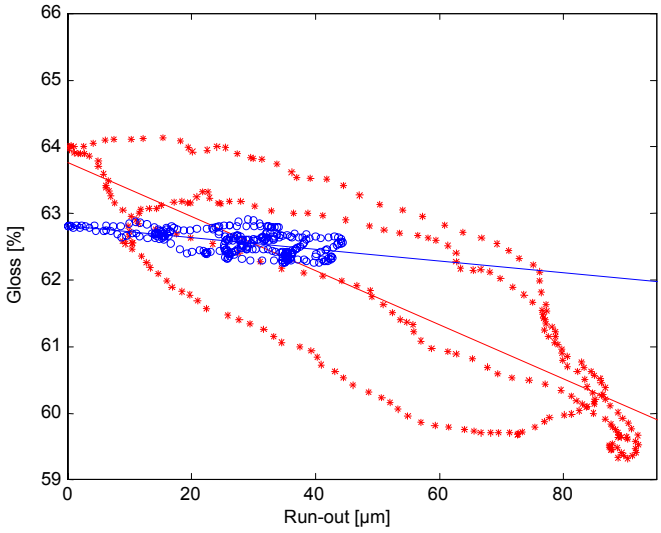

Figure 66 The correlation between gloss and run-out of the second coating station backing roll before (red stars) and after (blue circles) predictive 3D machining.

The correlation between gloss and run-out of the second coating station backing roll before and after predictive 3D machining is presented in Figure 66. The correlation reduced from strong (0.82) to moderate (0.55) as a result of predictive 3D grinding of the backing roll.

5.3.3 Basis weight variation in machine direction

The basis weight variation caused by the backing roll of the first coating station is presented in Figure 43. The run-out signal of the backing roll is presented in Figure 59. The time domain signal of ash variation during one roll rotation before and after predictive 3D machining is presented in Figure 67.

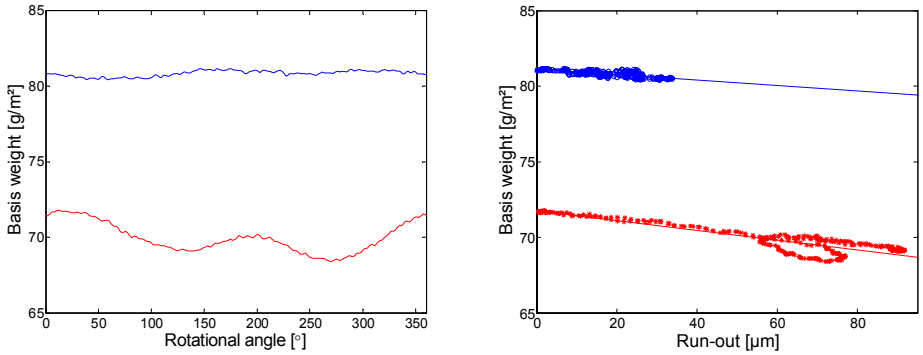

Figure 67 Basis weight variation caused by the first coating station backing roll (left) and the correlation between basis weight variation and run-out (right). Curves in both figures are measured before (red) and after (blue) predictive 3D machining.

The basis weight variation caused by the backing roll of the second coating station is presented in Figure 44. The time domain run-out signal of the backing roll is presented in Figure 61. The time domain basis weight signals are presented in Figure 68.

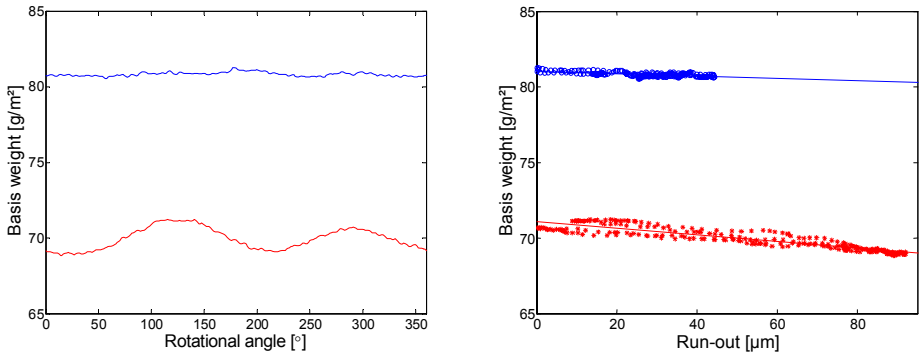

Figure 68 Basis weight variation caused by the second coating station backing roll (left) and the correlation between ash variation and run-out (right). Curves in both figures are measured before (red) and after (blue) predictive 3D machining.

The correlation between basis weight and run-out of the first coating station backing roll before and after predictive 3D machining is presented in Figure 67. The correlation reduced from strong (0.90) to substantial (0.72) as a result of predictive 3D grinding of the backing roll.

The correlation between basis weight and run-out of the second coating station backing roll before and after predictive 3D machining is presented in Figure 68. The correlation reduced from strong (0.91) to substantial (0.63) as a result of predictive 3D grinding of the backing roll.

5.3.4 Thickness variation in machine direction

The thickness variation caused by the backing roll of the first coating station is presented in Figure 47. The run-out signal of the backing roll is presented in Figure 59. The time domain signal of thickness variation during one roll rotation before and after predictive 3D machining is presented in Figure 69.

The thickness variation caused by the backing roll of the second coating station is presented in Figure 44. The time domain run-out signal of the backing roll is presented in Figure 61. The time domain signal of thickness variation during one roll rotation before and after predictive 3D machining is presented in Figure 70.

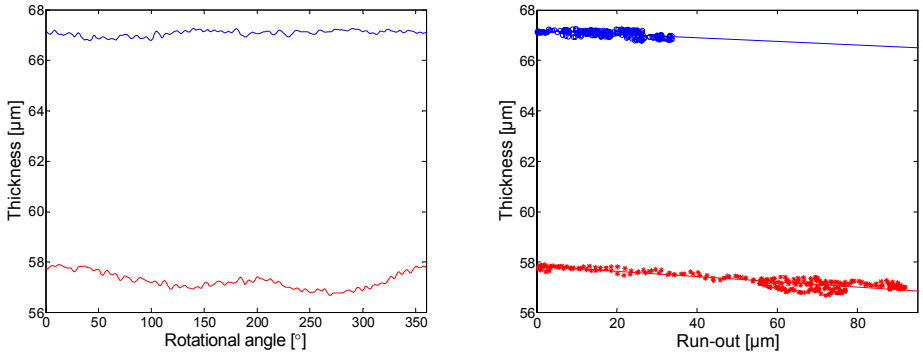

Figure 69 Thickness variation caused by the first coating station backing roll (left) and correlation between thickness variation and run-out (right). Curves in both figures are measured before (red) and after (blue) predictive 3D machining.

The correlation between thickness and run-out of the coating station backing rolls before and after predictive 3D machining are presented in Figure 69 and Figure 70. The correlation reduced from strong (0.86) to moderate (0.53) as a result of predictive 3D grinding of the first coating station backing roll. The correlation reduced from strong (0.89) to moderate (0.45) as a result of predictive 3D grinding of the second coating station backing roll.

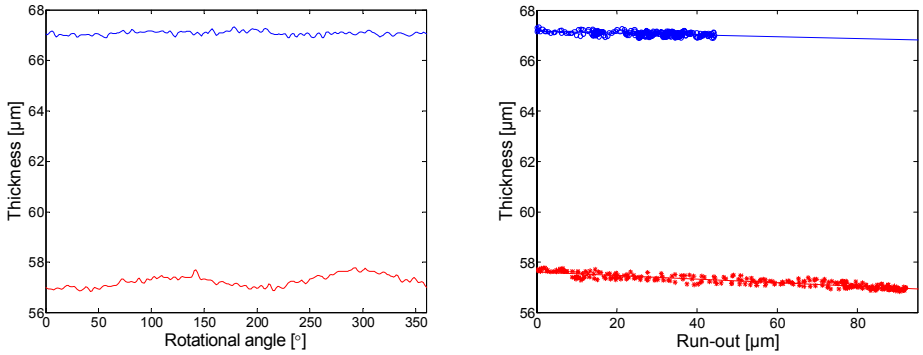

Figure 70 Thickness variation caused by the second coating station backing roll (left) and correlation between ash variation and run-out (right). Curves in both figures are measured before (red) and after (blue) predictive 3D machining.

The correlations between backing roll run-out and paper characteristics are presented after traditional grinding and after predictive 3D grinding of the backing rolls. The correlation is strong after traditional grinding because the backing rolls caused clear coating variation on the paper (Table 9). After predictive 3D grinding (Table 10) the correlation is still substantial. The variation has diminshed and the relative noise increased but what remains correlates to the run-out of the backing rolls.

Table 9 Correlation between backing roll run-out and paper characteristics after traditional grinding.

	Ash [g/m²]	*Basis weight* [g/m²]	*Thick-ness* [µm]	*Gloss st. 1* [%]	*Gloss st. 2* [%]
Runout st. 1 [µm]	0.92	0.90	0.86	0.79	-
Runout st. 2 [µm]	0.93	0.91	0.89	-	0.82

Table 10 Correlation between backing roll run-out and paper characteristics after predictive 3D grinding.

	Ash [g/m²]	*Basis weight* [g/m²]	*Thick-ness* [µm]	*Gloss st. 1* [%]	*Gloss st. 2* [%]
Runout st. 1 [µm]	0.81	0.72	0.53	0.72	-
Runout st. 2 [µm]	0.66	0.63	0.45	-	0.55

5.4 Importance of the results

The original features of this study are

- improved roll behaviour under production conditions because of predictive 3D grinding
- reduction of variations in paper quality because of predictive 3D grinding
- confirmed correlation between roll run-out and variations in paper quality

The original features are presented in more detail in Chapter 1.6. The results are significant for industries using rotating machines, such as paper machines, printing machines, and roller stands for the steel, aluminium, and plastics industries.

The benefit of the results for paper coating is that no extra energy is needed to dry an uneven layer of wet coating material. If the process is limited by drying capacity, the more even coating layer makes a speed increase possible. Paper with less coating material will no longer be overdried, which improves its strength properties. The main advantage, however, is the influence on printing quality. The effects of variations in paper quality on printing are summarised in more detail in Chapter 2.3.2.

The technology developed is cost-effective and can easily be applied to old paper production line machines where there is pressure to increase running speeds and paper quality. It has been proved that by means of this technology old rolls will run even better than the new rolls that are available. In new high-speed paper machines this technology provides a new tool to meet the tightening tolerances of rotational and geometric accuracy.

One major advantage of this technology is that in roll manufacturing emphasis can be placed on long-term stability and systematic roll behaviour rather than maximising machining accuracy on the shop floor. The accuracy will be achieved by predictive grinding technology. The technology cannot, however, predict, for example, stress relaxations.

Another major advantage is that roll machining accuracy is no longer bound to the accuracy of the machine tool but to the accuracy of the measuring system and the control system. Because of the measuring and control system, the major requirement for the machine tool is now stability, not mechanical accuracy.

The predictive grinding method eliminates the need for dynamic balancing when the run-out is in a reasonable range. Accurate balancing is difficult, especially for rolls with welded ends. Adding mass-balance weight inside a long roll in the middle cross-section is a laborious operation. Dynamic deflection compensation is included in the predictive external grinding geometry. The result is very accurate and can be readjusted at each service grinding if any changes have occurred.

The technology is not only limited to high-speed rotating paper machine rolls but the same method can be applied to compensate for the uneven thermal expansion or uneven stiffness of the rolls as well. The technology can also be applied in the steel, plastics, and aluminium industries. The method makes possible the use of rolls in applications which have requirements too high to be met by traditional technology.

5.5 Suggestions for further research

This research should now be focused on different applications. In the paper industry the main research field for predictive 3D grinding is compensation for the effects of thermal expansion. In some positions chilled roll temperatures can be over 250°C. The material layers of white cast iron and grey cast iron easily cause deflection of the roll under running conditions.

Another important application in the paper industry is the optimisation of the load in the nip rolls. The optimisation should be done in both CD and MD. Dynamic balancing with grinding should be applied to flexible rolls, which have high rotational accuracy requirements.

In the steel industry, the thickness profile of the steel strip after milling has periodical errors caused by the rolls. These systematic errors can be reduced by the technology presented here. The target should be an even

thickness profile for the strip. The technology can be applied both to hot strip mills and cold strip mills.

In the future, the frequency and amplitude of each component in the roundness profile and run-out spectrum should be considered separately according to the requirements of the installation position.

6 CONCLUSION

The motivation for this study was the observation that some paper machine rolls do not keep their geometry when their rotational speed is increased to running speed. Could it be possible to find a cost-effective method to avoid this problem? The problem became a real issue during the '90s as a result of increased running speeds. This trend seems to be continuing. At the same time, the paper produced must have a higher and more even quality. In printing papers the main end-use properties and quality components are runnability, printability, and print quality. These coexistent requirements impose new demands on the behaviour of the rolls under production conditions. High quality printing paper grades are coated. In blade coating the thickness of the coating film on the paper surface is found to be heavily dependent on the run-out of the backing roll which supports the paper web against the metering blade. The run-out tolerance of the backing rolls at running speed has recently been 50 µm and should be substantially reduced in the future. The new tolerances can no longer be met by tightening the traditional roll manufacturing tolerances.

A new predictive 3D grinding method was developed to improve roll behaviour in the paper production environment. It consists of a measuring system, which can verify the rotational and geometry errors of the roll at running speed, and a 3D grinding system, which controls the grinding process according to the information gained from the measurements.

In this study, the new method was applied to the backing rolls of a coating station. The experiments were carried out in a paper mill, in a medium-weight coated (MWC) paper production line. The paper was analysed before and after predictive 3D grinding to confirm the improvement in paper quality.

Both test rolls displayed remarkable asymmetric deformation as a function of running speed. Predictive 3D grinding improved the roll roundness by an average of 77%, from 76 µm to 17 µm at the production running speed in the middle cross-section. The roll run-out improved by 58%, from 92 µm to 34 µm. The first harmonic component of the run-out was also reduced by predictive 3D grinding. Traditionally, this was possible only with balancing.

Predictive 3D grinding reduced the machine direction (MD) ash variation caused by the backing rolls by an average of 76%. Ash variation has a good correlation to coating variation. As a result of a more even coating film, the MD gloss variation was reduced by 82%. Reduced gloss variation improves the print quality of MWC paper. Thickness variation caused by the backing rolls was reduced by 74%. A more even paper thickness reduces excitation and therefore improves runnability in calendering, winding, and printing.

A new paradigm for roll grinding was set. The applications of the technology developed are not limited to high-speed paper machine rolls; the method can be applied to different kinds of nips of rolls. The method can compensate for a systematic error causing nip force variation, such as the uneven thermal expansion or uneven flexural stiffness of the rolls. The technology can be applied to different industries, such as the steel, plastics, and aluminium industries. With this method, it is also possible to use rolls in applications which have requirements too high to be met by traditional technology.

REFERENCES

ANSI B89.3.1 (1972). Measurement of out-of-roundness. New York, The American Society of Mechanical Engineers. 27 pp.

Barth, U. (1984). Kombinierte Zweipunkt-Dreipunkt-Messung zum gleichzeitigen Bestimmen von Maß- und Kreisformabweichungen. Feingerätetechnik, Berlin 33 (1984). pp. 21-23.

Chen, Y.N., Boos, G. (1975). Calender barring on paper machines – practical conclusions and recommendations. Tappi Vol. 58, No. 8, pp. 147-151

Cutshall, K. A., Ilott G. E., Brooks B. W. (1979). Causes of MD Basis Weight Variation. Pulp and Paper Canada, June 1979.

Cutshall, K. (1990). Nature of Paper Variation. Tappi Journal, Vol. 73, No. 6, pp. 81-90

Ehrola, J. et al. (1999). Calendering p. 17. In: Papermaking Part 3, Finishing. Fapet Oy, Jyväskylä 1999: Papermaking Science and Technology. ISBN 952-5216-10-1.

Erho, T., Saari, J., Qvintus-Leino, P. (2002). Variations in paper and in print. Proceedings of the Technical Association of the Graphic Arts, TAGA, 2002, pp. 497-507

Finnish Forest Industries Federation (2002). Finnish Forest Industry transparency presentation sets, statistics in 2002. http://www.forestindustries.fi/ 24 pp.

Frank, A., Ruech, F. (1999). Thermographie an Werkzeugmaschinen: Visualisierung thermischer Effecte an Kugelrollspindeln in Positionsmeßsystemen von CNC-Maschinen. Österreichische Gesellschaft fur Thermographie. Jahrestagung 1999. Anif, Salzburg, 8-10 Oktober 1999.

Fu, C., Nuyan, S. (2002). Mill experiences on Cross-Machine Direction Troubleshooting, Proceedings of Tappi Technology Summit 2002, Atlanta GA. United States. 3-7 March, 2002.

Ghosh, A. K., Rae, C., Youdan, J. (2001). Off-line analysis of properties of the paper web: A diagnostic tool to reduce variability. Appita Journal, No. 5, September 2001, pp. 413-419, ISSN: 1038-6807

Girkmann, K. (1963). Flächentragwerke. Wien 1963, Springer-Verlag. pp. 473-475

Haikio, J. (1997). A turning system to minimize the geometrical error of a roll. Master's thesis, Helsinki University of Technology, Department of Mechanical Engineering. Espoo. 78 pp.

Higuchi, T., Yamaguchi, T., Tanaka, M. (1996). Development of a high speed non-circular machining NC-lathe for cutting a piston-head of a reciprocating engine by use of a new servomechanism actuated by electromagnetic attractive force. Journal of the Japan Society of Precision Engineering. March 1996; 62(3): pp. 453-7.

Hilden, K., Perento, J. (2000). Paper analysis: The key to optimizing and troubleshooting paper machines. Pulp and Paper Canada, Vol. 101, No. 7, July 2000, Don Mills, Ont, pp. 37-42, ISSN: 0316-4004

Herreman, G., Berry, F., Dowby, C. (1980). Laser measurement systems for machine tool testing. Hocken, R. J. Technology of Machine Tools, Vol. 5: Machine tool accuracy. Lawrence Livermore National Laboratory, University of California, USA.

Hybrid Dyna Test (2003). RollResearch International Ltd. http://www.rollresearch.fi.

International Organisation for Standardization (1993). Guide to the expression of uncertainty of measurements. Geneva. ISBN 92-67-10188-9.

ISO 11342 (1994). Mechanical vibration – Methods and criteria for the mechanical balancing of flexible rotors. Geneva. International Organization for Standardization. 31 pp.

Jaehn, A.H. (1985). Tappi Journal Vol. 68, No. 7, p. 112

Juhanko J. (1999). Dynamic behaviour of a paper machine roll. Licentiate's thesis, Helsinki University of Technology. Espoo, 82 pp.

Kato, H., Sone, R. Y., Nomura, Y. (1991). In-situ measuring system of circularity using an industrial robot and a piezoactuator. International Journal of Japan Society of Precision Engineering, Vol. 25, No. 2, pp. 130-135.

Kim, K.H., (1983). Forecasting compensatory control of roundness in cylindrical grinding. Ph. D. Thesis. University of Wisconsin, Madison, Wisconsin, USA, 1983. 148 pp.

Korpela, M.S. (1994). Mill Experiences at Kymmene-Kaukas. Proc., TAPPI Coating Conference, San Diego, CA., p. 310.

Kuosmanen, P. (1992). Optimization of the contact pressure in the nip of two non-ideal cylinders. Licentiate's thesis, Helsinki University of Technology. Espoo. 77 pp.

Kuosmanen, P. & Väänänen P. (1996). New Highly Advanced Roll Measurement Technology. Proceedings of 5th international conference on new available techniques. The world pulp and paper week June 4-7. 1996; Stockholm, Sweden. pp. 1056-1063.

Kuosmanen, P., Juhanko, J., Pullinen, J. (1998). Influence of the modernization on the dynamic behaviour of the backing roll. Paperi ja Puu - Paper and Timber 80 (3), pp. 162-166.

Kuosmanen, P. & Juhanko, J. (1999). Research and development in roll machining. Fortek Mill Maintenance Conference in Oulu 26-27 May 1999. 7 pp.

Lehtinen, E. (2000). Introduction to pigment coating of paper. Book 11: Pigment coating and surface sizing of paper, ed. E. Lehtinen. In: Papermaking Science and technology, eds. Gullichen, J. and Paulapuro, H. Fapet Oy, Helsinki 2000, 810 pp, ISBN 952-5216-11-X.

Makkonen, T. (1998). Procedure and means for measuring the thickness of a film-like or sheet-like web. U. S. Patent 4,773,760

McKeown, P. (1989). Kinematic design. Precision Engineering module of the integrated European course in mechatronics in Granfield UK 25.-29.9.1989. 47 pp.

Nevaranta, J. (1984). Barring of newsprint in the machine calender – The causes and elimination. Licentiate's thesis, University of Oulu, Department of Mechanical Engineering. Oulu. 53 pp.

Oinonen, H., (1998). Järvenpään teknologiakeskus uusittiin perinpohjin: Päällystysnopeus ei enää ole tuotannon lisäyksen pullonkaula. Paperi ja Puu. Vol. 80. No. 8 pp. 576-580.

Parker, J.R. (1965). Corrugation of calender rolls and the barring of newsprint. Paper Technology, Vol. 6, No. 1 pp. 33-41(T1-T9).

Patzig, C. (2002). Maschinenintegriertepost-Process Form-Messung beim CNC-Unrundschleifen. Dissertation zur Doktorin der technischen Wissenschaften. Technischen Universität Graz, im Februar 2002.

Perento, J. (1999). Paper trials help to improve quality and printability. Paper Asia, Vol. 15, No. 7, 1999, Singapore, pp. 15-17, ISSN: 0218-4540

Pullinen, J. (2001). Teladynamiikan mittalaitteen kalibrointi. Koneensuunnittelun laboratorio, sisäinen raportti. Otaniemi 2001. 15 pp.

Pullinen, J., et al. (1997). Kunnostuksen vaikutus päällystysaseman vastatelan dynaamiseen käyttäytymiseen. Teknillinen korkeakoulu, Koneensuunnittelun laboratorio, julkaisu nro C 286. ISBN 951-22-3741-5. Otaniemi 1997. 74 pp.

Savolainen, M. (1996). Development of the measuring and balancing system for the paper machine rolls. Master's thesis, Helsinki University of Technology, Department of Mechanical Engineering. Espoo. 68 pp.

Schnurr, B., (1998). Electrodynamisches Antriebsystem zur Unrundbearbeitung. Doctor's Thesis. Universität Stuttgart. 176 pp.

Sonozaki, S. & Fujiwara, H. (1989). Simultaneous Measurement of Cylindrical Parts Profile and Rotating Accuracy using Multi-Three-Point-Method. Bulletin of Japan Society of Precision Engineering. Vol. 23, No. 4. 1989.

Tapio Analyzator (2003). Tapio Technologies Oy. http:/www.tapiotechnologies.fi.

Tervonen, M. (1984). Barring of newsprint in the machine calender – The vibration models of the calendar. Licentiate's thesis, University of Oulu, Department of Mechanical Engineering. Oulu. 89 pp.

Uda, Y., et. al. (1996). In-process measurement and workpiece-referred form accuracy control system (WORFAC): application to cylindrical turning using an ordinary lathe. Precision Engineering 18: pp. 50-55, 1996.

US 5940969 (1999). Method and apparatus for continuously balancing and reducing the elastic asymmetry of a flexible rotor, particularly a roll or a cylinder. Valmet Corporation, Finland. (Kuosmanen, P. and Väänänen, P.) US 750005, Nov. 27, 1996. Pub. Aug. 24, 1999. 4 pp.

VTT (1999). Research report No. 75-99289. VTT Production technology. 31 pp.

Väänänen, P. (1993). Turning of flexible rotor by high precision circularity profile measurement and active chatter compensation. Licentiate's thesis, Helsinki University of Technology. Espoo. 104 pp.

Weck, M., Pyra, M., Özmeral, H. Non-Rotational-Symmetric Optics and their Applications. Proceedings of the 3rd International Conference on Ultraprecision in Manufacturing Engineering. Aachen, Germany, 2-6 May 1994.

Whitehouse, D. (1994). Handbook of surface metrology. Institute of Physics Publishing for Rank Taylor Hobson Ltd. pp. 139-142.